# Design and Modeling of the Navy Integrated Power and Energy Corridor Cooling System

by

### Ivan A. Reyes

Submitted to the Department of Mechanical Engineering in partial fulfillment of the requirements for the degrees of Master of Science in Naval Architecture and Marine Engineering

and

Master of Science in Mechanical Engineering at the

### MASSACHUSETTS INSTITUTE OF TECHNOLOGY

May 2022

© Massachusetts Institute of Technology 2022. All rights reserved.

Author	
	Department of Mechanical Engineering
	May 6, 2022
	Wlay 0, 2022
Certified by	
	Julie Chalfant
	Research Scientist
	Thesis Supervisor
Certified by	*
Cerumed by	Chryssostomos Chryssostomidis
	v
	Professor of Mechanical and Ocean Engineering
	Thesis Supervisor
Accepted by	
	Nicolas Hadjiconstantinou
(	Chairman, Department Committee on Graduate Theses

## Design and Modeling of the Navy Integrated Power and Energy Corridor Cooling System

by

#### Ivan A. Reyes

Submitted to the Department of Mechanical Engineering on May 6, 2022, in partial fulfillment of the requirements for the degrees of Master of Science in Naval Architecture and Marine Engineering and Master of Science in Mechanical Engineering

#### Abstract

As part of an ongoing U.S. Navy research consortium for next-generation warships, the Design Laboratory of the MIT Sea Grant Program is developing the Navy Integrated Power and Energy Corridor (NiPEC) to underpin the vessel's power distribution system. The corridor comprises several modular compartments capable of operating independently or as part of a network to execute energy storage, conversion, protection, control, isolation, and transfer functions. The power conversion process is carried out by the corridor's integrated Power Electronics Building Block (iPEBB) based architecture. The iPEBB is a comprehensive and self-contained converter configured to provide power-dense solutions to the ship's stochastic and dynamic loads. A key challenge with the iPEBB's advanced semiconductor technology is the mitigation of its thermal management, constrained by the provision of indirect liquid cooling methods and the objective of a sailor-centric design.

This thesis used numerical analysis and modeling to design an indirect liquid-cooling system aboard U.S. Navy Surface Vessels. Guided by Department of Defense and industry requirements, a new cooling paradigm was developed, promoting human-and intra-system operations, a comprehensive component design, and a robust cooling system architecture within the NiPEC compartment footprint. Documented are the initial investigation, equipment analysis, concept selection, and proof-of-concept testing that set the foundation for future prototyping and NiPEC cooling system development.

Thesis Supervisor: Julie Chalfant

Title: Research Scientist

Thesis Supervisor: Chryssostomos Chryssostomidis Title: Professor of Mechanical and Ocean Engineering

#### Acknowledgments

I would like to thank my thesis supervisors, Dr. Julie Chalfant & Professor Chryssostomos Chryssostomidis, for their invaluable feedback, advice, and encouragement. Their comprehensive knowledge in various fields of study guided me through critical points of my research. I feel remarkably fortunate to have had the opportunity to learn from them.

I am deeply grateful for the support and advice from several mentors who aided me in this educational endeavor, specifically Dr. Truc Ngo, Dr. Bradley Chase, Dr. Rick Olsen, Dr. Leonard Perry, and John Cavanaugh.

I would also like to thank my fellow Naval Officers and colleagues for their talents, insights, and friendship. A special thanks to LT Natasha Patterson, LT Eric Young, and LT Chris Tomlinson, without whom these degrees would not be possible.

I wish to acknowledge the contributions and sponsorship of Kelly Cooper and L.J. Petersen from the U.S. Office of Naval Research (ONR). This material is based upon research supported by, or in part by, the ONR under award numbers ONR N00014-16-1-2945 Incorporating Distributed Systems in Early-Stage Set-Based Design of Navy Ships and ONR N00014-16-1-2956 Electric Ship Research and Development Consortium.

Lastly, I owe eternal gratitude to my wife and daughter. Their patience, support, and understanding in this achievement are unparalleled and are a testimony to their amazing talents and capabilities.

# Contents

1	Intr	oducti	ion	17
	1.1	Backg	round	17
		1.1.1	Navy Integrated Power and Energy Corridor	18
		1.1.2	Navy integrated Power Electronics Building Block	20
	1.2	Proble	em Statement	21
	1.3	Base A	Assumptions	22
	1.4	Explo	ration of Cooling Methods	22
		1.4.1	Air Cooling	23
		1.4.2	Direct Liquid Cooling	24
		1.4.3	Cold Plate Cooling	25
		1.4.4	Advanced Methods	26
	1.5	Coolir	ng System Architecture	26
		1.5.1	Heat Exchanger	27
		1.5.2	Pump	29
		1.5.3	Other System Components	29
2	Hea	ıt Excl	nanger	33
	2.1	Heat 1	Exchanger Theory	33
	2.2	Heat 1	Exchanger Design Criteria and Modeling	41
		2.2.1	Two-pass Heat Exchanger Model	45
		2.2.2	Four-pass Heat Exchanger Model	47
		2.2.3	Heat Exchanger Modeling Conclusions	50

3	Pur	mp	51
	3.1	Pump Power & Sizing	51
4	Exp	pansion Tank	57
	4.1	Expansion Tank Volume	57
	4.2	Expansion Tank Pressures	59
5	Pip	es, Hoses, and Fittings	61
	5.1	Pipes and Flow Devices	61
		5.1.1 Corrosion	62
		5.1.2 Material Selection Conclusion	73
	5.2	Flexible Hoses	73
6	Wa	ter Chemistry Components	77
	6.1	Corrosion Analysis	77
	6.2	Chemistry Station and Filters	83
7	Col	d Plate	87
	7.1	Initial Design	87
	7.2	Second Design	91
	7.3	Third Design	91
	7.4	Final Design	93
8	Ove	erall NiPEC Cooling System Architecture	97
	8.1	iPEBB, iPEBB Assembly, and iPEBB Stack	97
		8.1.1 Condensation Mitigation	103
	8.2	NiPEC System and Compartment Layout	110
9	Fin	al System Design Summary	115
	9.1	Heat Exchanger	115
	9.2	Pump	116
	9.3	Expansion Tank	117
	9.4	Pipes, Hoses, and Fittings	118

	9.5	Water Chemistry Components	118
	9.6	Cold Plate	119
	9.7	Overall NiPEC Cooling System Architecture	119
10	T4-	Wash and Canalusians	101
ΤO	ruu	are Work and Conclusions	121
	10.1	Future Work	121
	10.2	Conclusion	122
A	Pipe	e Fittings Flow Friction Values	127
B	Flox	ible Hose End Fittings	129
D	I ICX	Tible Hose End Pittings	120
$\mathbf{C}$	Dini	ng Construction Materials	137
O	ı ıpı	ing Constituction Materials	191
D	Pipi	ng Insulation Materials	141
_	b.		
$\mathbf{E}$	Idea	l Tube Bank Correlation Graphs	143

# List of Figures

1-1	General view of the NiPEC in the notional ship [4]	19
1-2	Sample power corridor and stiffener positioning; not to scale [3]	19
1-3	Notional NiPEC compartment module [3]	20
1-4	(a) iPEBB design with a top view of the primary side, (b) iPEBB	
	topology, (c) switching-cell portion of the SiC H-bridges [35]	21
1-5	Plate Heat Exchanger [1]	28
1-6	Straight-tube two-pass shell-and-tube heat exchanger [32]	29
1-7	Centrifugal Pump [7]	30
2-1	Constants for ideal tube bank correlations	38
2-2	Heat Exchanger Construction Materials	42
2-3	Alternative Heat Exchanger Construction Materials	43
2-4	Two-pass heat exchanger chilled water flow velocities	45
2-5	Two-pass heat exchanger chilled water flow pressures	46
2-6	Two-pass heat exchanger demineralized water flow velocities	46
2-7	Two-pass heat exchanger demineralized water flow pressures	47
2-8	Four-pass heat exchanger chilled water flow velocities	48
2-9	Four-pass heat exchanger chilled water flow pressures	48
2-10	Four-pass heat exchanger demineralized water flow velocities	49
2-11	Four-pass heat exchanger demineralized water flow pressures	49
3-1	Cooling System Diagram	54
5-1	Galvanic series of some metals in ambient seawater [38]	63

5-2	Galvanic compatibility of bare conductive materials in a 1:1 A/C in	
	immersed artificial seawater [28]	66
5-3	Comparison of the general corrosion rates for various alloys in quiet	
	seawater, millimeters per year [11]	67
5-4	Crevice corrosion comparison of for various alloys in a cavitation tunnel	
	at 40 $m/s$ [10]	69
5-5	Comparison of fouling resistance for various alloys [11]	69
5-6	Erosion corrosion and pitting comparison for various alloys, (microns/year)	)
	[13]	70
5-7	Crevice corrosion comparison of for various alloys [38]	71
5-8	Localized corrosion comparison for various alloys [13]	72
5-9	Recommended safe maximum flow velocities [9]	72
5-10	Hose dimensions and pressures [20]	74
5-11	Hose construction and minimum bend radius [20]	74
6-1	Superposition of the Pourbaix diagrams for copper (dotted lines) and	
	nickel (solid lines) at 25 °C. E in V vs. SHE is the metal's potential	
	when measured by a standard hydrogen reference electrode [16] $$	80
6-2	Superposition of the Pourbaix diagrams for iron (dotted lines) and	
	chromium (solid lines) at 25 °C [16] $\ldots \ldots \ldots \ldots \ldots$	85
6-3	Air Eliminator [23]	85
7-1	Cold plate arranged as a single-pass heat exchanger Padilla et al. [31]	88
7-2	Cold plate arranged as a counter-flow heat exchanger Padilla et al. [31]	88
7-3	First iteration - single inlet, single outlet offset u-tube cold plate design	89
7-4	iPEBB stack design for first design iteration cold plates	90
7-5	Second iteration - double inlet, double outlet, opposing flow cold plate	
	design	92
7-6	iPEBB stack design for second design iteration cold plates	92
7-7	Third iteration - single inlet, single outlet, opposing flow cold plate	
	design	93

7-8	Cold plate arranged as a counter-flow heat exchanger	94
7-9	Cold plate demineralized water flow velocities	95
7-10	Cold plate demineralized water flow pressures	96
8-1	iPEBB being inserted into the operational position with cold plates in	
	the stowed position	98
8-2	iPEBB inserted into the operational position with electrical connec-	
	tions made and cold plates positioned to provide cooling $\ldots \ldots$	98
8-3	Unobstructed view of back-plate hinge mechanism and connection ter-	
	minals	100
8-4	View of hinge mechanism connecting the cold plates to the back-plate	101
8-5	iPEBB and cold plate front edge vertical clearances during iPEBB	
	insertion or removal	101
8-6	iPEBB and cold plate back edge vertical clearances during iPEBB	
	insertion or removal	101
8-7	Straight and angled swivel fittings [18]	102
8-8	Example of an S-bend required for cold plate lateral movement [30] .	103
8-9	Psychometric chart at sea-level atmospheric pressures [2]	104
8-10	Idealized iPEBB cabinet	108
8-11	Positive Pressure Unit Example [8]	110
8-12	Minimum machinery space working clearances [25]	112
B-1	End fittings for use with flexible hoses [21]	129
B-2	Flange to hose - straight (F) and 90-degree elbow (FL) [21]	130
B-3	37-degree flare swivel (A) [21]	131
B-4	O-ring seal union - straight (C) or 90-degree elbow (CL) [21] $\ \ldots \ \ldots$	132
B-5	Split clamp end fitting - straight (E) and 90-degree elbow (EL) [21] $$ .	132
B-6	Split clamp adapter assembly (SC) [21]	133
B-7	Tailpiece female adapter (TF) [21]	134
B-8	Tailpiece male adapter (TM) [21]	135
B-9	90-degree elbow [21]	136

C-1	Category C-1 and C-2, Freshwater, including feed, chilled water, con-	
	densate, electronic freshwater cooling, potable, freshwater firefighting,	
	and gas turbine washdown, 200 psig/250 °F [27] $\ \ldots \ \ldots \ \ldots$	138
C-2	Category C-1 and C-2, Freshwater, including feed, chilled water, con-	
	densate, electronic freshwater cooling, potable, freshwater firefighting,	
	and gas turbine washdown, 200 psig/250 °F - Continued [27] $$	138
C-3	Category C-1 and C-2, Freshwater, including feed, chilled water, con-	
	densate, electronic freshwater cooling, potable, freshwater firefighting,	
	and gas turbine washdown, 200 psig/250 °F - Continued [27] $$	139
D-1	Thickness of anti-sweat and refrigerant insulation for piping [26]	141
D-2	Thickness of anti-sweat and refrigerant insulation for machinery and	
	equipment [26]	142
D-3	Dimensional tolerance of form $1$ – tubular insulation and form $2$ – sheet	
	insulation [26]	142
E-1	Ideal tube bank correlation for triangular pitch [36]	143
E-2	Ideal tube bank correlation for square pitch [36]	144
E-3	Ideal tube bank correlation for diamond pitch [36]	145

# List of Tables

2.1	Chilled Water and Heat Exchanger Properties	35
2.2	Specific constants for ideal tube bank correlations	37
2.3	Demineralized Water and Heat Exchanger Properties	39
2.4	Heat Exchanger Characteristics	40
2.5	Two-pass heat exchanger model geometries and arrangement	43
2.6	Required tube outside diameter and thickness	44
2.7	Tube Design Criteria	44
2.8	Maximum Unsupported Tube Spans	44
2.9	Four-pass heat exchanger model geometries and arrangement	47
3.1	15 °C Water Properties	52
3.2	Equipment Pressure Losses	52
3.3	Suction & Discharge Piping Frictional Losses	53
3.4	Summarized Pressure Losses	55
4.1	One-Dimensional Thermal Resistance Values Per Semiconductor Switch	57
5.1	U.S. Navy surface ship alloys for construction of electronic cooling wa-	
	ter systems	61
6.1	Cu-Ni piping component gasket material	81
6.2	Demineralized Water Purity Requirements	82
8.1	Rubber flexible hose minimum lengths without fittings	103
A.1	Resistance Coefficient Fitting Values [29]	128

# Chapter 1

### Introduction

#### 1.1 Background

The Office of Naval Research (ONR) established the Electric Ship Research and Development Consortium (ESRDC) in 2002 to develop unprecedented integrated electric power system technologies. The ESRDC is an entity comprised of collaborating institutions and research centers working to advance electric ship concepts. The Power Electronic Power Distribution Systems (PEPDS) program seeks to build off these concepts to provide new power, energy, and control technologies to Navy shipboard electrical systems. The program focuses on five areas of study: Navy integrated Power Electronics Building Block (iPEBB), Power Corridor, Model is the Specification, control, and system simulation. In development by the Design Laboratory of the MIT Sea Grant Program, the Navy integrated Power and Energy Corridor (NiPEC) is a modular entity that houses and interfaces the ship's main-bus power distribution equipment via an iPEBB-based architecture. The iPEBB is a compact, plug-and-play, sailor-practical universal converter. The synthesis of these two technologies provides energy storage, conversion, protection, control, isolation, and transfer functions to system components and loads [33].

#### 1.1.1 Navy Integrated Power and Energy Corridor

The NiPEC constitutes a paradigm shift in energy and power handling technologies for naval applications. It is capable of coordinating the singular or simultaneous utilization of alternating-current (AC) and direct-current (DC) inputs to deliver power to AC and DC loads. Legacy systems, e.g. Integrated Power and Energy System, lack the fidelity and synchronization to provide comparable power output to the ship's dynamic and static electrical functions. They are limited in their capability of employing dual-source, AC and DC, parallel-power operations in support of the ship's power grid. Whereas, NiPEC is capable of receiving and applying AC and DC power simultaneously from various sources, e.g. batteries, turbine generators, diesel engines, fly-wheels, capacitor banks, uninterruptible power supplies [33].

The NiPEC is designed to the reserved space concept. Early in the ship's design, relevant system components are co-located into predetermined compartment modules. Cables, circuit breakers, converters, and such complementary system components work in concert within these compartments to provide primary and back-up power to ship loads. del Águila Ferrandis et al. [4] explored the concept of source-to-load power delivery and provided a model and algorithm to ensure system flexibility and redundancy. The model used a four-corridor layout for a notional destroyer-sized vessel as seen in Fig. 1-1. Each of the corridors lies in a separate quadrant of a transverse cross-sectional view. Two of the corridors are positioned on the 2<sup>nd</sup> Deck, and the other two corridors are on the 4<sup>th</sup> Deck. The corridors closely mirror each other port-to-starboard across the ship's longitudinal center-line. Each corridor is separated into twelve modular compartments by the ship's watertight bulkheads, enabling each compartment to provide zonal power to the equipment within in its boundaries. Each load is connected in such a way that it is able to receive power from alternate compartments if its primary zonal compartment is disabled, thus providing a robust system architecture that increases the ship's survivability. This model serves as the ship-wide basis for assumptions made in this thesis.

A study by Cooke et al. [3] provided the design case for the NiPEC and compart-

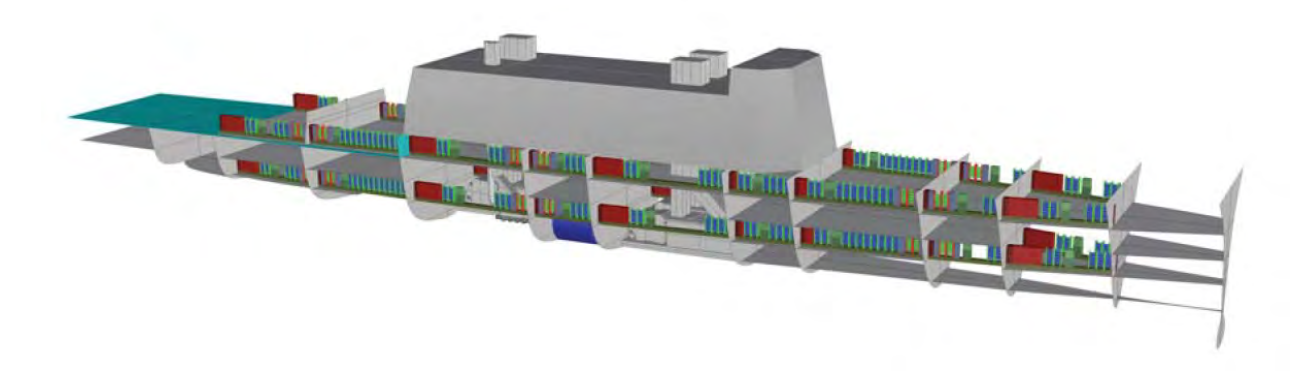


Figure 1-1: General view of the NiPEC in the notional ship [4].

ment modules. Each NiPEC is positioned and sized accordingly to avoid interference with the ship's girders and stiffeners. An example of such transverse placement is seen in Fig. 1-2.

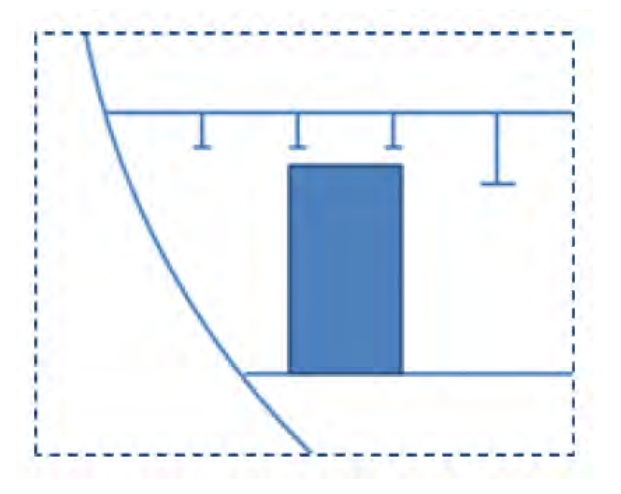


Figure 1-2: Sample power corridor and stiffener positioning; not to scale [3].

Each NiPEC is comprised of modular compartments that are longitudinally connected and run parallel to the ship's center-line. The dimensions and equipment layout of a notional NiPEC compartment module are seen in Fig. 1-3. All dimensions are displayed in inches, and an overview of the represented major components includes:

- Bus cable and conduit (magenta)
- Power converter stack (dark blue and brown)

- Interface junction box (orange)
- Energy storage (salmon)
- Circuit breaker or disconnect (teal)
- Bulkhead penetration (gray)

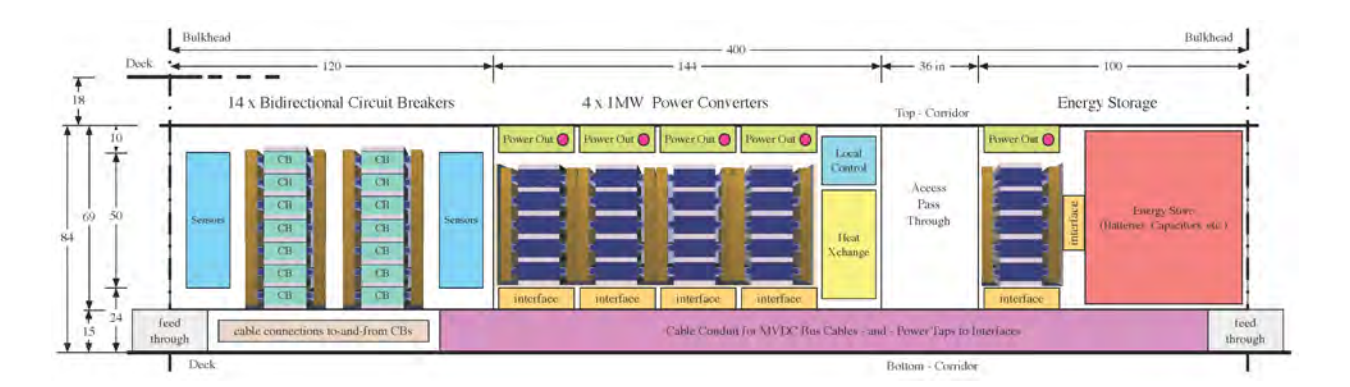


Figure 1-3: Notional NiPEC compartment module [3].

The compartment topography and assumptions made by Cooke et al. [3] serve as the baseline for the design iteration covered in this thesis.

#### 1.1.2 Navy integrated Power Electronics Building Block

The iPEBB uses Silicon-Carbide (SiC) semi-conductor technology to deliver efficient, power-dense solutions tailored to end-use needs. It possesses the inherent electrical inertia to provide stable and reliable energy to a wide array of dynamic loads. It surpasses the capabilities of traditional Silicon-based devices by achieving a higher breakdown voltage, faster switching speed, lower switching losses, and higher operating temperatures [35].

The iPEBB is designed as the least replaceable unit and the most common denominator. For example, instead of replacing individual components that make-up the converter, the entire unit would be removed and replaced. It streamlines maintenance and repair operations and minimizes system downtime. Its self-contained modular framework facilitates unit replacement through its physical construction and software control. The commonality between units mitigates the need to procure and store different parts while enabling and simplifying user training and familiarity. The current design iteration measures  $500 \ mm$  long,  $300 \ mm$  wide, and  $100 \ mm$  tall and weighs approximately  $35 \ lbs$ . The unit's dimensions and general internal layout are depicted in Fig. 1-4 and serve as the basis for designs covered in this thesis.

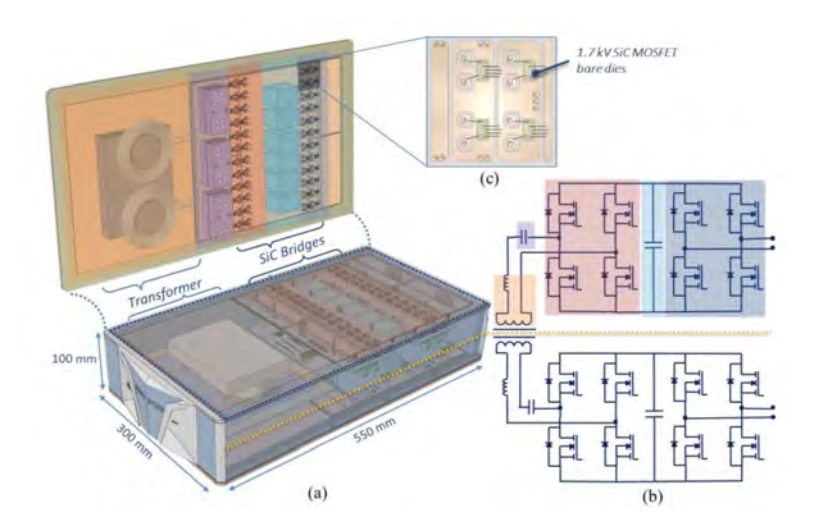


Figure 1-4: (a) iPEBB design with a top view of the primary side, (b) iPEBB topology, (c) switching-cell portion of the SiC H-bridges [35].

#### 1.2 Problem Statement

Electrical losses from the internals of the iPEBB generate heat that must be removed to prevent component damage and system degradation. The current design and analysis of the iPEBB assumes a heat load of approximately  $10\ kW$  and serves as the base assumption for this study. The heat is transmitted and spread through component substrates and the unit's baseplate to the top and bottom faces of the iPEBB. The amount of heat requiring removal is not extreme by current industry standards, but it is complicated by imposed design constraints. First, the iPEBB is prohibited from having any liquid cooling connections. This eliminates the possibility of direct cooling methods, which functionally have a greater thermal capacity. Second, the iPEBB must be compact, light-weight, and resilient to physical damage. This prevents the use of casing fins to dissipate heat to the air and surrounding environment. Third, the

unit's anchoring mechanism must interface with the casing's outer surface to secure the unit from static and dynamic forces. The cooling method and anchoring interface must develop an integrated design approach to prevent interference and promote synergistic operations. Lastly, the thermal management solution must conform to industry and military design standards.

#### 1.3 Base Assumptions

A four-corridor NiPEC system serves as the base model for assumptions made in this study. Each corridor is comprised of 12 compartments, with each compartment housing 20 iPEBBs. The 20 iPEBBS are distributed into five cabinets which are termed iPEBB stacks. Each iPEBB stack contains four iPEBBs stacked in vertical alignment.

The iPEBB mainly operates in two different load conditions. The first condition assumes an equal heat load distribution across all semi-conductor switches. The second condition assumes that half the switches produce 80% of the heat load and the other half 20% (80/20 condition). Assuming the iPEBB produces 10kW of heat and is designed with 96 switches, the maximum heat load per switch in each condition is 104W at even load and 167W for the 80/20 condition. Therefore, the 80/20 condition is the most thermally limiting situation and serves as the basis for cooling system assumptions and requirements [31].

#### 1.4 Exploration of Cooling Methods

An exploration of shipboard PEBB cooling strategies conducted by Yang et al. [40] discussed the limitations and requirements of traditional and emerging cooling methods for the PEBB 6000. The PEBB 6000 and iPEBB are of similar purpose and design, with the PEBB 6000 providing more robust power capabilities. Both PEBBs produce an approximate 10 kW of heat and share a similar topography, allowing parallel arguments to be made for the iPEBB based on the PEBB 6000 study. Fur-

thermore, the constraints and assumptions from the study are consistent with those made for the iPEBB. Therefore, the following assessment of cooling strategies is heavily influenced by Yang et al. [40].

#### 1.4.1 Air Cooling

Air cooling methods require no additional provisions after PEBB installation. No auxiliary pipes, connections, or other interface requires attachment for system operation. Notionally, heat would be removed by the convection of forced air over the top and/or bottom surfaces of the PEBB. Analysis was performed and showed that the number of cooling fins and PEBB casing material were significant factors that affected the thermal interface. Increasing the number of cooling fins and thermal conductivity of the cover material resulted in improved thermal diffusivity and heat transfer capacity. These conditions allowed the PEBB to achieve lower operating maximum temperatures.

The drawback to the effective use of this method requires a large mass flow rate of air and a substantial PEBB surface area. The air flow rate would necessitate a large fan, which in turn demands a large power requirement. Additionally, a larger fan, or system of fans, would increase the noise of the compartment and presents personnel safety concerns with regards to the produced decibel level. If the air were cooled prior to use, then the mass flow rate and surface area could correspondingly be reduced. This trade-off would require the use of a localized cooling system.

The mission area or operating theater of naval warships can vary along with the atmospheric conditions it experiences. The humidity and dew point of the surrounding environment risks compromising the PEBB if condensation is enabled or introduced via the air intake of the cooling system. The use of protective coatings to mitigate the issue could potentially reduce the PEBB's thermal performance. The use of an atmospheric conditioning system introduces complexity to a cooling strategy with simple design objectives.

The PEBB's cooling fins augment the size and increase the vulnerability of the unit, both of which infringe upon the goals of the PEBB's design basis. The in-

creased size, weight, and external surface would make transportation and handling difficult and likely exceed the desired limits of the design. Traditionally, cooling fins are constructed to maximize the effective surface area while occupying minimal volume. The design makes the cooling fins susceptible to physical damage due to their structural fragility. If damage occurs to the cooling fins, it introduces the possibility of reduced thermal performance. Given the operational commitments and environment of a naval warship, a more rugged design is better suited for PEBB life-cycle performance. Furthermore, the PEBB's larger volumetric footprint would effectively reduce the unit's power density and occupy more space within the NiPEC. More space occupied by fewer PEBBs reduces the electrical power capacity of the NiPEC and diminishes the available domain for other NiPEC system components.

#### 1.4.2 Direct Liquid Cooling

Direct cooling methods deliver liquid to each PEBB by connecting pipes or tubing from a source to individual units. Operationally this functions by inserting the PEBB into its location and then having an operator or system make-up the liquid connections. The strategy uses demineralized water or dielectric liquid to mitigate electrical conductivity between components. Non-conductive connectors provide electrical isolation to the remainder of the cooling system, and the use of no-leak disconnects protects components from potential liquid damage. This method was determined by [40] to be more effective at removing heat from the PEBB than the air cooling method. It had a higher heat transfer coefficient by an entire order of magnitude and utilized a significantly smaller heat transfer area.

The issues with this strategy are that it negates the constraint of direct cooling connections and places liquid in close proximity to electrical components. A leak, fluid contamination, or internal malfunction could result in catastrophic component or system damage. Corrosion and wear present significant risk factors requiring further consideration and analysis, and likely reduce the operational life-cycle of the PEBB. The PEBB's swapability is compromised by the direct connections, which requires considerable interaction by the user to manipulate. For example, if the liquid

connection is a threaded union, then the operation required for removal or installation of the PEBB is relatively more time-intensive and physically intricate than the idealized plug-and-play capability. Such operator dependencies deviate from the design goals and constraints of the iPEBB.

#### 1.4.3 Cold Plate Cooling

Cold plates are heat sinks with internal fluid channels that transfer heat away from the source. This cooling strategy is achieved by the conduction of heat through the in-contact, dry and solid surfaces of the PEBB and cold plate. This method requires no cooling connection to the PEBB, prevents liquid contact of electrical components, and is capable of providing some measure of electrical isolation from the PEBB. The drawback is the considerable contact resistance at the PEBB-to-cold plate interface. Debris, surface roughness, and contact pressure are significant factors that affect the interface conductance. [40] postulated the use of a thermally conductive interface pad to improve surface contact and promote the effective utilization of this cooling strategy. The thermal pad would be dependent on a secondary mechanical support system to provide adequate and uniform contact pressure across the interface surface area.

The heat capacitance of liquid-based cooling strategies surpasses air cooling methods. Although air cooling methods could provide the immediate thermal solution, they risk providing insufficient cooling to future iPEBB design iterations. Further justification in pursuing liquid-based cooling strategies is provided by the requirement in DOD-STD-1399 [6] that states when the temperature difference between the inlet and outlet of the cooling air exceeds 14 °C, liquid cooling methods shall be employed. Current convective air cooling performance estimations conducted by CPES show air cooling strategies exceeding this limit which necessitates the investigation of liquid-based cooling strategies. In their examination of PEBB cooling strategies, [40] concluded that direct liquid cooling slightly outperformed the cold plate cooling method from a purely thermal standpoint. However, as discussed, the direct liquid cooling strategy violates iPEBB design goals and presents the need to further examine

cold plate cooling strategies as a viable thermal solution.

#### 1.4.4 Advanced Methods

Other cooling strategies such as solid-state cooling, impinging jet, immersion cooling, electro-wetting, and liquid-metal heat exchangers could provide improved capabilities required of higher heat flux applications. However, these methods are typically more complex and can introduce greater vulnerability. [40] concluded that given the estimated heat output of the PEBB and capabilities of liquid-cooled strategies, further analysis of advanced methods would be unnecessary.

#### 1.5 Cooling System Architecture

The notional NiPEC cooling system is a closed-loop, pressurized, demineralized water cooling system. It is comprised of components required to ensure continuous flow and adequate cooling of the iPEBB architecture within the NiPEC compartment. Heat exchangers, pumps, water chemistry control instruments, pipes and fittings, expansion tanks, cold plates, and water filters are the major components to be assessed in meeting this goal. Cooling water flow, temperature, system pressure, and water purity monitoring and alarm equipment are support systems required for the safe and proper operation of the system.

Design standards and assumptions are based on DOD-STD-1399 [6], which provides the requirements for water cooling of shipboard electronic equipment. Demineralized water is the chosen NiPEC cooling system medium as it eliminates or lessens the risk of electrical conductivity between components and corrosion of equipment. The system water pressure must be within the operating range of 10 to  $110 \ lbs/in^2$  and be capable of withstanding a hydrostatic test pressure of  $150 \ lbs/in^2$ . Analysis and modeling assume an  $100 \ lbs/in^2$  system operating pressure to mitigate the risk of water contamination from support system leakage. The likely source of potential contamination would be from the secondary water of the heat exchanger. The heat exchanger's cooling water is required to be sourced from the ship's seawater or chilled

water systems. Therefore, the NiPEC cooling water system pressure must be greater than those systems to prevent the introduction of water in the event of a leak across the heat exchanger's fluid-to-fluid interface. If a leak were to occur, the secondary water would not meet NiPEC cooling water purity specifications and increase the conductivity and corrosive properties of the demineralized water. Additionally, the NiPEC cooling water system is a closed-loop design to aid in maintaining water chemistry, making effective use of system resources, and minimizing head losses incurred by an open system design.

#### 1.5.1 Heat Exchanger

The heat exchanger transfers heat between fluids via an interface that prevents direct contact and intermixing. The fluid being cooled in the heat exchanger is demineralized water, which provides cooling to the iPEBBs by means of a cold plate. Based on assumptions made by [31], 15 °C cold plate inlet water is required to provide adequate cooling to the iPEBB. Military design standards mandate that cooling water at or below 40 °C be cooled by the ship's chilled water system [6]. Therefore, the secondary fluid in the heat exchanger is chilled water. Chilled water passes through the heat exchanger, cooling the demineralized water, and deposits heat energy into the ship's surrounding water via the refrigerant system.

Heat exchangers used in Navy shipboard electronic cooling water systems are either plate-type or shell-and-tube coolers. Plate-type heat exchangers (PHE) are constructed of stacked and gasketed titanium sheets supported by a fixed chassis. Illustrated in Fig. 1-5, cold cooling water enters the heat exchanger at the bottom left inlet. As the cooling water flows towards the back of the heat exchanger, some flow is diverted up between the plates, alternating between plates. The cooling water flows up and returns to the outlet at the front face of the heat exchanger. The liquid being cooled follows a similar, but opposite flow path; its alternating intra-plate path is offset from the cooling liquid. Heat from the cooled liquid is transferred across the thin plates to the cooling liquid by convection and conduction.

Shell-and-tube heat exchangers are shell vessels that house numerous small tubes

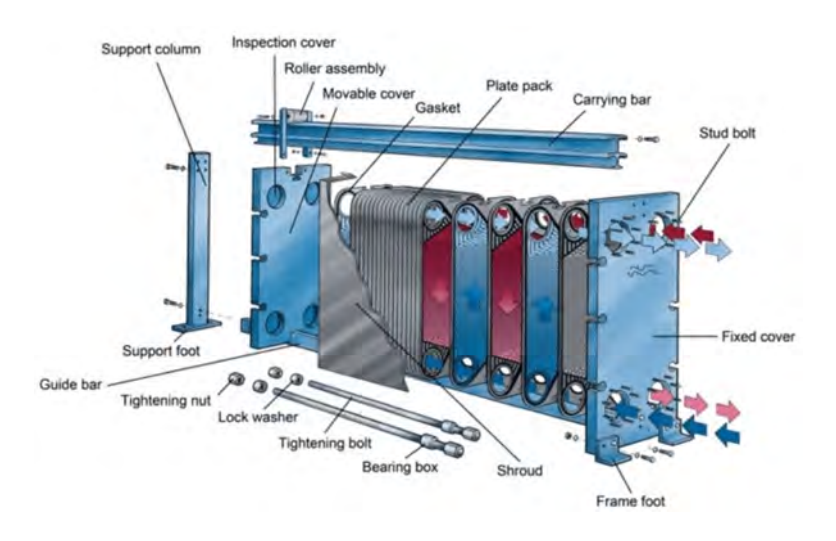


Figure 1-5: Plate Heat Exchanger [1].

oriented along the length of the structure and patterned symmetrically at the vessel's circular cross-section. Fluid flow relations exist between the fluid inside the tubes and the fluid outside the tubes. Different design flow arrangements exist depending on the equipment's application. The example of a two-pass parallel flow heat exchanger is shown in Fig. 1-6. Cooling water flows into the top half of tubes via the inlet plenum, accumulates at the end-bell, and exits the outlet plenum via the bottom set of tubes. The cooling water flow is referred to as tube-side flow. The water to be cooled enters the shell at one end of the heat exchanger, flows around the tubes and exits at the heat exchanger's other end. The cooled water flow is referred to as shell-side flow. Baffles typically exist on the shell-side of the heat exchanger so that a serpentine path exists to minimize stagnant flow and maximize heat transfer.

Shell-and-tube heat exchangers are considered for further analysis as they traditionally are capable of operating with higher system temperatures and pressures, produce a smaller pressure loss across the heat exchanger, enable easier leak identification and repair, require less complicated maintenance, and are less prone to physical damage.

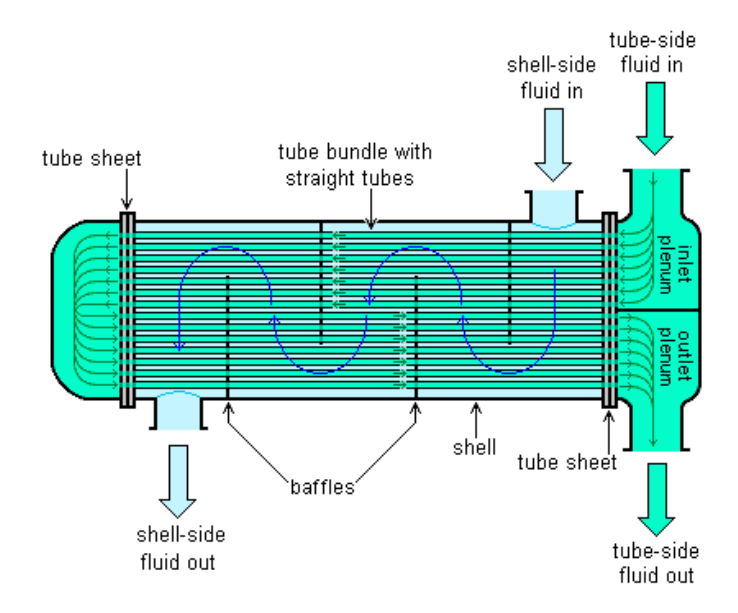


Figure 1-6: Straight-tube two-pass shell-and-tube heat exchanger [32].

#### 1.5.2 Pump

The pump component of the NiPEC cooling system provides the motive force for the cooling fluid to ensure continuous flow to the electronic components and through the system. Pumps used in Navy shipboard electronic cooling water systems are centrifugal pumps as they are more efficient at providing large amounts of flow to fluids at lower viscosities. They are typically simpler in design, more compact, and less difficult to maintain than positive displacement pumps. The centrifugal pump's design enables the operator to more readily adjust system flow and pressure characteristics. Therefore, further analysis of the NiPEC cooling system assumes the use of centrifugal pumps for system operations.

#### 1.5.3 Other System Components

The expansion tank is a closed-shell water reservoir that provides net positive suction head for the pump, supplies make-up water for system losses, and mitigates the thermal expansion and contraction of the cooling liquid.

The water chemistry control instruments maintain or enhance the cooling medium's purity by circulating the demineralized water through resin beds to extract corrosion

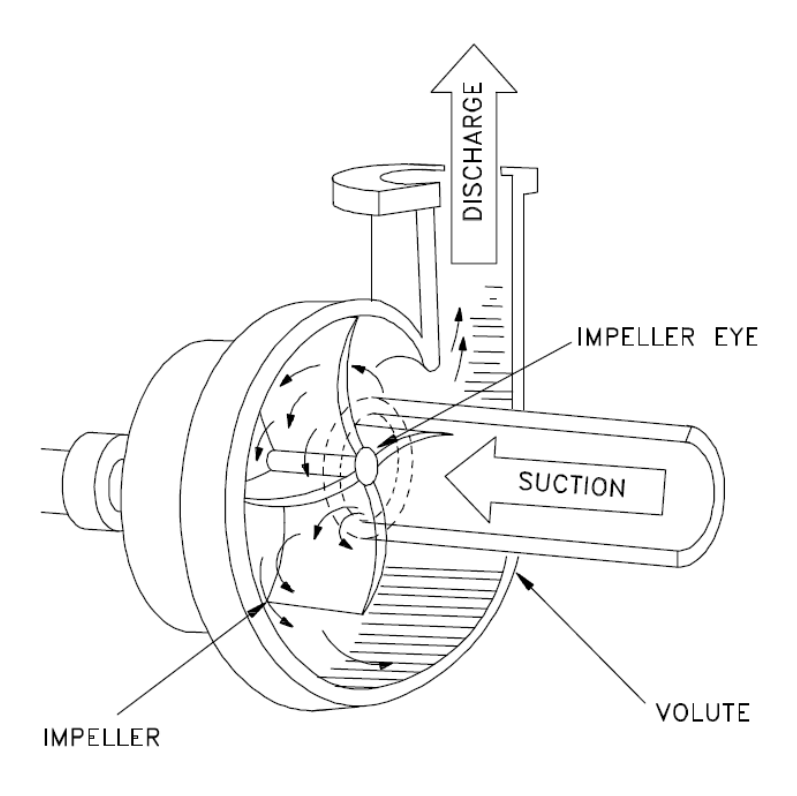


Figure 1-7: Centrifugal Pump [7]

inducing compounds and wear products. The demineralized water has all inorganic salts removed by ion exchange. A mixed-bed resin uses cations to convert dissolved salts within in the water into acid, which is subsequently removed and retained by the resin's anions.

Mechanical filters are used to extract particulate matter from the coolant to protect downstream components. Pump bearings and valve seats can be damaged from particulates due to impingement or interstitial friction between surfaces. Flow restrictions and system degradation can occur from particulates accumulating in bends, elbows, and fine passages of equipment.

Pipes, tubing, and fittings utilized in the NiPEC cooling system are made of copper alloy or stainless steel materials and use Normal Pipe Size (NPS) and Pipe Schedule (SCH) standards to define their dimensions. SCH 40 piping is assumed for all piping analyses conducted within this study. Flexible hoses utilized in the cooling system are made of rigid rubber to enable freedom of movement between components

and some measure electrical isolation protection.

The cold plate provides the interface by which heat is removed from the iPEBB and transferred to the demineralized cooling water. Each iPEBB is designed with top and bottom cold plates, as those surfaces are internally mounted with the heat-producing components and provide the greatest heat transfer area.

# Chapter 2

# Heat Exchanger

To develop a baseline assessment for the design characteristics of each cooling system component, direct calculations were performed and iterated to achieve the desired results. The design characteristics are based on the specifications of the iPEBBs, spatial constraints of the NiPEC, and governance set forth by technical authority.

#### 2.1 Heat Exchanger Theory

Determining the appropriate design criteria and geometries for the cooling system heat exchanger requires the calculation and iteration of heat transfer variables and their conformance to standards. The subsequent calculations follow the derivations of Serth [36] and Lienhard IV and Lienhard V [15]. A derivation of Fourier's Law, Eqn. 2.1, for multi-composite structures is the fundamental equation used to characterize the heat exchanger design.

Individual material heat transfer coefficients were calculated ahead of determining the overall heat transfer coefficient. The heat transfer coefficient for the heat exchanger cooling medium (i.e. chilled water) was determined by the following means at a temperature of 7°C:

$$\dot{Q} = UA\Delta T \tag{2.1}$$

where  $\dot{Q}$  is the rate of heat transfer (W), U is the overall heat transfer coefficient  $(\frac{W}{m^2-K})$ , A is the external surface area for the tube bundle  $(m^2)$ , and  $\Delta T$  is the log mean temperature difference (K).

Based on cold plate cooling assumptions for the NiPEC corridor system by Padilla et al. [31] and the requirements of DOD-STD-1399 [6], the fluid inside the heat exchanger tubes is assumed to be ship's chilled water at 7°C with the characteristics listed in Table 2.1. The Reynolds number determines the flow pattern of the fluid inside the heat exchanger tubes and is calculated using

$$Re = \frac{\rho v D_{ID}}{\mu} \tag{2.2}$$

where  $\rho$  is the density of the fluid  $(kg/m^3)$ , v is the mean flow velocity (m/s),  $D_{ID}$  is the internal diameter of the pipe (m) and  $\mu$  is the dynamic viscosity. In calculating the convective heat transfer of the chilled water flowing through the pipe, the Nusselt number was determined. The Gnielinski Correlation was used to calculate the Nusselt number. It is valid for the turbulent flow of liquid and forced convection in pipes within the following ranges:

$$0.5 \le Pr \le 2000$$
  
 $3000 \le Re \le 5E6$ 

$$Nu = \frac{\frac{f_D}{8}(Re - 1000)Pr}{1 + 12.7(\frac{f_D}{8})^{\frac{1}{2}}(Pr^{\frac{2}{3}} - 1)}$$
 (2.3)

where  $f_D$  is the Darcy Friction Factor and Pr is the Prandtl number. The Prandtl number, which is the ratio of dynamic viscosity to thermal diffusivity, is defined as

$$Pr = \frac{c_p \mu}{k} \tag{2.4}$$

where  $c_p$  is the specific heat capacity of water,  $\mu$  is the dynamic viscosity of water and k is the thermal conductivity of water. The Darcy Friction Factor,  $f_D$ , is calculated using the Petukhov approximation for smooth pipes and Reynolds values between

 $10^4 \le Re \le 10^5.$ 

$$f_D = (0.79 \ln(Re) - 1.64)^{-2} \tag{2.5}$$

The Nusselt number, the ratio of the convective to conductive heat transfer across a boundary, is defined as

$$Nu = \frac{h_{CW}}{k/D_{ID}} \tag{2.6}$$

where Nu is the Nusselt number,  $h_{CW}$  is the heat transfer coefficient for the chilled water  $(W/m^2K)$ , and  $D_{ID}$  is the internal diameter of the tube (m). Using Eqn. 2.6, the convective heat transfer for the chilled water inside the heat exchanger tubes was determined. The results for the calculated parameters are shown in Table 2.1.

Density	ρ	$kg/m^3$	999.86
Fluid Velocity	v	m/s	2.5
Internal Diameter	$D_{ID}$	in	0.305
Dynamic Viscosity	$\mu$	$N - s/m^2$	1.43-3
Reynolds number	Re	non-dim	13541.81
Specific Heat Capacity	$c_p$	J/kg - K	4200
Thermal Conductivity	k	W/m-K	0.574
Prandtl number	Pr	non-dim	10.46
Darcy Friction Factor	$f_D$	non-dim	0.029
Nusselt number	Nu	non-dim	122.09
Chilled Water Heat Transfer Coefficient	$h_{CW}$	$W/m^2 - K$	9046.37

Table 2.1: Chilled Water and Heat Exchanger Properties

In determining the convective heat transfer of the demineralized water flowing over the tubes, the Bell-Delaware method was utilized. It uses empirical correlations for shell-and-tube heat exchangers to calculate the heat transfer coefficient and friction factor for the flow on the shell-side of the heat exchanger passing perpendicular to the tubes. Perpendicular flow is achieved when the shell side fluid passes through the region between baffle tips. Deviations from the ideal tube bank condition are integrated using heat transfer and pressure drop correction factors. Bypass streams and leakage, such as parallel flow across baffle tips, are accounted for by flow area correlations. The following calculations use a version of the Bell-Delaware method for a one-pass shell (TEMA Type E), single-cut segmented baffles, and un-finned tubes Serth [36].

The Colburn Factor for heat transfer, j, is a dimensionless number that relates heat transfer, mass transfer, and friction factors, and can be expressed as

$$j = \frac{h_{DI}Pr^{\frac{2}{3}}}{c_PG\phi} \tag{2.7}$$

where  $h_{DI}$  is the ideal heat transfer coefficient for the demineralized water  $(W/m^2 - K)$ , Pr is the Prandtl number,  $c_P$  is the specific heat capacity (J/kg - K), G is the mass flux on the cross-flow area  $(kg/m^2 - s)$ , and  $\phi$  is the viscosity correction factor. The mass flux on the cross-flow area was determined using Eqn. 2.8 and expected chilled water system conditions. Assuming a NiPEC system with four ship corridors, as discussed in Section 1.1.1, each corridor would be provided chilled water by a dedicated chilled water pump. With four designed corridors, it would require the ship to maintain 4 online chilled water pumps. Each pump was assumed to provide 600 gpm at 100  $lbf/in^2$  to each quadrant of the ship. 60 gpm of the 600 gpm would be used for loads not associated with the NiPEC cooling system, and the remaining 540 gpm would be divided equally among the 12 compartments of their respective corridor. At 45 gpm, each compartment's heat exchanger would receive a chilled water mass flow rate of 2.839 kg/s.

$$G = \frac{\dot{m}}{Sm} \tag{2.8}$$

where G is the mass flux of the cross-flow area  $(kg/m^2 - s)$ ,  $\dot{m}$  is the mass flow rate (kg/s), and Sm is the cross-flow area of the region between baffle tips. The viscosity correction factor was calculated by the following means:

$$\phi = \left(\frac{\mu}{\mu_W}\right)^{0.14} \tag{2.9}$$

where  $\mu$  is the dynamic viscosity of the demineralized water  $(N-s/m^2)$  and  $\mu_W$  is the dynamic viscosity at the average temperature of the tube wall  $(N-s/m^2)$ . The

average tube wall temperature is calculated using the following equation:

$$T_w = \frac{h_{DI}t_{ave} + h_{CW}(D_{ID}/D_{OD})T_{AVE}}{h_{DI} + h_{CW}(D_{ID}/D_{OD})}$$
(2.10)

where  $T_w$  is the average tube wall temperature (C),  $t_{ave}$  is the average temperature of the chilled water (C),  $T_{AVE}$  is the average temperature of the demineralized water (C), and  $D_{OD}$  is the outside diameter of the tube (m). Initial calculations for  $\phi$  assume a value of 1 until values for conductive heat transfer are determined by follow-on calculations.

The Colburn Factor, j, is calculated using

$$j = a_1 \left(\frac{1.33}{P_T/D_{OD}}\right)^a Re_{OD}^{a_2} \tag{2.11}$$

where  $P_T$  is the tube pitch (m) assumed to be 0.5 in from MIL-DTL-15730 [17] and  $Re_{OD}$  is the Reynolds number for flow on the outside of the tubes calculated by

$$Re_{OD} = \frac{D_{OD}G}{\mu_{DI}} \tag{2.12}$$

All a constants are listed in Table 2.2 and are derived from Fig. 2-1.

$$a = \left(\frac{a_3}{1 + 0.14(Re)^{a_4}}\right) \tag{2.13}$$

Table 2.2: Specific constants for ideal tube bank correlations

Tube Layout Angle	~ -	_	$a_2$	$a_3$	$a_4$
90°	$10^5 - 10^4$	0.370	-0.395	1.187	0.370

A square tube pitch formation was selected based on the criteria from MIL-DTL-15730 [17]. An alternative method for deriving ideal tube bank correlations, such as the Colburn factor, is by using the charts found in Appendix E for various tube pitch formations.

After calculating the ideal shell side heat transfer coefficient  $h_{CW}$ , flow correction factors are incorporated by

Layout angle	Reynolds number	a <sub>1</sub>	a <sub>2</sub>	a <sub>3</sub>	a <sub>4</sub>	b <sub>1</sub>	b <sub>2</sub>	b <sub>3</sub>	b <sub>4</sub>
30°	10 <sup>5</sup> -10 <sup>4</sup>	0.321	-0.388	1.450	0.519	0.372	-0.123	7.00	0.500
	10 <sup>4</sup> -10 <sup>3</sup>	0.321	-0.388		i a	0.486	-0.152		
	10 <sup>3</sup> -10 <sup>2</sup>	0.593	-0.477			4.570	-0.476		
	10 <sup>2</sup> –10	1.360	-0.657			45.100	-0.973		
	<10	1.400	-0.667			48.000	-1.000		
45°	10 <sup>5</sup> -10 <sup>4</sup>	0.370	-0.396	1,930	0.500	0.303	-0.126	6.59	0.520
	10 <sup>4</sup> -10 <sup>3</sup>	0.370	-0.396			0.333	-0.136		
	10 <sup>3</sup> -10 <sup>2</sup>	0.730	-0.500	1	1	3.500	-0.476		
	10 <sup>2</sup> -10	0.498	-0.656		11.11	26.200	-0.913		
	<10	1.550	-0.667	1		32.000	-1.000		
90°	10 <sup>5</sup> -10 <sup>4</sup>	0.370	-0.395	1.187	0.370	0.391	-0.148	6.30	0.378
	10 <sup>4</sup> -10 <sup>3</sup>	0.107	-0.266	11	1 1 4 4	0.0815	+0.022		
	10 <sup>3</sup> -10 <sup>2</sup>	0.408	-0.460			6.0900	-0.602		
	10 <sup>2</sup> –10	0.900	-0.631		1-	32.1000	-0.963		
	10	0.970	-0.667			35.0000	-1.000		

Figure 2-1: Constants for ideal tube bank correlations

$$h_{DIcorr} = h_{DI}J_CJ_LJ_BJ_RJ_S (2.14)$$

where  $h_{DIcorr}$  is the corrected heat transfer coefficient for the demineralized water  $(W/m^2 - K)$ ,  $J_C$  is the correction factor for baffle window flow,  $J_L$  is the correction factor for baffle leakage effects,  $J_B$  is the correction factor for bundle bypass effects,  $J_R$  is the laminar flow correction factor, and  $J_S$  is the correction factor for unequal baffle spacing. Practical estimates provided by [36] were used for calculating  $h_{DIcorr}$ .

Using the methodology of [31], expected demineralized water temperatures were derived and the 80/20 condition, discussed in Section 1.1.1, was determined to be the most thermally limiting situation. The follow-on calculations differ in that the number of semi-conductors internal to the iPEBB has increased in the latest design iteration from 72 to 96. Using the following equation, the temperature rise from semi-conductor to cooling liquid is determined:

$$\dot{Q} = \Delta T_{Net} / R_{Tot} \tag{2.15}$$

where  $\Delta T_{Net}$  is the temperature difference between the semi-conductor switch and cooling water (K) and  $R_{Tot}$  is the total thermal resistance from the semi-conductor

switch to cooling water (K/W).

Using the  $R_{Tot}$  calculated by [31] of 0.6064 K/W and a  $\dot{Q}$  of 167 W per semi-conductor, the  $\Delta T_{Net}$  is 101.3 °C. The maximum component temperature to prevent damage to the iPEBB semi-conductors is 180 °C. Using a 30 °C safety margin criteria established by [31], a 150 °C upper-temperature limit is defined. Using the calculated  $\Delta T_{Net}$  and 150 °C limit, the maximum permissible coolant temperature passing through the cold plate is 48 °C. Furthermore, the expected coolant temperature difference across the cold plate is assumed to be 2 °C based on the requirements of DOD-STD-1399 [6]. Therefore, a maximum cold plate coolant inlet temperature of 46 °C is assumed for the heat exchanger's demineralized coolant outlet temperature.

The demineralized water's thermal properties at 46 °C are used in the following calculations and are listed in Table 2.3. A heat exchanger with an internal shell diameter of 8 in and a baffle spacing of 4 in was assumed for initial calculations based on commercially comparable geometries for capable thermal loads.

Dynamic Viscosity	$\mu$	$N-s/m^2$	5.866E-4
Specific Heat Capacity	$c_p$	J/kg - K	4180
Thermal Conductivity	k	W/m-K	0.639
Prandtl number	Pr	non-dim	5.22
Mass Flow	$\dot{m}$	kg/s	20.98
Cross-Flow Area	Sm	$m^2$	0.0206
Mass Flux	G	$kg/m^2 - s$	137.5
Colburn Factor	j	non-dim	0.01758
DI Water Heat Transfer Coefficient	$h_{DI}$	$W/m^2 - K$	4122.58

Table 2.3: Demineralized Water and Heat Exchanger Properties

Applying the definition of the Overall Heat Transfer Coefficient from [15], Eqn. 2.1 is rewritten:

 $h_{DIcorr}$ 

Corrected Heat Transfer Coefficient

$$U = \frac{\dot{Q}}{A\Delta T} = \frac{1}{\frac{1}{h_{CW}} + \frac{L}{k} + \frac{1}{h_{DI}}}$$
 (2.16)

 $W/m^2-K$ 

1681.70

where U is the overall heat transfer coefficient  $(\frac{W}{m^2-K})$ , A is the external surface area for the tube bundle  $(m^2)$ ,  $\Delta T$  is the log mean temperature difference (K), L

is the thickness of the tube (m), k is the thermal conductivity of the tube material (W/m-K). Per [17], the tubes are assumed to have an outside diameter of 0.375 in, a wall thickness of 0.035 in, and a thermal conductivity for CuNi 90/10. A fouling resistance is incorporated into the calculation as required by [36].  $\dot{Q}$  is determined to be 240 kW based on the heat load of the 20 iPEBBs in the NiPEC compartment with a 20-percent margin of safety. The log mean temperature difference is calculated by

$$\Delta T = \frac{(T_{hin} - T_{cout}) - (T_{hout} - T_{cin})}{\ln\left(\frac{T_{hin} - T_{cout}}{T_{hout} - T_{cin}}\right)}$$
(2.17)

where  $T_{hin}$  is the demineralized water temperature entering the heat exchanger (°C),  $T_{hout}$  is the demineralized water temperature leaving the heat exchanger (°C),  $T_{cin}$  is the chilled water temperature entering the heat exchanger (°C), and  $T_{cout}$  is the chilled water temperature leaving the heat exchanger (°C).  $T_{hout}$  is 46 °C based on maximum semi-conductor temperatures,  $T_{hin}$  is 44 °C based on a maximum 2 °C  $\Delta T$ ,  $T_{cin}$  is 7 °C based on expected chilled water system temperatures, and  $T_{cout}$  is 27 °C.  $T_{cout}$  was calculated using the expected thermal heat load of the 20 iPEBBs, a 45 gpm flow rate, and the thermal properties of the chilled water. Assuming that each of the 20 iPEBBS is emitting 10 kW of heat, and incorporating a 20% safety margin, the total heat load for the cooling system is 240 kW. Utilizing Eqn. 2.1 and previously derived factors, the required heat exchanger shell-side tube surface area is  $7.42 m^2$ , as shown in Table 2.4.

Table 2.4: Heat Exchanger Characteristics

Heat Transfer	$\dot{Q}$	kW	240
Log Mean Temperature Difference	$\Delta T$	C	26.93
Tube Thickness	L	in	0.035
Thermal Conductivity of Tube	k	W/m-K	40
Chilled Water Heat Transfer Coefficient	$h_{CW}$	$W/m^2 - K$	9046.37
Corrected DI Water Heat Transfer Coefficient	$h_{DIcorr}$	$W/m^2 - K$	1681.70
Fouling Resistance Coefficient	$R_f$	$hrft^2F/Btu$	0.0005
Overall Heat Transfer coefficient	$h_{CWcorr}$	$W/m^2 - K$	1226.22
Tube Surface Area	A	$m^2$	7.42

## 2.2 Heat Exchanger Design Criteria and Modeling

Heat exchanger construction must abide by the design constraints set forth by [17] and the industry specifications (*i.e.* ASTM, ASME, SAE) it incorporates. Any specifications or restrictions described in this section are derived from [17] unless otherwise stated. Given the heat exchanger's purpose and defined fluid, it is classified as a Type I Class 5 cooler. Type I is a shell-and-tube design, with the cooling water circulated through the tubes and the cooled water passing through the shell region. Class 5 is the designation for fresh water cooled surface ship applications.

During material procurement, mercury, cadmium, magnesium, asbestos, and carcinogenic materials shall not be selected for use in the manufacturing, testing, or servicing of the heat exchanger. The restrictions apply to the listed material's compounds and alloys as well. Personnel and equipment may suffer deleterious effects if the listed materials are implemented into the heat exchanger's design or processing. The primary materials permitted for use in the heat exchanger's design and construction are copper alloys, nickel alloys, aluminum alloys, bronze, and tin. A tabulated list of materials and applicable documentation are listed in Fig. 2-2. Alternative construction materials specifically permitted for Type I Class 5 heat exchangers are listed in Fig. 2-3. Material selection should consider the compatibility of interfacing components [28] and the structural properties to meet the requirements of shock testing [22] and ships motion [5] not covered by this study. Copper-nickel and bronze alloys are recommended based on their compatibility and material properties discussed in later chapters.

Two-pass and Four-pass demineralized water heat exchangers were modeled using SOLIDWORKS and its supplemental Flow Simulation software. Cooler geometry and arrangement are based on the assumptions and calculations performed in Section 2.1. The two-pass heat exchanger's length was determined to be 76 in based on the calculated tube surface area, assumed tube circumference, and heat exchanger water-box heads having the same radius of curvature as the main body. The requirement for waterbox head depth is that it shall not be less than 0.5D for a single-pass heat

Part	Material	Applicable document
Shells	Copper-nickel alloy	MIL-C-15726
	Tubing, copper-nickel alloy	MIL-T-16420
	Copper-nickel alloy, alloy C70600 or C71500	ASTM B171/B171M
	Copper-nickel alloy, alloy C70600 or C71500, temper 08035	ASTM B151/B151M
	Copper-aluminum alloy, copper alloy C61400	QQ-C-450
	Bronze, tin, sand castings, alloy C90500 or C92200	ASTM B584
	Bronze, nickel-aluminum casting	MIL-B-24480
Waterboxes	Copper-nickel alloy	MIL-C-15726
	Tubing, copper-nickel alloy	MIL-T-16420
	Copper-nickel alloy	ASTM B369/B369M
	Bronze, nickel-aluminum casting	MIL-B-24480
	Aluminum bronze, alloy C95400 as cast, or alloy C95200	ASTM B148
	Bronze, tin, sand castings, alloy C90500 or C92200	ASTM B584
Tubesheets	Copper-nickel alloy	MIL-C-15726
	Nickel-aluminum, bronze, alloy C63000	ASTM B171/B171M
	Aluminum bronze, nickel-aluminum, alloy C61400	ASTM B171/B171M
Tubes	Copper-nickel alloy, composition 90-10	MIL-T-15005
		MIL-T-22214
Gland rings and lantern rings	Bronze, tin, centrifugal castings, alloy C90300 or C92200	ASTM B271/B271M
	Bronze, tin, sand castings, alloy C90300 or C92200	ASTM B584
	Copper-nickel alloy	MIL-C-15726
Baffles	Copper-nickel alloy	MIL-C-15726
Spacers	Copper-nickel alloy	MIL-T-15005
		MIL-T-16420
Spacer rods and spacer rod nuts	Copper-nickel alloy	MIL-C-15726
Bolts, studs, and nuts	Nickel-copper, grade 400 or 405	MIL-DTL-1222
	Nickel-copper-aluminum, grade 500	
Jackscrews	Copper-aluminum alloy, copper alloy C61400	ASTM B150/B150M
	Phosphor bronze C51000, C54000, or C52400	ASTM B139/B139M
	Copper-silicon alloy C66100	ASTM B98/B98M
Flat gaskets	Rubber, synthetic, class 1, grade 80	MIL-PRF-6855
	Rubber, synthetic, type II, class 5	MIL-PRF-1149
Washer	Copper-aluminum alloy, copper alloy C61400	ASTM B150/B150M
		ASTM B169/B169M
		QQ-C-450
Plugs and adapters	Copper-nickel alloy	MIL-C-15726
Caralla again	Copper-nickel alloy, alloy C71500, temper 0S035	ASTM B122/B122M
Packing rings	Rubber, synthetic, type II, class 5	MIL-PRF-1149
O-ring gaskets	Rubber, synthetic, type I	MIL-G-21610
an and Francisco	Rubber synthetic	SAE AMS7276
		SAE AMS7259
		SAE AMS-P-83461

Figure 2-2: Heat Exchanger Construction Materials

Part	Material	Applicable document
Waterboxes	Aluminum-bronze, alloy C95400 as cast, or alloy C95200	ASTM B148
Tubesheets	Copper-aluminum alloy, copper alloy C61300	QQ-C-450
	Aluminum bronze D, copper alloy C61400	ASTM B171/B171M
Tubes	Copper-nickel alloy, composition 90-10	MIL-T-15005
		MIL-T-22214

Figure 2-3: Alternative Heat Exchanger Construction Materials

exchanger, 0.345D for a two-pass heat exchanger, and 0.25D pass for a four-pass heat exchanger; where D is the shell diameter for the heat exchanger. A summary of the heat exchanger geometries are listed in Table 2.5.

Table 2.5: Two-pass heat exchanger model geometries and arrangement

Geometry	Value	Unit
Waterbox head depth	4	in each
Exposed tube length	66	in
Tube sheet thickness	1	in each
Overall heat exchanger length	76	in
Heat exchanger internal shell radius	8	in
Tube spacing (centerline-to-centerline)	0.5	in
Tube sheet thickness	1	in
Total number of tubes	148	non-dim
Number of inlet tubes	74	non-dim
Baffle thickness	0.125	in
Baffle spacing	4	in

The exposed tube length of 66 in was calculated based on the required surface area of  $7.42 m^2$ , the number of first-pass tubes that could be accommodated on the tube sheet face, and the outside circumference of the 3/8 in tube. Tube outside diameters and wall thickness are limited to those listed in Table 2.6. The tube size restriction is based on preventing tube cracking, erosion-corrosion, flow-induced vibrations, and damage from external vibrations and shock. The tube sheet design assumed the use of inlet-end flared tubes. The tube sheet thickness was not to be less than the depth of expansion, plus the depth of flare, plus 1/8 in; 0.5 in and 0.376 in respectively for a 3/8 in tube. The tube sheet wall thickness calculation is less limiting when using non-flared tubes or for the inner tube sheets of double tube sheet design heat

exchangers. Values for other diameter tubes are found in Table 2.7. A U-tube design heat exchanger was not chosen due to the complexity of maintenance. A U-tube design requires the tube bundle to be removable and have a floating tube sheet for its back-end support. A straight tube design can have a fixed tube sheet and perform maintenance without the removal of the tube sheet. In regards to the heat exchanger's baffles, alternating top and bottom semi-circle baffles rising up to the heat exchanger's centerline were used in the design. The baffles must have a thickness not less than 1/8 in and a spacing in accordance with Table 2.8. If the maximum unsupported tube span for 3/8 in tubes is 30 in then the spacing between baffles shall not be more than 15 in. Lastly, a difference between the tube hole diameter in the baffles and the outside diameter of the tube must be greater than 1/64 in.

Table 2.6: Required tube outside diameter and thickness

Outside Diameter (in)	Minimum Tube Wall Thickness (in)					
5/8	0.049					
1/2	0.049					
3/8	0.035					

Table 2.7: Tube Design Criteria

Tube outside diameter $(in)$	Minimum depth of tube expansion $(in)$	Depth of flare (in)	Tube spacing $(in)$
5/8	5/8	1/2	13/16
1/2	5/8	3/8	21/32
3/8	1/2	5/16	1/2

Table 2.8: Maximum Unsupported Tube Spans

Outside Diameter $(in)$	Maximum Unsupported Tube Spans (in)
5/8	45
1/2	38
3/8	30

The heat exchanger must meet the following flow and heat transfer characteristics. The allowable pressure drops across the heat exchanger for both the cooling and cooled fluid must not exceed  $6 lbf/in^2$ . Cooling water velocities for the chilled water shall not exceed 9 ft/s through the heat exchanger tubes and 11 ft/s through the

heat exchanger inlet piping. Assuming a 45 gpm chilled water flow rate, a limit of  $11 \ ft/s$ , and the continuity equation for mass, a 1.5 in pipe diameter was chosen for the chilled water inlet and outlet piping. Using the same equation and similar assumptions, an expected tube velocity of 2.67 ft/s for  $3/8 \ in$  tubes. Cooling water inlet temperatures for large surface ship heat exchangers utilizing fresh water shall not exceed 95°F. The 95°F criteria is met using the assumptions derived in the previous section for calculating the log mean temperature difference. Heat transfer surfaces for fresh water coolers shall incorporate a fouling coefficient of 0.0005  $(hr \ ft \ F/BTU)$  into the design heat transfer coefficient. The factor was incorporated into the calculation for the overall heat transfer coefficient.

### 2.2.1 Two-pass Heat Exchanger Model

A model was constructed, and a fluid simulation was performed on the two-pass heat exchanger. The simulation assumed a chilled water inlet pressure of  $100 \ lbf/in^2$  and a mass flow rate of  $2.893 \ kg/s$ , or  $45 \ gpm$  at  $27 \ ^{\circ}C$ . Fig. 2-4 and 2-5 show the flow trajectories and pressure and velocity ranges across the model.

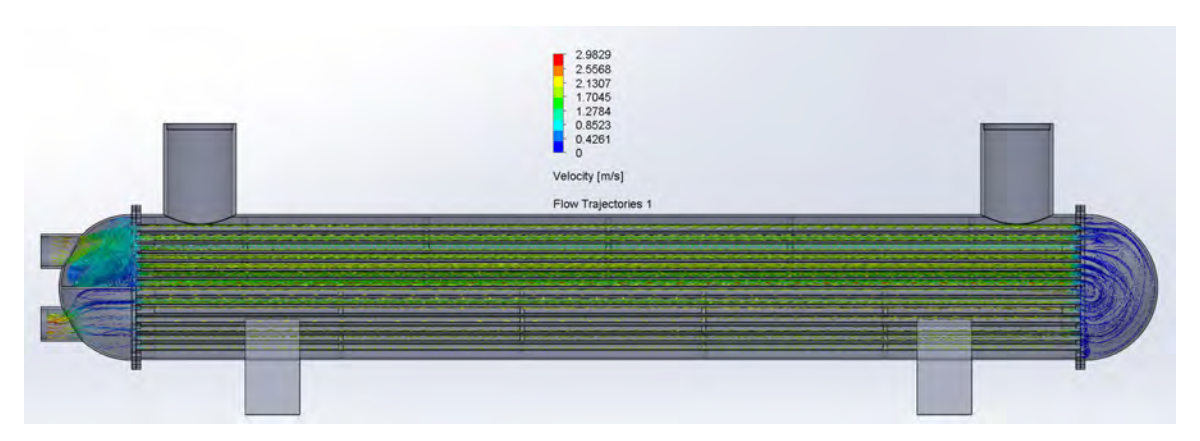


Figure 2-4: Two-pass heat exchanger chilled water flow velocities

Neither the 11 ft/s (3.3528 m/s) for the chilled water inlet piping or the 9 ft/s (2.7432 m/s) for the tubes is expected to be exceeded. Additionally, flow trajectories do not create vortices that impede the flow path.

A pressure drop of approximately (11.7371  $lbf/in^2$ ) is calculated and does not meet the required design criteria of (6  $lbf/in^2$ ). Follow-on designs that optimize the

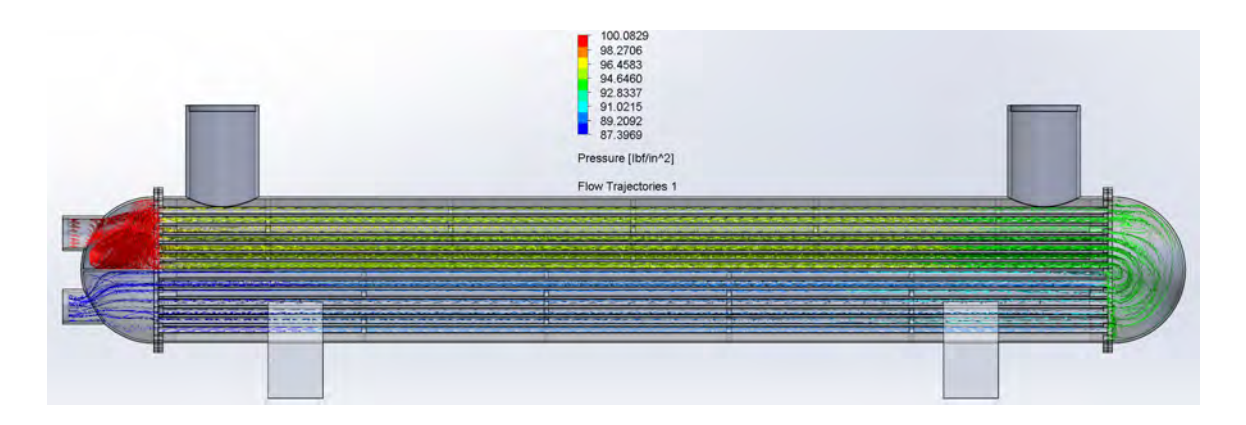


Figure 2-5: Two-pass heat exchanger chilled water flow pressures

heat exchanger's performance should investigate increasing the tube diameter and minimizing the number of passes to resolve the pressure drop issue.

A second simulation was performed for the demineralized water portion of the heat exchanger. The simulation assumed an inlet pressure of  $100 \ lbf/in^2$  and a mass flow rate of  $20.9829 \ kg/s$ , or  $336 \ gpm$  at  $46 \ ^{\circ}C$ . Fig. 2-6 and 2-7 show the flow trajectories and pressure and velocity ranges across the model.

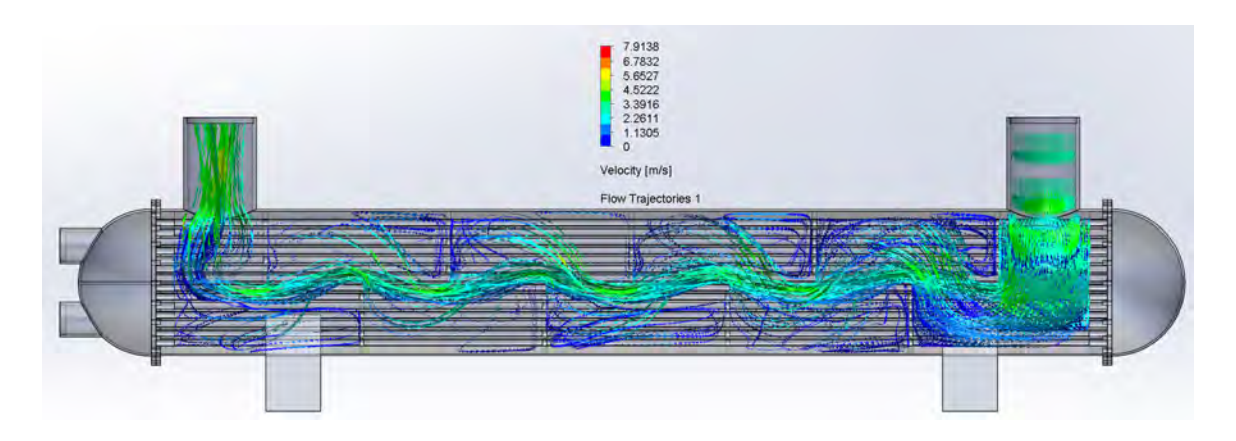


Figure 2-6: Two-pass heat exchanger demineralized water flow velocities

The flow velocities are projected to marginally be within the safe limits for the heat exchanger's internal components. A limit of  $3.5 \ m/s$  is derived given the heat exchanger's diameter and material selection of copper-nickel. Increasing the heat exchanger's diameter can provide an additional buffer to operate safely within the velocity limits.

A pressure drop of approximately  $(29.5810 \ lbf/in^2)$  is calculated and does not

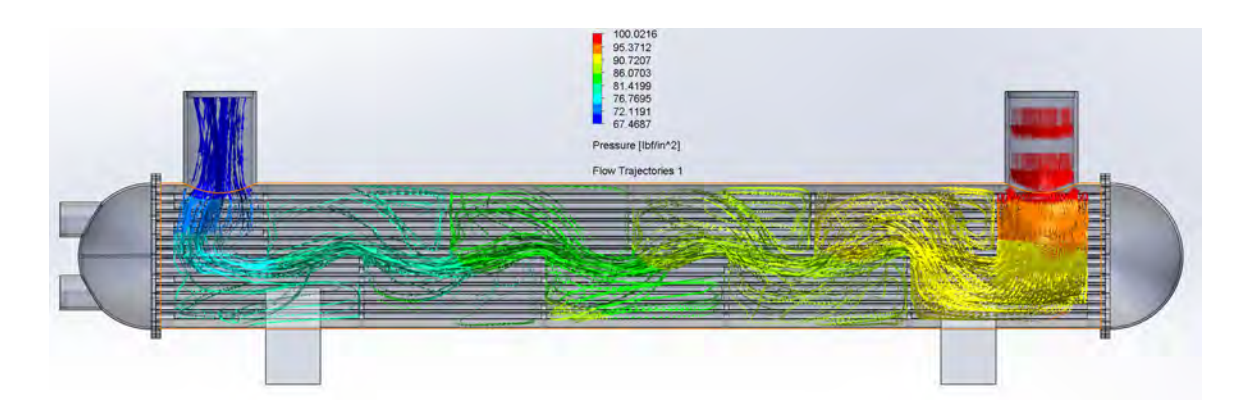


Figure 2-7: Two-pass heat exchanger demineralized water flow pressures

meet the required design criteria of  $(6 lbf/in^2)$ . Follow-on designs that optimize the heat exchanger's performance should investigate increasing the baffle spacing, reducing the baffle cross-sectional area, and increasing the tube spacing to resolve the pressure drop issue.

### 2.2.2 Four-pass Heat Exchanger Model

The four-pass heat exchanger was modeled with the characteristics in Table 2.9. The internal shell diameter, number of tubes, tube diameter, and effective tube length remained consistent to achieve the required tube surface area. The tube and baffle spacing were increased to lower the demineralized water pressure drop across the heat exchanger.

Table 2.9: Four-pass heat exchanger model geometries and arrangement

Geometry	Value	Unit
Waterbox head depth	7	in each
Exposed tube length	50	in
Tube sheet thickness	1	in each
Overall heat exchanger length	66	in
Heat exchanger internal shell radius	7	in
Tube spacing (centerline-to-centerline)	0.65	in
Tube sheet thickness	1	in
Total number of tubes	296	non-dim
Number of inlet tubes	74	non-dim
Baffle thickness	0.125	in
Baffle spacing	6	in

The fluid simulation was performed on the four-pass heat exchanger using the same chilled water flow assumptions as the two-pass simulation. Fig. 2-8 and 2-9 show the flow trajectories and pressure and velocity ranges across the model.

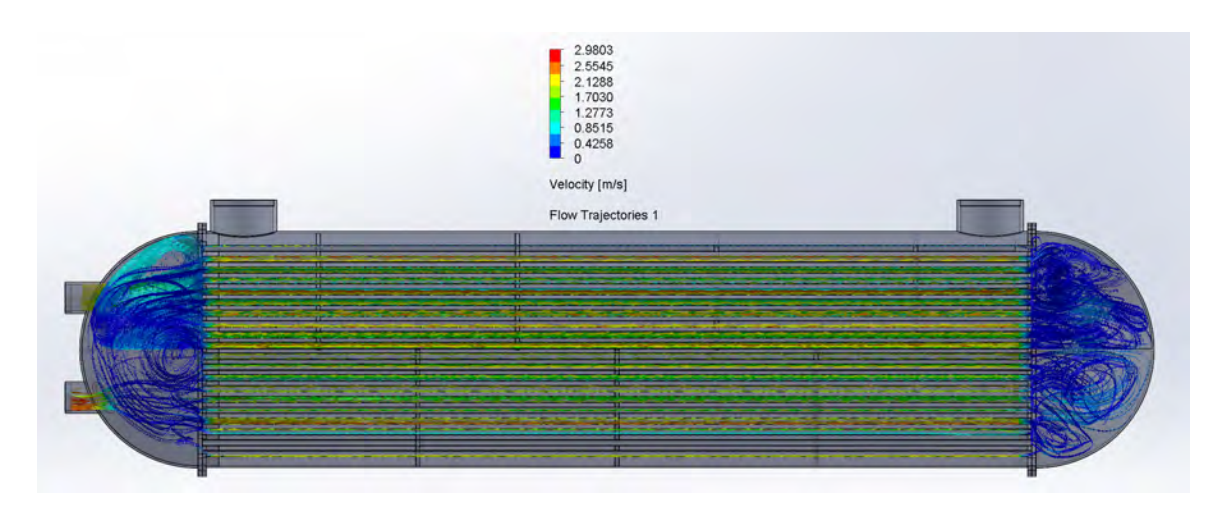


Figure 2-8: Four-pass heat exchanger chilled water flow velocities

Neither the 11 ft/s (3.3528 m/s) for the chilled water inlet piping or the 9 ft/s (2.7432 m/s) for the tubes is expected to be exceeded. Additionally, flow trajectories do not create vortices that impede the flow path.

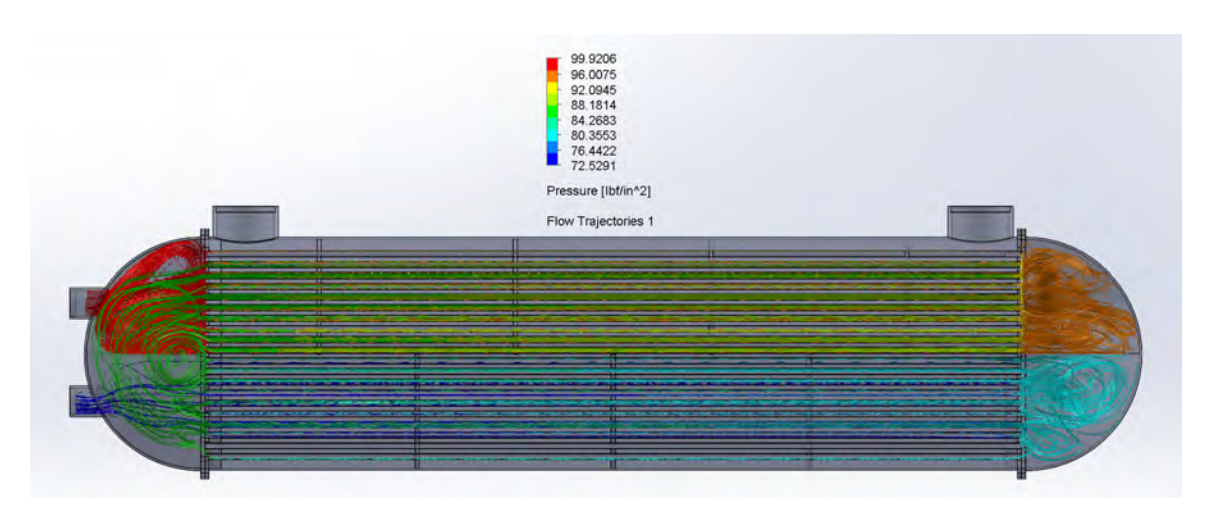


Figure 2-9: Four-pass heat exchanger chilled water flow pressures

A pressure drop of approximately  $(27.39 \ lbf/in^2)$  is calculated and does not meet the required design criteria of  $(6 \ lbf/in^2)$ . A larger chilled water pressure drop across the heat exchanger was expected due to increasing the number of passes, but was explored to observe the magnitude of change. The pressure drop increased by a factor of 2.33 from the two-pass model given that the number of passes doubled.

A second fluid simulation was performed on the four-pass heat exchanger using the same chilled water flow assumptions as the two-pass simulation. Fig. 2-10 and 2-11 show the flow trajectories and pressure and velocity ranges across the model.

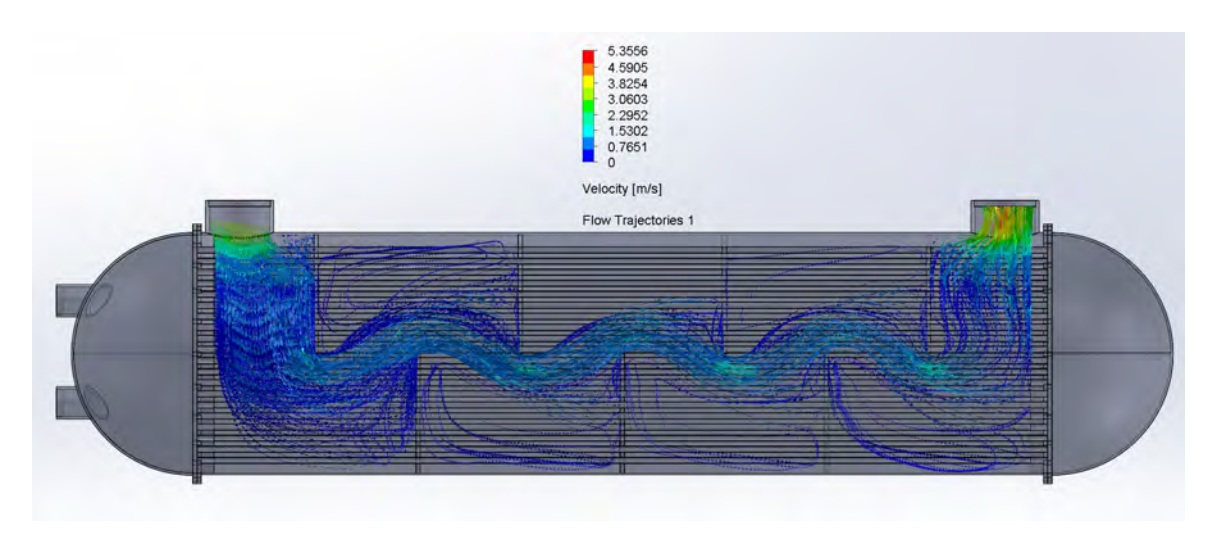


Figure 2-10: Four-pass heat exchanger demineralized water flow velocities

The flow velocities are projected to be well within the safe limits for the heat exchanger's internal components, but of sufficient magnitude to minimize the probability of biological surface fouling.

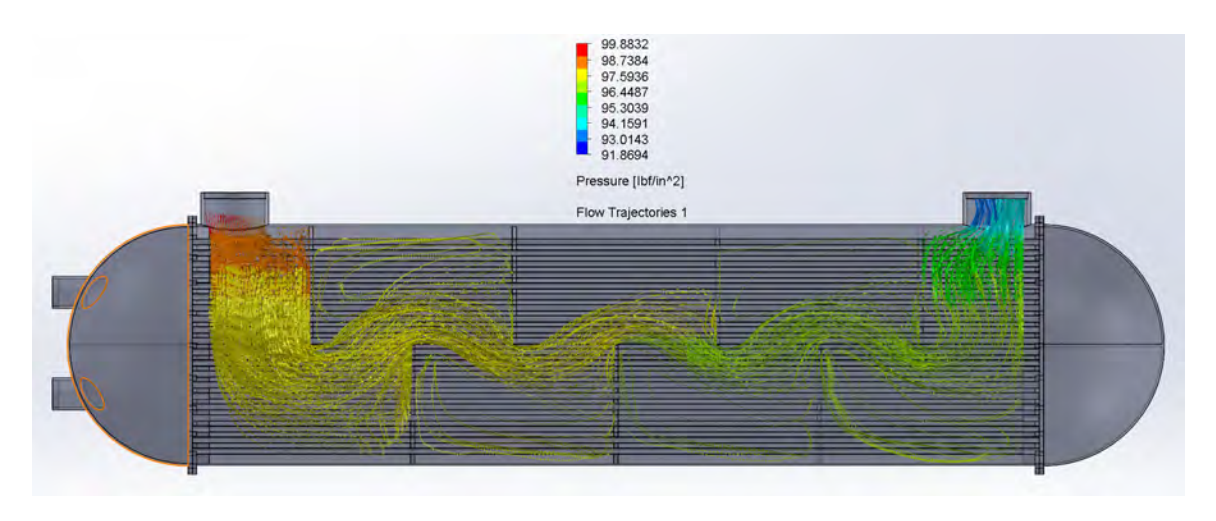


Figure 2-11: Four-pass heat exchanger demineralized water flow pressures

A global pressure drop of approximately  $(5.5323 \ lbf/in^2)$  is calculated and meets

the required design criteria of  $(6 lbf/in^2)$ .

### 2.2.3 Heat Exchanger Modeling Conclusions

The two-pass heat exchanger model resulted in lower chilled water pressure losses. The smaller pressure drop was primarily due to having fewer passes for the same number of inlet tubes as compared to the four-pass heat exchanger. A disadvantage to this model was the pressure drop on the shell-side of the heat exchanger for the demineralized water. The larger pressure drop is attributed to having a smaller internal shell diameter and more closely spaced baffles. However, a more compact baffle arrangement provides greater heat transfer capability to the heat exchanger. The two-pass heat exchanger is 10~in longer than the four-pass model in order to maintain sufficient exposed tube surface area for heat transfer. Both heat exchangers have approximately the same heat load capability of 240~kW given the differences in their design.

Based on the simulation results, all flow requirements were met by the four-pass heat exchanger, with the exception of the chilled water pressure drop. It is recommended that further heat exchanger optimization is performed to determine the solution that meets all requirements. Modifying the four-pass heat exchanger to a two-pass design with 1/2 in or 5/8 in diameter tubes should be pursued. The number of inlet tubes should scale with the tube diameter in order to maintain a safe but sufficient fluid flow velocity.

## Chapter 3

# Pump

### 3.1 Pump Power & Sizing

Choosing the appropriate pump design boundaries was based on the requirements of military standards, conventional factors of safety, and industry standards.

Based on the assumptions made by [3] for equipment allocation and vertical spatial allowances, five iPEBB stacks, each consisting of four iPEBBs would optimally fit within the footprint of the model NiPEC. Ongoing development by the ESRDC Virginia Tech project team characterized 96 semi-conductors and one transformer as the main heat-producing elements within the iPEBB [35]. Each MOSFET was determined to emit 70W of heat, and each transformer 1158W. Therefore, with applied conservatism and data margin, each iPEBB is considered to produce 10 kW of heat. Applying a 20% safety factor, the 20 iPEBBs within the NiPEC compartment produce 240 kW of heat.

The maximum volumetric flow rate for a shipboard cooling water system must be adjusted to 1.4 gallons per minute per kilowatt load and a maximum rise in water temperature of 2  $^{\circ}C$  as stated in DOD-STD-1399 [6]. Therefore, for a 240 kW load, the required maximum volumetric flow rate is 336 gpm. As the pump takes suction directly from the system's heat exchanger and expansion tank, it is assumed that the demineralized water enters the pump at a maximum temperature of 44  $^{\circ}C$  based on the assumptions in Chapter 2.1. Table 3.1 provides the characteristic water properties.

Table 3.1: 15 °C Water Properties

Density	ρ	$kg/m^3$	990.66
Dynamic Viscosity	$\mu$	$N - s/m^2$	6.078E-4
Vapor Pressure	$P_{vap}$	kPa	9.112

In determining the total dynamic head of the cooling system, frictional losses from system equipment, fittings, and piping were considered. The piping run with the greatest anticipated pump head was used for calculations as it presented the most conservative approach. Estimated equipment head losses are tabulated in Table 3.2. The chemical resin bed and micron filter components are not in-line with the main cooling path and were therefore not incorporated into the total dynamic head calculation. The pump suction filter is y-strainer with expected pressure losses equivalent to commercial products. The iPEBB stack and heat exchanger losses were assumed to be the maximum permissible design standards from [17].

Table 3.2: Equipment Pressure Losses

	Suction	Discharge
	(psi)	(psi)
iPEBB Stack	0	10
Heat Exchanger	0	6
Mechanical Filter	6	0

Piping frictional losses were calculated using the Darcy-Weisbach equation,

$$\Delta p = f_D \frac{L}{D} \frac{\rho}{2} (v)^2 \tag{3.1}$$

where  $f_D$  is the Darcy friction factor, L is the length of the pipe (m), D is the internal diameter of the pipe (m),  $\rho$  is the density of the fluid  $(kg/m^3)$  and v is the mean flow velocity (m/s).

The diameter for the suction and discharge piping of the pump were assumed to be 4 in and 3.5 in, respectively. Smaller branches of piping along the main cooling path were determined to be 2 in leading into and out of the iPEBB stack and 1 in for the cold plate inlet and outlet piping. The piping sizes were derived by the safe flow velocities determined in Chapter 5, the thermal properties of the demineralized

water, a total volumetric flow rate of 336 gpm, and the continuity of mass equation. 8 m of piping were estimated for each of the main cooling water headers and 2.5 m for each branch of the iPEBB stack. The pipe lengths were derived from NiPEC cooling system CAD modeling. The Darcy Friction Factor was calculated using Eqn. 2.5 and Reynolds values based on the selected piping diameter. The resulting values are shown in Table 3.3.

Table 3.3: Suction & Discharge Piping Frictional Losses

			Suction	Discharge
Volumetric Flow Rate	V	$m^3/s$	0.0212	.0212
Pipe Internal Diameter	$D_{ID}$	in	4.029	3.548
Pipe Length	L	m	10.5	10.5
Fluid Velocity	v	m/s	2.577	3.323
Reynolds Number	Re	non-dim	429,877	488,155
Darcy Friction Factor	$f_D$	non-dim	0.01350	0.01319
Piping Pressure Loss	$P_{Pipe}$	psi	0.7157	1.142

Fitting frictional losses were calculated using the resistance coefficient fitting assumption and a derivation of Eqn. 3.1 for dimensional analysis. A table of pertinent resistance coefficients for various fittings can be found in Appendix A. The values were used in calculating the cumulative fitting system head loss as follows:

$$h_L = K \frac{v^2}{2q} \tag{3.2}$$

where K is the resistance coefficient, v is the mean flow velocity (m/s), and g is the gravitational acceleration  $(m/s^2)$ . Fitting quantity and header allocation was determined from the initial system design layout of Fig. 3-1.

A summarized table of pressure losses and the total dynamic head is found in Table 3.4.

Typical pump efficiencies for small AC-powered centrifugal pumps range between 55% and 71%. Centrifugal pumps operate with higher efficiencies when supplying maximum volumetric flow against a relatively benign pump head. Therefore, a 70% pump efficiency was chosen. The power required by the pump was calculated using

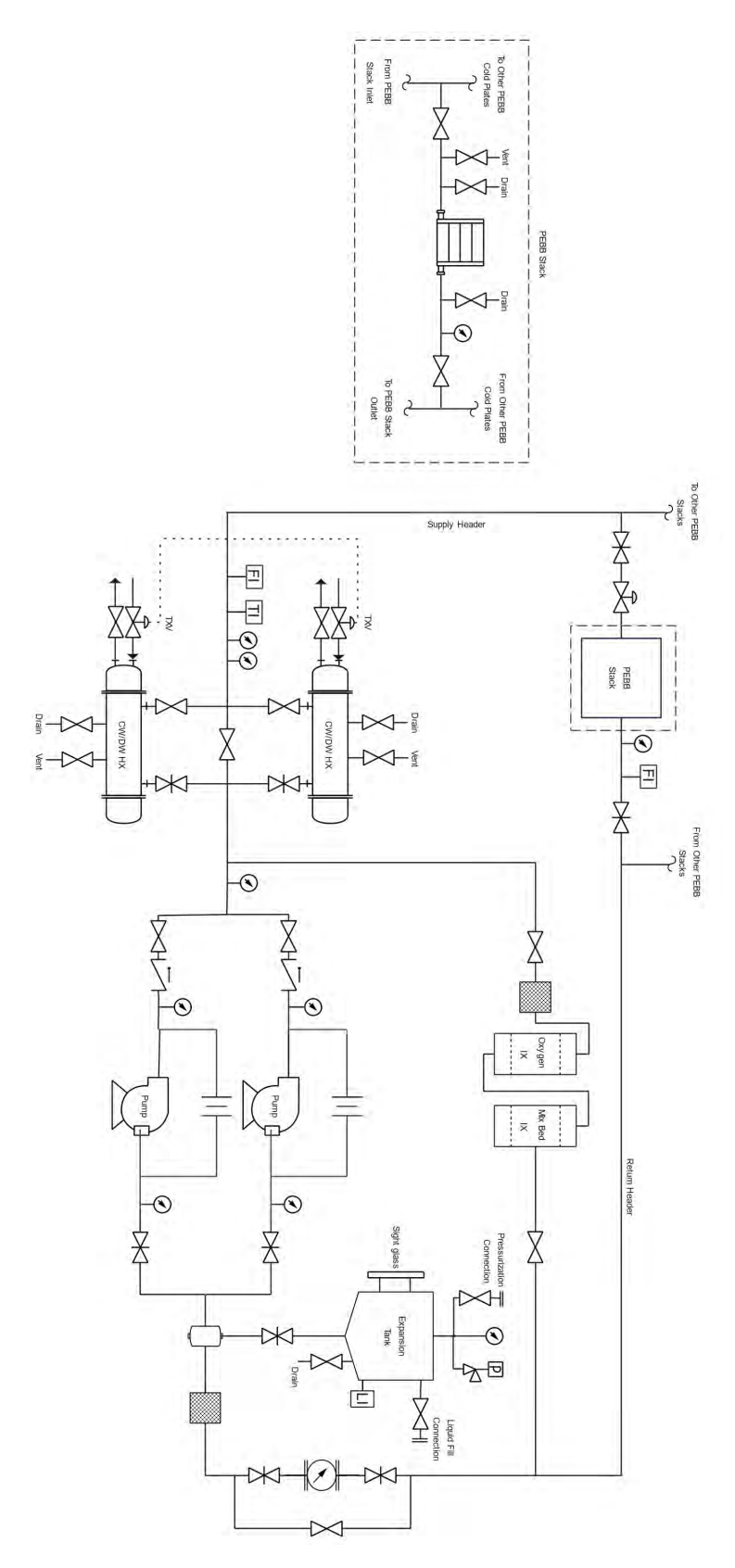


Figure 3-1: Cooling System Diagram

Table 3.4: Summarized Pressure Losses

			Suction	Discharge
Equipment Pressure Loss	$P_{Equip}$	psi	6	16
Piping Pressure Loss	$P_{Pipe}$	psi	0.7157	1.1411
Fitting Pressure Loss	$P_{Fitting}$	psi	8.26	23.30
Total Pressure Loss	$P_{Tot}$	psi	14.98	40.44
Total Dynamic Head	TDH	psi	5.	5.42

the pump power equation

$$P = \frac{\dot{V}\rho g(TDH)}{\eta} \tag{3.3}$$

where P is the pump power (kW),  $\dot{V}$  is the volumetric flow rate  $(m^3/s)$ , TDH is the total dynamic head (m), and  $\eta$  is the pump efficiency. The required pump power is calculated to be 16.21 kW or 21.87 hp.

## Chapter 4

# **Expansion Tank**

## 4.1 Expansion Tank Volume

The expansion tank shall be sized to accommodate the thermal expansion of the system coolant, a conservative operating volume, and sufficient safety margins. The thermal expansion volume is based on a cooling water temperature range from 0 to 79 °C, where 0 °C is the minimum phase temperature, and 79 °C is based on the maximum possible temperature seen by the liquid. The maximum temperature assumes that the main heat-producing components within the iPEBB are the semi-conductor switches. Based on the assumptions and methodology of Padilla et al. [31], Table 4.1 provides the one-dimensional thermal resistance values per semi-conductor switch for the thermal network of interfacing materials.

Table 4.1: One-Dimensional Thermal Resistance Values Per Semiconductor Switch

Semiconductor	$R_{SC}$	K/W	0.4
iPEBB Casing	$R_{Case}$	K/W	0.0188
Thermal Pad	$R_{TP}$	K/W	0.1103
Piping Wall	$R_{PW}$	K/W	0.0773
Total	$R_{Tot}$	K/W	0.6064

If iPEBB operates in the 80/20 load condition described in 2.1, a 167 kW heat load per semi-conductor is expected. Assuming a 180 °C maximum functional temperature for the semi-conductor, and a loss of flow casualty to the cooling system,

maximum cooling water temperature of 79 °C is reached utilizing Eqn. 2.15. This worst-case scenario is how the perceivable temperature range for the cooling liquid was determined.

The volume required for expansion of the liquid in the system considers only the cooling water in the piping and components. Based on the assumed piping and component volumes, a total estimated system volume of 200 gallons is derived. The 200 gallons assumes two heat exchangers, two pumps, two demineralizers, approximately 25 meters of varying pipe sizes, and 40 cold plates (5 iPEBB stacks, each with 4 iPEBBs and two cold plates per iPEBB). The volume required to accommodate the thermal expansion of the demineralized water was calculated using

$$\Delta V_E = V_\theta \beta \Delta T_{Range} \tag{4.1}$$

where  $\Delta V_E$  is the change in cooling volume due to thermal effects (gal),  $V_{\theta}$  is the initial volume of cooling water within the system (gal),  $\beta$  is the volumetric temperature expansion coefficient of water (1/K), and  $\Delta T_{Range}$  is the possible difference of cooling water temperature range (K). Assuming the value of  $\beta$  is  $6.21 \cdot 10^{-4}$  at its most limiting temperature, the required expansion volume is 9.81 gallons.

Typically, the operational volume allowance  $V_O$  used in determining the total expansion tank volume is based on the need to fill portions of the system from a shutdown condition. The criteria prevents having to refill and check the chemistry of the added water multiple times to fill the system's limiting component (i.e. the heat exchanger). As the NiPEC compartment cooling system is not expected to be shut down on a frequent basis, the heat exchanger does not serve as the basis for this volume.  $V_O$  is assumed to be 4 gallons and is based on having to fill and restore a single iPEBB stack from a maintenance condition.

A low-level tank margin of 20% total volume is applied to ensure that operators can take timely action to diagnose and restore expansion tank pressure and level conditions. If tank level and pressure were not promptly restored, cavitation and/or air-binding of the pump could occur, leading to loss of flow and cooling to the iPEBBs.

A high-level tank margin of 10% total volume is applied as a buffer to prevent the inadvertent wetting of equipment at the top of the tank not intended to come in contact with water.

The total liquid volume of the expansion tank is therefore

$$V_{Tot} = 0.1 * V_{Tot} + V_E + V_O + 0.2 * V_{Tot}$$
(4.2)

where  $V_{Tot}$  is the total liquid volume of the expansion tank (gal),  $V_E$  is the thermal expansion volume (gal), and  $V_O$  is the operating volume (gal). Using the previously determined values for  $V_E$  and  $V_O$ ,  $V_T$  is calculated to be 19.71 gallons.

## 4.2 Expansion Tank Pressures

To calculate the normal operating expansion tank pressure, a minimum system pressure of  $10 \ psi, P_{min}$ , is maintained [6]. The criteria ensures the system can operate under normal conditions and provides a minimum positive pressure to prevent the introduction of oxygenated air into the system. The pressure is assumed to occur for the limiting case of an expansion tank level at the low-level margin. The total pressure at the tank level is therefore given by the following equation:

$$P_{Low} = P_{min} + \rho g H_{Tank} \tag{4.3}$$

where  $P_{Low}$  is the pressure in the tank at the low-level margin and  $H_{Tank}$  is the vertical distance between the tank level and the highest point in the remaining cooling system. Assuming an available compartment height of 102 in, a 60 in tall iPEBB stack that sits 9 in off the deck, and a 18in tall expansion tank that is anchored 6 in from the overhead,  $H_{Tank} \approx 9 \ lbf/in^2$ . Equipment spacing and size are based on assumptions discussed in Chapter 8 and criteria from [24] and [25]. Therefore,  $P_{Low} = 10.32 \ lbf/in^2$ .

The volume of air at the low-level margin is  $V_1 = 0.8V_{Tot}$ , and the absolute pressure is  $P_1 = P_{atm} + P_{Low}$ . The volume of air at the normal operating level is

 $V_2 = 0.8V_{Tot} - V_O$ , and the absolute pressure is  $P_2 = P_{atm} + P_{Norm}$ , where  $P_{Norm}$  is the normal operating pressure of the expansion tank. Using Boyle's law for fluids at constant temperature, the expansion tank's normal charge pressure was determined by

$$(P_{atm} + P_{Low})(0.8V_{Tot}) = (0.8V_{Tot} - V_O)(P_{atm} + P_{Norm})$$
(4.4)

The minimum expansion tank pressure must be greater than  $18.82\ lbf/in^2$  to maintain the system low-pressure criteria.

## Chapter 5

# Pipes, Hoses, and Fittings

## 5.1 Pipes and Flow Devices

The piping and tubing of the demineralized cooling circuit must functionally compliment the equipment and materials it supports. Surface ship electronic cooling water systems which use distilled or fresh water as the cooling medium must fabricate the cooling circuit from copper or copper-alloy materials. However, for demineralized water systems, copper-alloy, bronze, or corrosion-resistant steel (CRES) materials are required. The specific alloys permitted for use in the construction of the demineralized cooling circuit are listed in Table 5.1.

Table 5.1: U.S. Navy surface ship alloys for construction of electronic cooling water systems

Material	Alloy Designation	Trade Name
Copper-Nickel Alloy	C70600	CuNi 90/10
Copper-Nickel Alloy	C71500	CuNi 70/30
Bronze	C92200	Navy M Bronze
Bronze	C90300	Tin Bronze
Stainless Steel	SAE 304	CRES, 0.08% Carbon
Stainless Steel	SAE 316	CRES, 0.03% Carbon
Stainless Steel	SAE 316L	CRES, 3% Molybdenum

The materials must be electrochemically compatible with other construction substances and contain limited carbon content [6]. This restriction minimizes the possibility and severity of the system's degradation from various corrosion mechanisms.

Copper or lightly-alloyed copper stock is not used in demineralized systems due to its production of copper carbonate fouling and ion contamination of the cooling water's purity. The following is a list of copper-composed alloys that may be used in distilled or fresh water applications but not for use with high-purity water as in this design.

- Copper, C10100 (Oxygen-Free-Electronic)
- Copper, C10200 (Oxygen-Free)
- Copper, C10300 (Oxygen-Free Extra Low Phosphorous)
- Copper, C10800 (Oxygen-Free Extra Low Phosphorous)
- Copper, C12000 (Phosphorus-Deoxidized, Low Residual Phosphorus)
- Copper, C12200 (Phosphorus-Deoxidized, High Residual Phosphorus)
- Copper, C14200 (Phosphorus-Deoxidized, Arsenica)

An analysis of the properties and capabilities of the materials in Table 5.1 determined that Copper-Nickel is the most suitable material for the construction of the demineralized water cooling circuit.

### 5.1.1 Corrosion

As the application of this cooling system exists in a marine environment, the likelihood for an electrolytic fluid, such as seawater or chloride-contaminated liquids, to interact with cooling circuit materials increases. The liquid contaminant can originate from various sources such as atmospheric condensation, heat exchanger tube failure, external system leakage, and piping insulation. It creates an environment that fosters and accelerates corrosion. Therefore, the following assessments assume that seawater or a chloride-contaminated liquid interacts with the cooling circuit's components, as is the case with most marine applications.

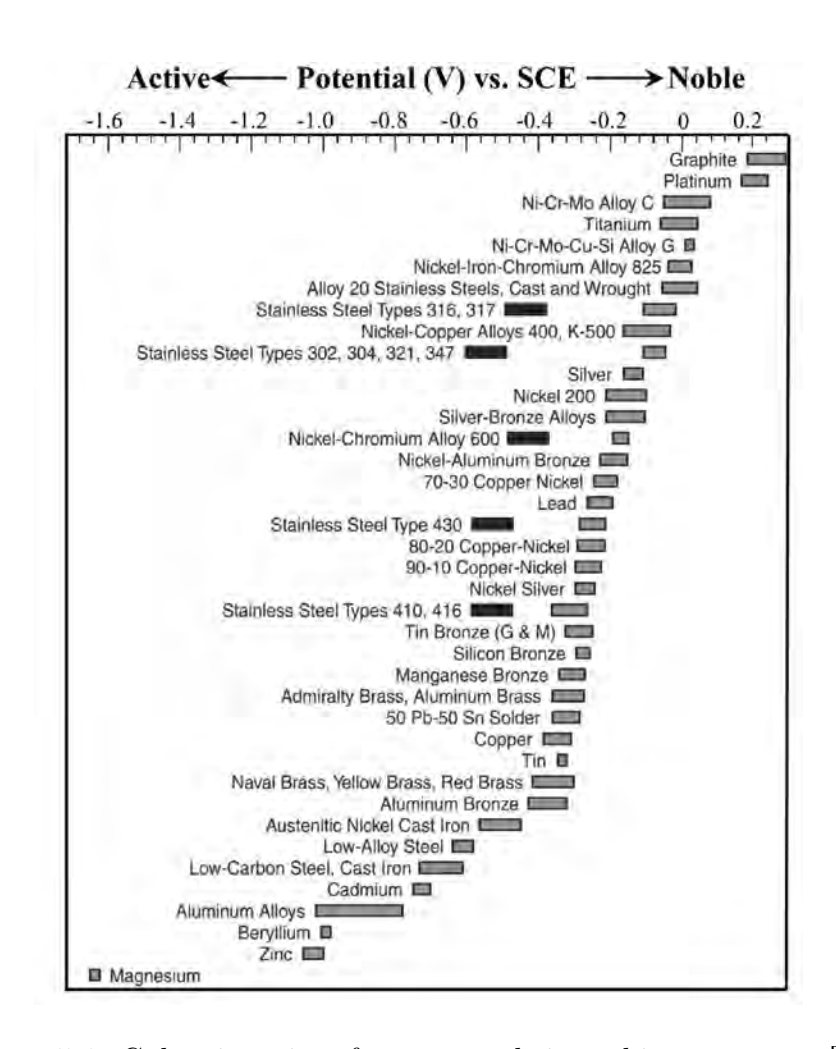


Figure 5-1: Galvanic series of some metals in ambient seawater [38]

#### Galvanic Corrosion

Galvanic corrosion is an issue when dissimilar metals or alloys, having different surface potentials, are in electrical contact with each other and a common electrolyte. As the proposed heat exchanger design requires the use of predominantly copper-nickel alloy construction materials, the corrosion potential between these metals and those listed in Table 5.1 were assessed. The heat exchanger was chosen for comparison as it is the most limiting component due to its likelihood and severity for failure. Fig. 5-1 shows the steady-state electrode material potential (volts) referenced to a saturated calomel half-cell. The different shaded ranges for specific materials are for when the metal is in an active or passive state. The dark-shaded range represents the metal's active state, which can occur in acidic water conditions. These conditions may exist in localized cervices, stagnation or low-flow points, or in poorly aerated systems. The lightlyshaded range represents the metal's passive state, when the surface of the metal is covered by a protective corrosion layer. The stainless steel alloys from Table 5.1 have a 0.1 to 0.3 volt difference in potential with the copper-nickel alloys and a 0.2 to 0.4 volt difference with the bronze alloys. A 0.05 to 0.15 volt difference in potential exists between the bronze alloys and copper-nickel alloys. An even smaller difference in potentials exists when comparing the various copper-nickel alloys. The greater potential between materials increases the likelihood and severity of galvanic corrosion, causing the less noble material to corrode. Since the copper-nickel or bronze alloys are less noble than stainless steel, the materials they comprise would deteriorate. Based on the construction materials of the heat exchanger and galvanic compatibility, coppernickel alloys are the preferred materials to avoid degraded component performance or premature failure.

In a study by the European Stainless Steel Development Association [12], it was found that a galvanic cell between an equivalent grade of stainless steel from Table 5.1 and CuNi 90/10 enabled a corrosion rate of 0.07 mm/yr for a 4:1 anode-to-cathode area ratio (A/C). The maximum compatibility corrosion rate defined by MIL-STD-889D is 0.009 mm/yr for a 1:1 A/C. Using the following equation from MIL-STD-889

[28], a comparison of corrosion rates can be made:

$$A/C = \frac{CR}{0.009mm/yr} \tag{5.1}$$

where A/C is the anode-to-cathode area ratio and CR is the corrosion rate between the galvanic couple (mm/yr). Normalized to a 1:1 A/C, the stainless steel and CuNi 90/10 corrosion rate of 0.0175 mm/yr exceeds the 0.009 mm/yr limit. Exceeding the limit requires the component or system to have a form of corrosion protection installed. Such protection methods include, but are not limited to, sacrificial metal coatings, seals between faying surfaces, painting of surfaces, and barrier installation between faying surfaces. Therefore, to limit the possibility of galvanic corrosion and system constraints, copper-nickel or bronze alloys are the preferred construction materials. The corrosion rate between stainless steel and bronze is captured in Fig. 5-2. SEA 304 and 316 (passivated) have a compatibility rank of 0 (<0.009 mm/yr). However, when the stainless steels are active, as is possible with corrosion or a water chemistry disruption, the corrosion cell is galvanically incompatible with a rank of 3 (1-4.99 mm/yr).

Overall, the need for a cathodic protection system in copper-nickel or bronze alloy systems is limited or unnecessary. Galvanic corrosion is not a concern when copper-nickel is used with other copper-based components, such as bronze. Specifically, CuNi 90/10 can be safely coupled to tin bronze, CuNi 70/30, and nickel-aluminum bronze.

#### General Corrosion

Other types of corrosion considered were general corrosion, impingement attack, pitting corrosion, crevice corrosion, erosion-corrosion, and stress corrosion cracking. A comparison of the general corrosion rates by the Copper Development Association in Fig. 5-3 shows that SAE 304 and 316 typically have higher general corrosion rates compared to CuNi 90/10 and CuNi 70/30. Copper-Nickel alloys have excellent corrosion resistance in low flow or stagnant fluid system conditions, the ideal material for systems in overhaul or commissioning status.

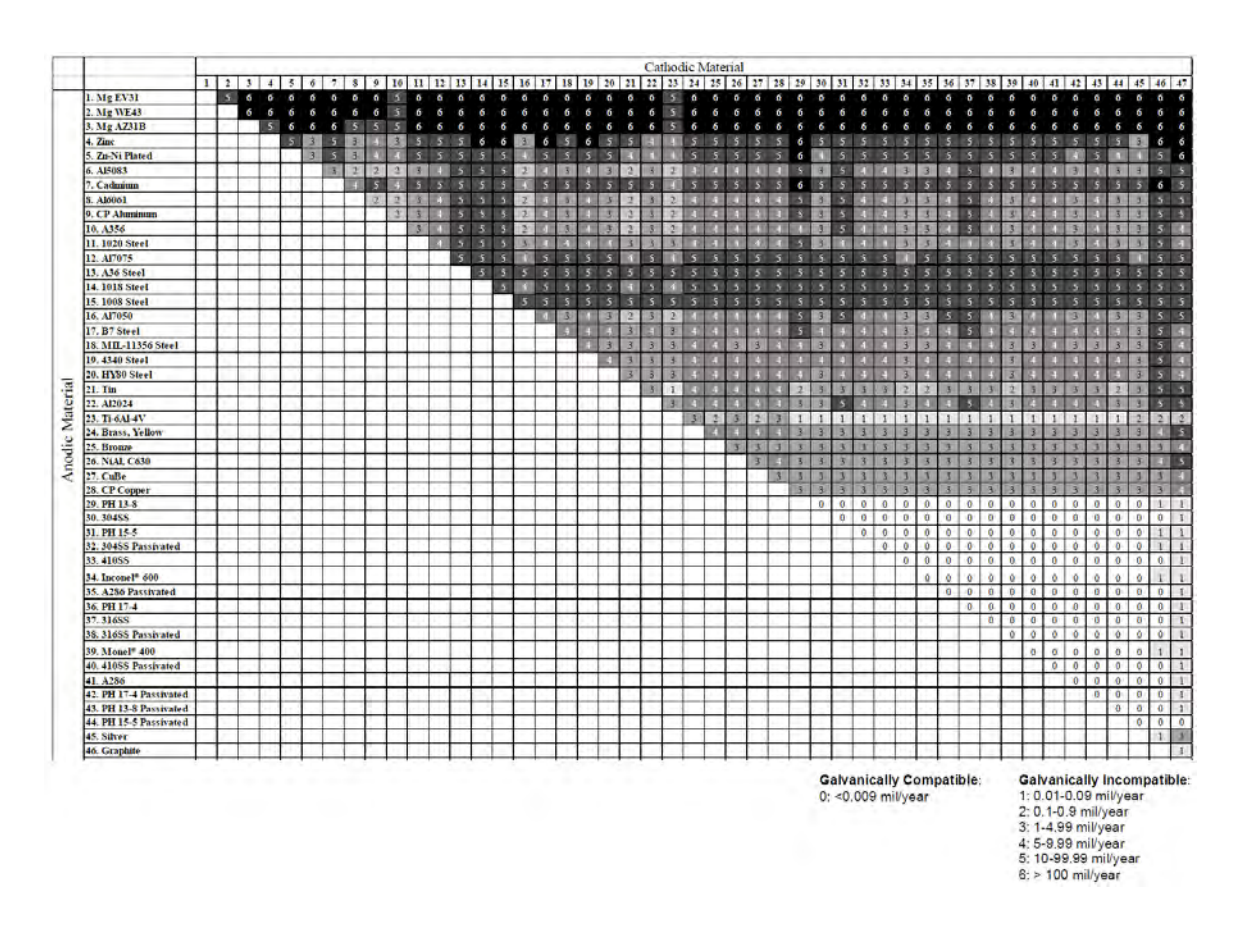


Figure 5-2: Galvanic compatibility of bare conductive materials in a 1:1 A/C in immersed artificial seawater [28]

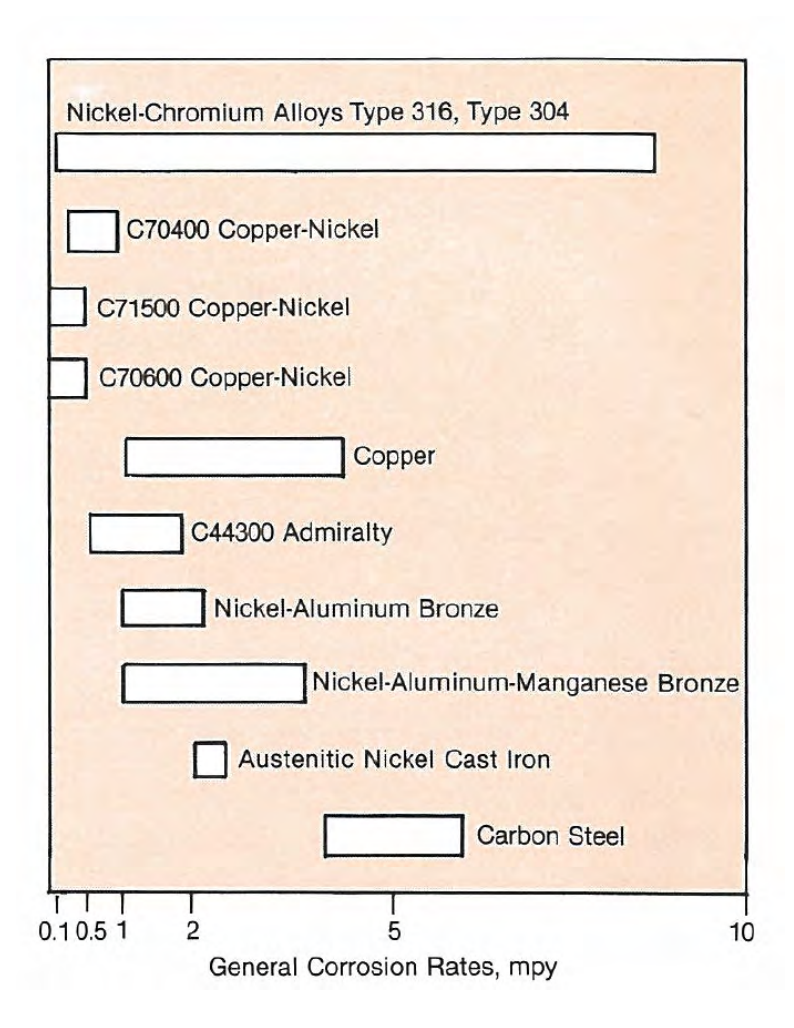


Figure 5-3: Comparison of the general corrosion rates for various alloys in quiet seawater, millimeters per year [11]

### Impingement Attack

Impingement attack can be caused by excessive piping velocities, bubble or particulate entertainment, and internal surface roughness can be reduced by the use of Copper-Nickel alloys. Particulates suspended in the cooling fluid can develop from fouling or contamination. CuNi 90/10 and Cu-Ni 70/30 have excellent resistance to fouling when compared to stainless steel, with CuNi 90/10 having the superior characteristic. The CuNi alloys perform better in this metric due to copper ions creating an inhospitable environment for biological organisms. Maintaining fluid velocities >1 m/s will remove bio-fouling from materials with relatively good fouling resistance. Alloys lacking this capability enable biological organisms to grow and thrive. In the case of equipment or systems that are offline, alternating components, periodic cycling, or lay-up conditions should be executed in accordance with existing navy procedures.

A ranking of the fouling resistance of several comparable alloys, including those from table Table 5.1, was conducted by the Nickel Institute and is shown in Fig. 5-5. Bubble impingement can develop from dissolved gasses coming out of the bulk solution due to reaching saturation conditions, such as with pump cavitation. To combat this issue, water chemistry is strictly adhered to, and designed pump operations provide sufficient net positive suction head. Of note, copper-nickel alloys are more susceptible to cavitation damage than stainless steel. Fig. 5-4 shows the volume loss rate of alloys in a cavitation tunnel at 40 m/s. Typical values of piping roughness depend on the material and method of fabrication. Generally, stainless steels have larger absolute roughness coefficients than CuNi and Bronze alloys, which translates to a smoother internal piping surface for the latter. Furthermore, as stainless steel is more susceptible to corrosion, its internal surface roughness increases along its life cycle and enables more corrosion [34].

#### Pitting Corrosion

Pitting corrosion occurs when small holes develop in the alloy's protective oxide layer and create a corrosion cell between the anodic region of the hole and the surrounding

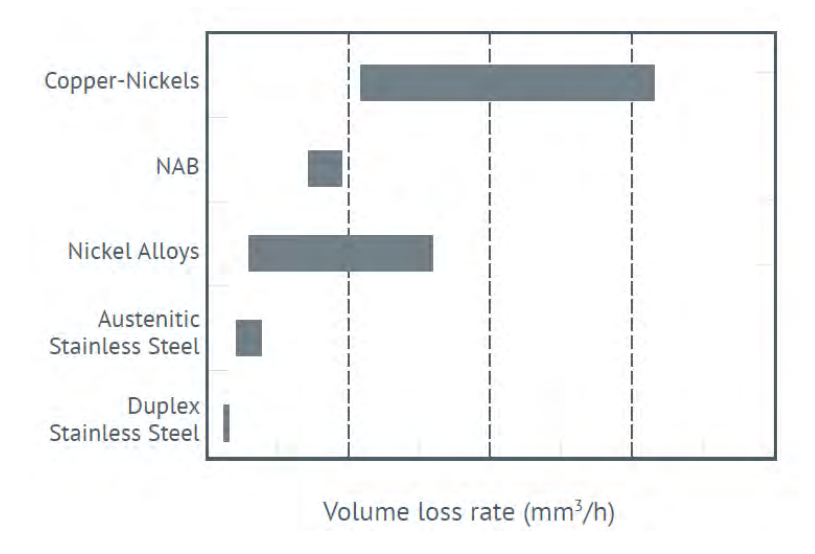


Figure 5-4: Crevice corrosion comparison of for various alloys in a cavitation tunnel at  $40\ m/s\ [10]$ 

Arbitrary Rating Scale of Fouling Resistance		Materials	
90-100	Best	Copper 90/10 copper-nickel alloy	
70-90	Good	Brass and bronze	
50	Fair	70/30 copper-nickel alloy, aluminium bronzes, zinc	
10	Very Slight	Nickel-copper alloy 400	
0	Least	Carbon and low alloy steels, stainless steels, nickel-chromium-high molybdenum alloys Titanium	

Figure 5-5: Comparison of fouling resistance for various alloys [11]

cathodic material. The Copper-Nickel and Bronze alloys are not notably susceptible to pitting corrosion, whereas stainless steel alloys 304 and 316 are. This can be seen in Figures 5-6 and 5-7 developed by the Copper Development Association and [39].

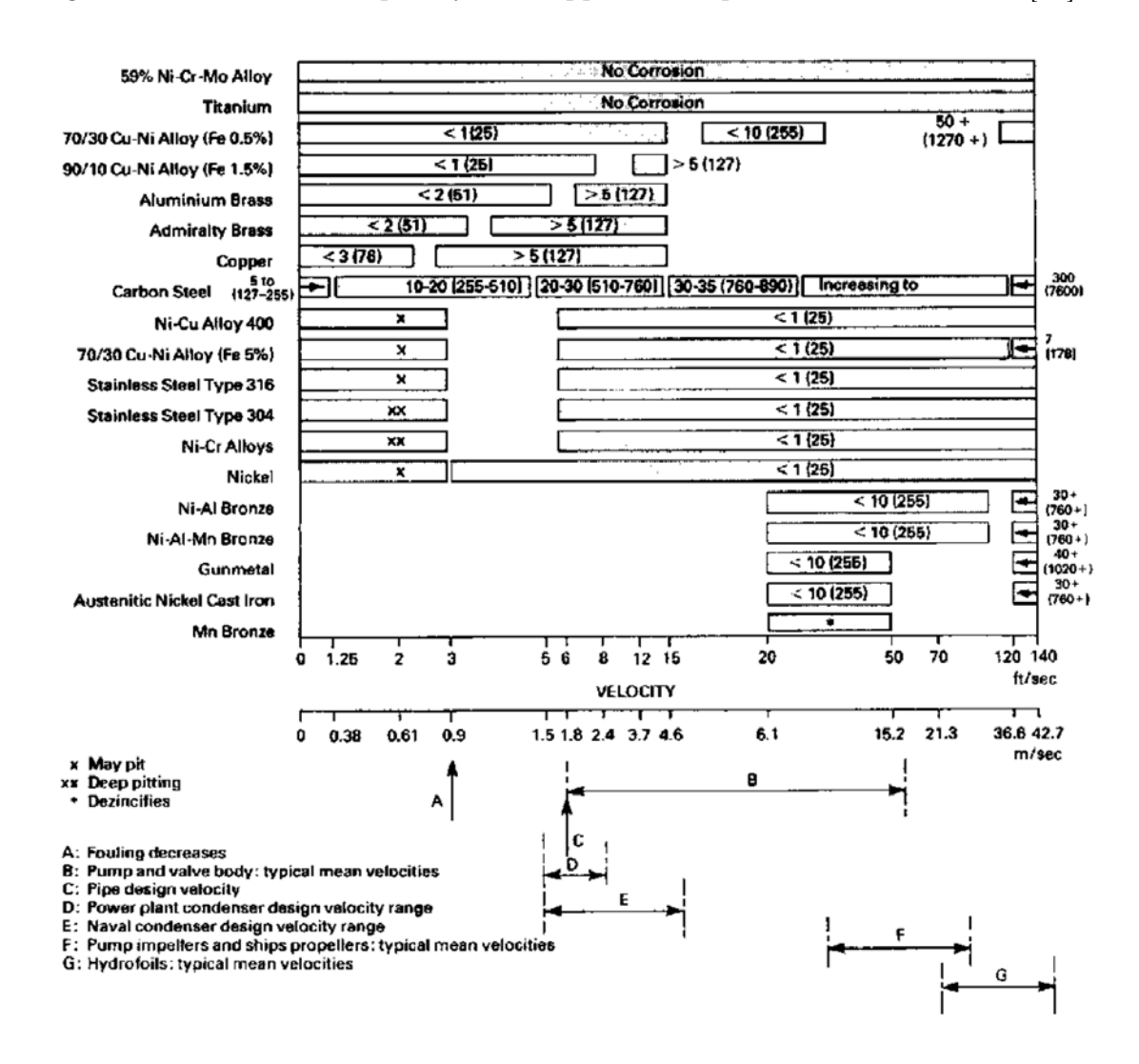


Figure 5-6: Erosion corrosion and pitting comparison for various alloys, (microns/year) [13]

#### Crevice Corrosion

The mechanism for crevice corrosion is similar to pitting corrosion, with the general distinction being that pitting occurs on the surface of the material. Crevice corrosion occurs in areas such as the interfaces of joints and fasteners, preexisting flaws, under bio-fouling, sharp corner low-flow areas, and oxygen-deprived regions. Fig. 5-8

Crevice corrosion resistance		Crevice induced serious pitting		
Excellent	Good	Moderate	Inferior	
Ti Hastalloy C	90 ~ 10 CuNi1.5Fe 70 ~ 30 CuNi0.5Fe Bronze Brass	Cast iron Carbon steel	Incoloy 825 NiCu alloy Cu	AISI 316, 304, 400 series stainless steel

Figure 5-7: Crevice corrosion comparison of for various alloys [38]

provides a summary of localized corrosion comparisons for various alloys.

#### **Erosion-Corrosion**

Erosion corrosion occurs when flow velocities cause the removal or dissolution of the alloy's protective oxide layer and exceed the layer's ability to regenerate. The flow velocity at which this mechanism occurs is called the critical velocity. Fig. 5-6 shows the correlation of erosion-corrosion to piping velocity for various alloys. Stainless steels have a higher resistance to erosion-corrosion than copper-nickel or bronze alloys but exceed the necessary range of the NiPEC cooling design velocities. Therefore, CuNi alloys are more appropriate given the design parameters. Recommended maximum safe flow velocities by the Copper Development Association are provided in Fig. 5-9 and incorporate undisclosed safety factors. Additionally, Fig. 5-9 considers local speed increases due to changes in direction and points of divergence.

#### Stress Corrosion Cracking

Copper-Nickel alloys are susceptible to stress corrosion cracking (SCC) from aqueous solutions of ammonium ion, nitrites, mercury compounds, and moist atmospheres containing sulfur dioxide. Conversely, stainless steels are susceptible to SCC from chloride ions and no other known chemicals.

Copper-nickel is more thermally conductive than stainless steel and therefore requires additional considerations in mitigating this issue. The installation of pipe lagging and other insulators are recommended to prevent heat losses to ambient of the cooling water and deter condensation build-up from atmospheric conditions. A recommended list of insulation and lagging components is listed in Appendix E. Stainless steel alloys achieve higher material strength characteristics, but the low-pressure

Crevices can normally	Titanium Alloy C Alloy 625	These metals foul but rarely pit.  Titanium will pit at temperatures above 120°C.  Alloy 625 after 2-3 years show signs of incipient pitting in some tests in quiet seawater.
be tolerated in designs	90/10 copper-nickel (1.5 Fe) Admiralty Brass	Shallow to no pitting. 90/10 copper-nickel is standard seawater piping alloy.
using these materials	70/30 copper-nickel Copper Tin and aluminium bronzes Austenitic nickel cast iron	Good resistance to pitting. Useful in piping applications.
Useful although	Nickel-copper alloy 400	Pits tend to be self-limiting in depth at about 1-6 mm. No protection required for heavy sections. Cathodic protection from steel or copper base alloys will prevent pitting on O Ring, valve seats, and similar critical surfaces.
Cathodic protection	CN7M (Alloy 20)	Occasional deep pits will develop.
required	All 005	Protection not normally required for all alloy 20 pumps.
on critical surfaces	Alloy 825	Cathodic protection from less noble alloys may be necessary for O Ring and similar critical surfaces.
200.0000	Type 316 Stainless Steel	Cathodic protection from zinc, aluminium, or steel is required except when part is frequently removed from seawater and thoroughly cleaned.
Crevices cannot be tolerated	Nickel	Many deep pits develop. Cathodic protection from less noble alloys required.
in designs (Excellent, however, in above-	Type 304 Stainless Steel	Many deep pits develop. Cathodic protection from steel may not be fully effective.
the- waterline marine applications)	Precipitation Hardening Grades of Stainless Steel	Many deep pits develop. Cathodic protection with zinc or aluminium may induce cracking from hydrogen.
Severe crevice	Type 303 Stainless Steel	Severe pitting. Cathodic protection may not be effective.
corrosion limits usefulness	Series 400 Stainless Steel	Severe pitting. Cathodic protection with zinc or aluminium may induce cracking from hydrogen.

Figure 5-8: Localized corrosion comparison for various alloys [13]

Alloy	Heat Exchanger Tube	Pipe (≤ NPS 3) (DN ≤ 80 mm)	Pipe (> NPS 3) (DN > 80 mm)
Aluminium Brass	1.5-2.0	1.5-2.0	2.0-2.5
90/10 Copper-nickel	2.0-3.0	2.0-3.0	3.0-3.5
70/30 Copper-nickel	2,5-3.5	2.5-3.5	3.5-4.0
66/30/2/2 Cu-Ni-Fe-Mn	3.0-3.5	3.0-3.5	3.5-4.5
Nickel Aluminium Bronze		2.5-3.5	2.5-3.5

Figure 5-9: Recommended safe maximum flow velocities [9]

applications of the design are well-conforming to the abilities of copper-nickel and do not require the added strength provided by stainless steel.

#### 5.1.2 Material Selection Conclusion

Considering the alloys from Table 5.1, copper-nickel alloys are the superior choice in cooling circuit material due to their flow performance characteristics and corrosion resistance. While CuNi should be used for most applications, Tin bronze is recommended for bearings and pump impellers due to its good wear resistance. Using the list of permitted piping component materials in Appendix C, material selection should proceed in the following prioritized order: CuNi 90/10, CuNi 70/30, Bronze.

Further design considerations are that fluid distribution is primarily controlled via the cross-sectional area of piping, tubing, and hoses and augmented by flow control devices such as orifice plates, flow regulators, and valves. When flow control devices are used, they are chosen based on their necessity while minimizing their flow disrupting characteristics. The cooling circuit is designed with a limited the number of bends, fitting, valves, and branches to minimize head loss and corrosion, as seen in Fig. 3-1. Lastly, the recommended model is designed to dissipate heat using flow paths that are short, direct, and have feasibly low thermal resistances.

#### 5.2 Flexible Hoses

Flexible hose requirements are in accordance with naval technical directives and standards. The variations of hoses used in naval applications use rubber, polymer-based, or metal materials. For use in the demineralized water cooling circuit, rubber or polytetrafluoroethylene (PTFE) hoses shall be used. The rubber hose is constructed of synthetic rubber reinforced by metal or synthetic fibers. The PTFE hose is constructed of a PTFE tube reinforced by braided stainless steel wire. As the flexible hose design would be used in electronic cooling applications, electrical conductance through the hose materials is a risk. Electrical conductance could cause damage to the flexible hose and downstream components. There are documented cases of pin-hole

leaks developing in the PTFE hoses due to arcing across the metal braiding [20]. Furthermore, hose end fittings are to be made of copper-nickel, bronze, or nickel-copper alloys in accordance with [21]. Therefore, To minimize the probability of galvanic corrosion and electrical conductance, a rubber hose reinforced by synthetic fibers should be used.

For application in the cooling circuit, the flexible hose would be used in piping segments that direct water to the PEBB stack. The hoses would accommodate movement between components and provide some measure of electrical isolation. These segments correspond to the military standard for synthetic rubber hoses reinforced with synthetic fiber in low-pressure applications and nominal inside diameters of 1/4 in to 2 in. The required specifications are listed in Figures 5-10 and 5-11. The dash number represents the nominal inside diameter of the hose in sixteenths.

Hose size (dash number)	Pressure (psi)		Hose dimensions (inches)						
			I	D	OD				
	Working (max)	Burst (min)	Min	Max	Min	Max			
-4	1,000	4,000	0.188	0.214	0.500	0.539			
-5	800	3,200	0.250	0.281	0.562	0.601			
-6	650	2,600	0.313	0.394	0.656	0.695			
-8	625	2,500	0.406	0.437	0.743	0.789			
-10	600	2,400	0.500	0.539	0.899	0.945			
-12	550	2,200	0.625	0.667	1.055	1.101			
-16	500	2,000	0.875	0.917	1.203	1.265			
-20	450	1,800	1.125	1.172	1.469	1,531			
-24	400	1,600	1.375	1.422	1.719	1.781			
-32	350	1,400	1.812	1.859	2.172	2.266			

Figure 5-10: Hose dimensions and pressures [20]

Hose size (dash number)	Hose re	einforcement	Minimum bend	Impulse peak pressure (psi)	
	Construction	Number of layers	radius (inches)		
-4 Braided 2		2	3.00	1,500	
-5	Braided	2	3.38	1,200	
-6	Braided	2	4.00	975	
-8	Braided	2	4.62	938	
-10	Braided	2	5,50	900	
-12	Braided	2	6.50	825	
-16	Braided	2	7.38	750	
-20	Braided	2	9.00	675	
-24	Braided	2	10.50	600	
-32	Braided	2	13.25	525	

Figure 5-11: Hose construction and minimum bend radius [20]

The following designs for hose end fittings are listed below and detailed in Appendix C:

- Flange to Hose
- 37-degree Flare Swivel
- O-ring Seal Union
- Split Clamp
- Tailpiece
- 90-degree Elbow

The principal limitations of using flexible hoses are the permitted configurations, minimum hose lengths, temperature ratings, and life-cycle specifications. The permitted acceptable hose configurations for the cooling circuit are listed below:

- 90-degree dog leg hose assembly two straight hose lengths connected by a 90-degree elbow fitting.
- U or 180-degree return bend hose assembly two straight hose lengths connected by a 180-degree elbow fitting.
- Single hose assembly one straight hose with a fittings at each end.

Of note, Single hose assemblies require specific NAVSEA approval and are not recommended for installation on new construction ships due to their sound attenuating characteristics.

The minimum free hose length, or visible length between fittings, is 9 in for hose sizes -4 (1/4 in) through -64 (4 in), and 24 in for hoses larger than -64 (4 in). The hose length requirement also applies to each hose length for the 90-degree and 180-degree assemblies. This constraint increases the cooling circuit's size and likely increases the effective cooling system's footprint within the compartment.

The maximum allowed temperature is 200 °F for rubber hoses, 380 °F for PTFE hoses, and 600 °F for metal hoses. For the NiPEC cooling system, temperatures are not expected to exceed 200 °F.

Life-cycle specifications include shelf life, service life, logistics, and maintenance requirements. Shelf life is defined as the period from manufacture to approximately the installation time frame. Service life is defined as the period from installation to end-of-life and accounts for periods when removed from the system. The shelf life and service life for metal and polymer-based hoses are unlimited as they do not degrade from atmospheric conditions. However, the shelf life and service life for rubber hoses, if used in a NiPEC cooling capacity, are 12 years each. The increased use of flexible hoses in shipboard applications requires a linear increase in the amount of onboard spare parts. All hoses require at least an annual inspection, with some rubber hoses requiring a more frequent periodicity. The inspection criteria for rubber hoses is more involved and potentially disrupting to system operations than the inspection required of other flexible hoses. Hydrostatic tests of rubber hoses are more intrusive and frequent than those required of other flexible hoses. However, rubber hoses are less prone to kinking during installation.

Naval administration strongly recommends the use of PTFE hoses on new construction ships when a flexible hose is required. The life-cycle specifications and costs nominally support the recommendation with some exceptions. As the design stands, the current NiPEC cooling system does not necessitate or benefit from the use of flexible hoses though future design iterations may choose to incorporate this component.

## Chapter 6

# Water Chemistry Components

## 6.1 Corrosion Analysis

Consideration is given to the effect corrosion has on cooling system components and its possible curtailment of the overall system lifespan. Design choices, enabled by military and commercial standards, mitigate the negative effects of corrosion mechanisms. However, they rely on robust administrative programs and technician follow-through to ensure that proper operation and maintenance are conducted.

In all states of operation, the cooling system is vulnerable to general corrosion. The process thins the affected metal by the oxidation of the exposed surface. Specifically, the oxygen interacts with the metal ions to create a thin passive-oxide layer on the material's surface. If the passive-oxide layer is removed by physical or chemical means, the process repeats and the metal continues to thin. Alternatively, if the passive layer is maintained, studies have shown that the general rate of corrosion can be reduced. Adherence to the chemistry standards set forth and the design recommendations of piping design reduce the vulnerability of the protective passive-oxide layer to chemical attack and dissolution. Although oxidation of alloy surfaces is generally considered detrimental, passivation of system components and maintenance of the oxide layer enhance the cooling system's longevity and reduce life-cycle costs [14].

Galvanic corrosion, as previously discussed, preferentially corrodes the anode in a galvanic cell. The mechanisms that enable this reaction should be removed or reduced.

The installation of an electrically resistant material at the junction of components can accomplish this. Specific to the design, the use of a gasket or o-ring should be used when interfacing piping or piping components. If SAE 304, 304L, or 316L is the build material, flat rubber gasket material shall be used. Cu-Ni or bronze components shall use fluorocarbon o-rings and gasket materials from Table 6.1 [27]. When considering the use of other non-metallic insulating materials, the following guidance is provided by MIL-STD-889 [28] for selection:

- Free of corrosive agents (salts)
- Free of acid or alkaline materials (leachant must be neutral pH)
- Free of carbon or metallic particles
- Are not electrically conductive (>104 ohm-cm resistivity)
- Are not subject to significant bio-deterioration
- Will not support fungal growth
- Do not absorb or wick water in amounts that make them electrically conductive

The recommended design utilizes demineralized water as the cooling medium for the iPEBB. This choice reduces the electrolytic content of the fluid, therefore lessening the effects and severity of corrosion. Faying surfaces should be water-tight sealed to prevent introducing fluid, with inherent or acquired electrolytes, into areas vulnerable to galvanic corrosion. One reason is that the performance requirements for the pipe insulation require that it not exceed 250 ppm water-leachable chlorine, fluorine, and bromine. If the fluid inside the piping were to leak past joints and contact the insulation, it could cause substantial amounts of corrosion due to the leached chemicals. The leakage or corrosion beneath the insulation and lagging would not be readily visible to operators and maintainers. Special care and attentiveness should be taken to detect and prevent such occurrences.

When differential surfaces must be connected without an electrical insulator, the anode to cathode area ratio (A/C) should be minimized as reasonably achievable. As

seen in Eqn. 5.1, the A/C has an approximately linear relationship with the corrosion rate for galvanic cells [28]. An example of this approach can be seen with the use of bolts made of a different material than the flanges it connects. The use of a less noble metal for the joining materials without an electrical insulator prevents corrosion of the high-value component and preferentially corrodes the more expendable parts. If the bolts were made of the same material as the flanges, the possibility exists of the flange material becoming a more active metal and corroding in submission to the bolts.

The following components or processes were not adopted for the proposed design but should be considered and investigated for future use:

- Sacrificial coatings or components such as zinc anodes
- Coatings or additive manufacturing which increase the material's electrical resistance
- Active corrosion protection such as an impressed current cathodic system

Electrolytic corrosion uses a similar mechanism to galvanic corrosion, but the reaction is amplified by a sustained electrical current. The electrical current can result from coolant contacting electrical components or surfaces at high potential. A specific caution, "piping systems should never be used as a ground return [23]." Furthermore, non-metallic piping sections are recommended for use between the electronic equipment being cooled and the rest of the cooling system.

Most metal alloys used for construction and build applications have a higher corrosion rate in acidic solutions. Furthermore, some metals such as iron, zinc, aluminum, and magnesium react poorly in acidic solutions. However, if the solution becomes excessively alkaline, it may cause dissolution or rapid corrosion of soluble metal oxides. Therefore, a cooling fluid with a neutral to slightly alkaline pH is recommended.

The Pourbaix diagrams for copper and nickel are superimposed in Fig. 6-1. The diagrams allow for an evaluation of the general corrosion resistance of metals in aqueous solutions. They can provide a basis of expectation for the passivity of metals

in various conditions. The diagram shows the relationship between the metals' potential and the pH of the liquid. pH can be adjusted by increasing or decreasing the liquid's alkalinity. Similarly, the potential can change based on the metal's fabrication, inherent qualities, or imposed current, such as that from cathodic protection systems. Pourbaix diagrams assume that the metal is at equilibrium at approximately 25 °C. The diagram gives no information on the actual corrosion rate, nor does it give consideration to localized corrosion.

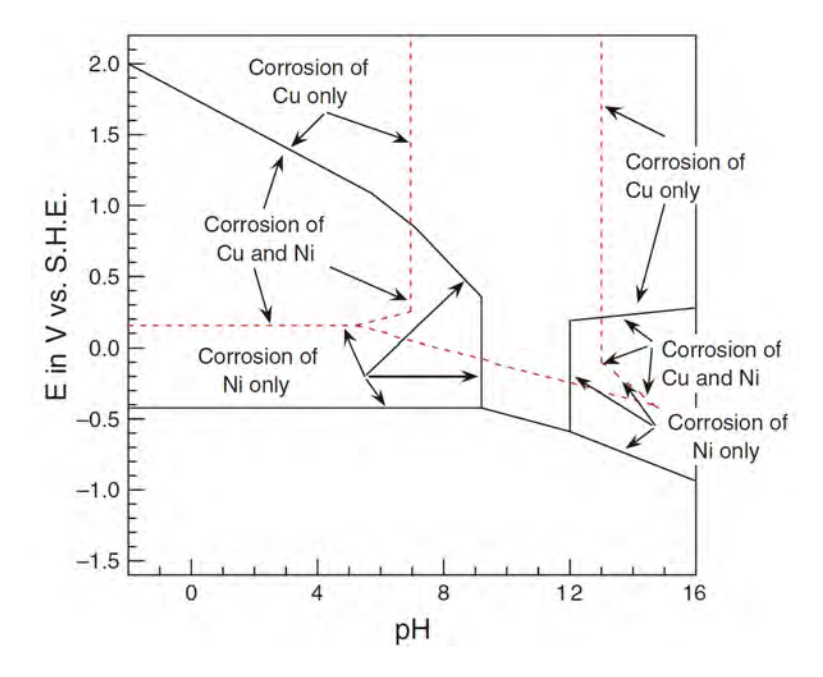


Figure 6-1: Superposition of the Pourbaix diagrams for copper (dotted lines) and nickel (solid lines) at 25 °C. E in V vs. SHE is the metal's potential when measured by a standard hydrogen reference electrode [16]

Fig. 6-1 shows that  $Cu_2O$  and CuO, the predominant oxide layers for Cu-Ni 90/10 and 70/30, provide passivity at neutral to mildly alkaline values of pH. For a similar range, the oxidation of SAE 304 and 316 alloys also show passivity. Fig. 6-2 shows this by superimposing the Pourbaix diagrams for chrome and Iron. SAE 316 develops a  $Cr_2O_3$  and  $Fe_2O_3$  oxide bi-layer, with the latter being the outermost layer. Alloy 304 develops a  $FeCr_2O_4$  oxide layer with more restricting passivity limits than SAE 316.

From this analysis, the water chemistry for the demineralized water should be maintained within pH range for the selected alloy to enhance the corrosion resistance properties of the system. The pH can be achieved and maintained with chemical additions or installed filters. However, chemical additions should minimize changes in conductivity, total dissolved solids, and chemicals deleterious to the construction materials. Challenging this effort is the ionization of carbon dioxide to carbonic acid, and subsequently to bicarbonate and hydronium ions. The increased concentration of hydronium ions lowers the pH of the liquid, which makes it more acidic and prone to corrosion. Though the demineralized water may start out at a pH of 7 when freshly produced or demineralized, exposure to the carbon dioxide in the air can reduce pH to about 4.8 and should therefore be mitigated.

Humidity and condensation increase the likelihood of corrosion. Therefore, the proposed design counters this challenge by encasing critical components in a controlled environment cabinet. The cabinet seeks to reduce the moisture vapor content to preclude the formation of condensation at the lowest expected service temperature. Corrosion protective strategies against humidity and condensation must consider whether the cabinet is hermetically sealed. If the cabinet cannot guarantee an air-tight atmosphere, then corrosion strategies shall be designed to expect the worst potential environment [28].

Table 6.1: Cu-Ni piping component gasket material

Material	Applicable Documents	Remarks
Non-Asbestos	MIL-DTL-24696, Type II	Preferred gasket for butterfly valves
Nylon inserted rubber	804-5284201, Type 1	UNAFLEX® SBR CI-Type #96
Nylon inserted rubber	804-5284201, Type 2	UNAFLEX® Neoprene CI Sheet-Type #87
Nylon inserted rubber	804-5284201, Type 4	UNAFLEX® Buna-N CI
EPDM	MIL-DTL-22050	Ethylene propylene diene monomer rubber

High purity reverse osmosis (HPRO) water, 0.065 equivalents per million (elm) chlorides maximum, is normally used for filling electronic cooling water systems. However, the proposed design requires the use of demineralized water when filling or augmenting the cooling system. This can be achieved by passing water from a desalination plant through a demineralizer, or transferring water from a ship or shore established demineralized water source. Furthermore, chemistry tests should be performed in accordance with naval administration to ensure that the incoming water

is sufficiently pure prior to admitting it to the cooling system. The following are the minimum water chemistry standards required for the cooling system's demineralized water:

Table 6.2: Demineralized Water Purity Requirements

Total Dissolved Solids	< 10	parts per million (ppm)				
Chloride Concentration	$\leq 0.065$	equivalents per million (elm)				
Conductivity	<b>≤</b> 2	micromhos per cm ( $\mu$ mho/cm) corrected to 25 °C				
Oxygen Concentration	$\leq 0.5$	ppm by weight				
Particulate Size	$\leq 0.5$	micrometers $(\mu m)$				

The total dissolved solids (TDS) specification refers to the amount of organic or inorganic material dissolved in the cooling liquid. Examples of dissolved material include, but are not limited to metals, salts, biomass, and chemical pollutants. An increase in TDS accelerates impingement attack, erosion-corrosion, and pitting directly; it could also indicate the presence of deleterious constituents such as mercury, chlorides, and such.

The chloride specification of 0.065 elm is equal to 0.25 grains of sea salt per gallon, or 4.3 ppm TDS. Chlorides for stainless steel and copper-nickel alloys induce localized breakdown and dissolution of the protective oxide layer. Furthermore, chlorides migrate to the newly exposed pits and crevices to maintain their charge neutrality. The concentration of chlorides in these localized regions form a highly corrosive and acidic internal electrolyte.

An increase in oxygen concentration, external or internal to the cooling system components, exacerbates various corrosion mechanisms. As little can be done to change the oxygen concentration in the surrounding environment, the design focuses on minimizing the oxygen concentration within the bulk cooling solution. Oxygen is the catalyst for general corrosion. It creates a potential difference in crevice and pitting corrosion, and increases the susceptibility of some metals to stress corrosion cracking. Abidance to the chemistry specification listed in Table 6.2 greatly reduces the system's susceptibility to corrosion.

The cooling circuit is designed to minimize the effects of oxygen and carbon dioxide, from air absorption, on water chemistry. Vent valves are strategically installed on components and piping to allow the venting of trapped air and the release of liquid-entrained gasses. The first method uses high-point manual vent valves on components such as the pumps and heat exchangers to vent the components during various operations or as required. The second method is by using an air eliminator near the suction of the pump, to which the return header and expansion tank piping are attached. The device is located near the pump suction as it is nominally the system's lowest point of pressure. At this location, the solubility of non-condensing gasses is the lowest, which facilitates gasses coming out of the solution. Fig. 6-3 shows an example of a typical air eliminator. Other means of preventing air absorption that were not incorporated into the design, but should be further investigated, are the use of a neutral gas to pressurize the expansion tank, a membrane or diaphragm style expansion tank, and the use of automatic high-point vent valves to supplement or replace manual means.

Conductivity measures the ion content of the bulk fluid. The analysis provides an insight into what other contaminants may be in the fluid aside from chlorides. For example, if an unintentional air addition was suspected, an increase in conductivity would be expected from the ionization of carbon dioxide to bicarbonate and hydronium ions. A pH analysis could also aid in detecting an air addition, as pH is expected to lower with the formation of carbonic acid. The conductivity analysis is not limited to this example but demonstrates how it can be used to detect a change in ion content from the baseline concentration and determine if hazardous constituents are present.

## 6.2 Chemistry Station and Filters

Filters and demineralizers mitigate the severity of water chemistry casualties and promote the health and longevity of the cooling system against corrosion. Filters remove the particulate content from the bulk fluid to protect pump bearings and valve seats, and prevent the build-up of matter in flow-restricting passages. Two

filters are designed for use in the cooling system. One filter is installed on the return header, upstream of the pump's suction. Its purpose is to remove particulates from the return header or expansion tank prior to directing it to vulnerable downstream components. The second filter is installed in-line and upstream of the demineralizer as seen in Fig. 3-1. Its purpose is to prevent the early exhaustion or damage of the resin bed, as a filter in this location is more readily replaced and maintained than the demineralizer.

The demineralizer is designed as a recirculation loop about the pumps. It draws its suction at the discharge of the pumps, and its return is connected near the pump's suction. The demineralizer shall be capable of filtering the entire contents of the liquid cooling system within a 24-hour period with a 20% margin. A flow regulating device shall be used to maintain the required rate of coolant flow to the demineralizer. The consequences of excessive flow could damage the demineralizer components, whereas insufficient flow may not provide adequate filtering needs. An oxygen cartridge is the first component in the demineralizer. It houses an anion resin designed to remove oxygen from the bulk fluid. The second cartridge is a mixed-bed resin, made up of anions and cations, designed in-line and downstream of the first cartridge. The mixed-bed resin is designed to remove metallic particles, hard water ions, and carbon dioxide. The filter and demineralizer shall be selected to maintain the chemistry specifications listed in Table 6.2.

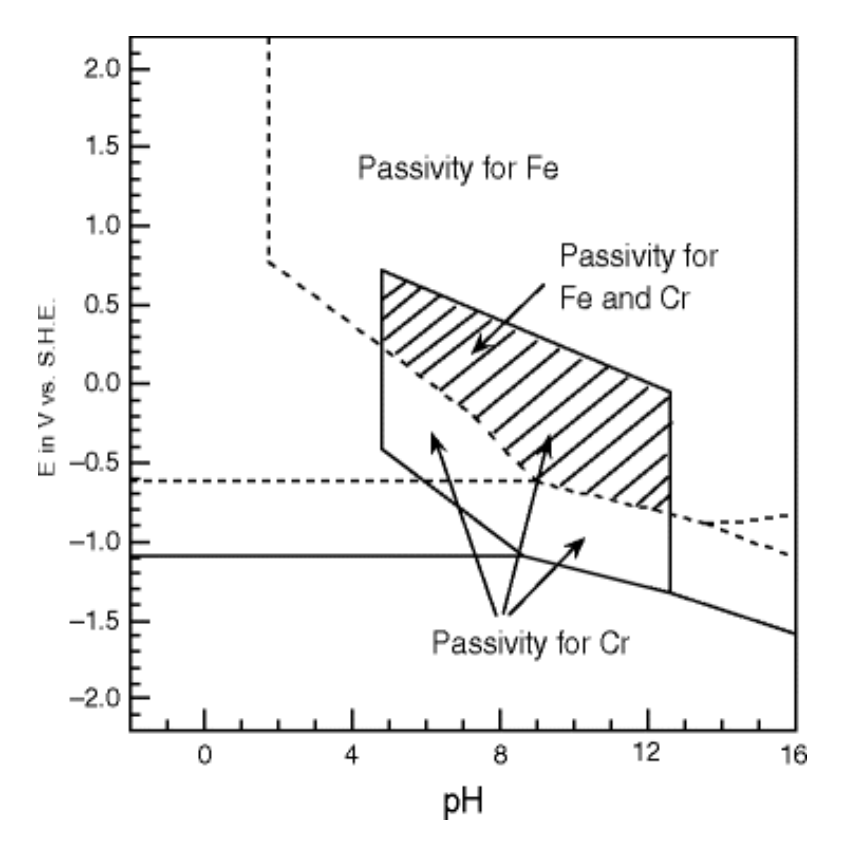


Figure 6-2: Superposition of the Pourbaix diagrams for iron (dotted lines) and chromium (solid lines) at 25  $^{\circ}\mathrm{C}$  [16]

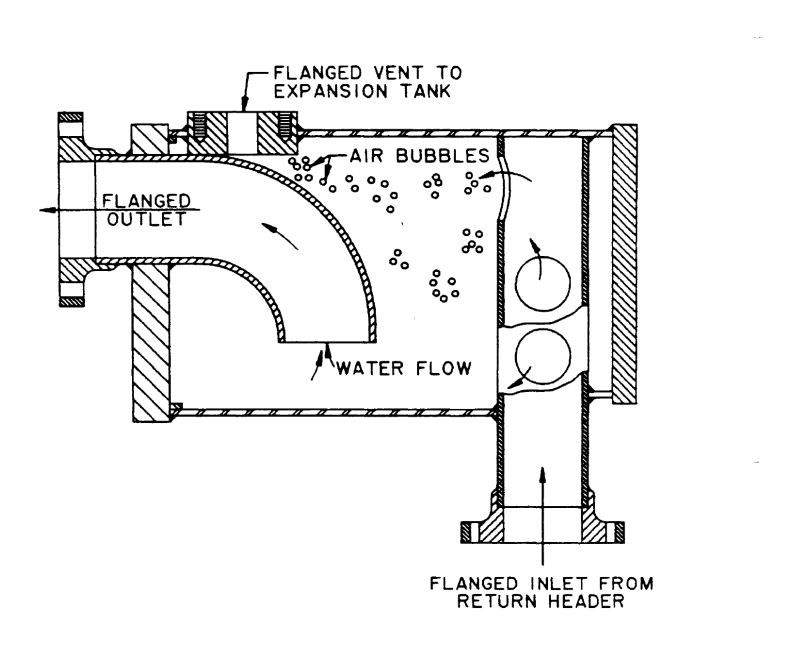


Figure 6-3: Air Eliminator [23]

# Chapter 7

## Cold Plate

## 7.1 Initial Design

Initial cold plate designs were based on the work done by Padilla et al. [31]. The study identified that the limiting operational iPEBB heat load occurs when half the semi-conductors operate at 80% load and the remaining at 20% load, vice an equal distribution of load. The study considered two cold plate designs, a single-pass serpentine arrangement and a counter-flow-style heat exchanger. The designs are depicted below in Figures 7-1 and 7-2. The heat removal performance of the counter-flow design enabled a lower maximum temperature per semi-conductor. This was in part due to each semi-conductor being exposed to multiple loops with lower maximum water temperatures. Other notable discussions are that the counter-flow heat exchanger required less pumping power due to less flow resistance from shorter pipe lengths with fewer bends. Additionally, diminishing returns in semi-conductor temperature decrease were observed at water velocities greater than 2.5 m/s for the finalized piping diameter of 3/8".

Four design iterations were assessed to optimize flow performance and operational synergy with interfacing systems. The first design iteration, Fig. 7-7, continued the design basis from [31] for a counter-flow arrangement, with slight modifications. Flow from the inlet piping, attached to the side of the cold plate, is directed into a 1" diameter inlet plenum. In the inlet plenum, water is directed through 3/8" diameter

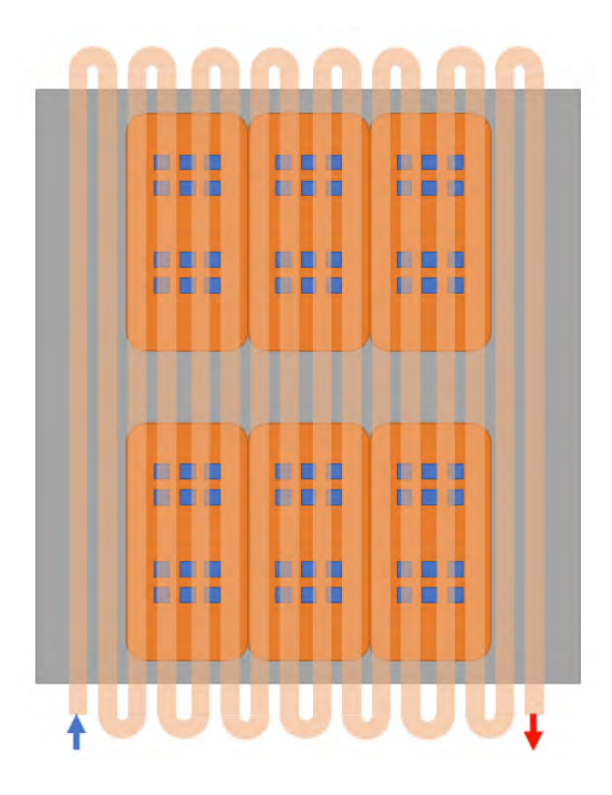


Figure 7-1: Cold plate arranged as a single-pass heat exchanger Padilla et al. [31]

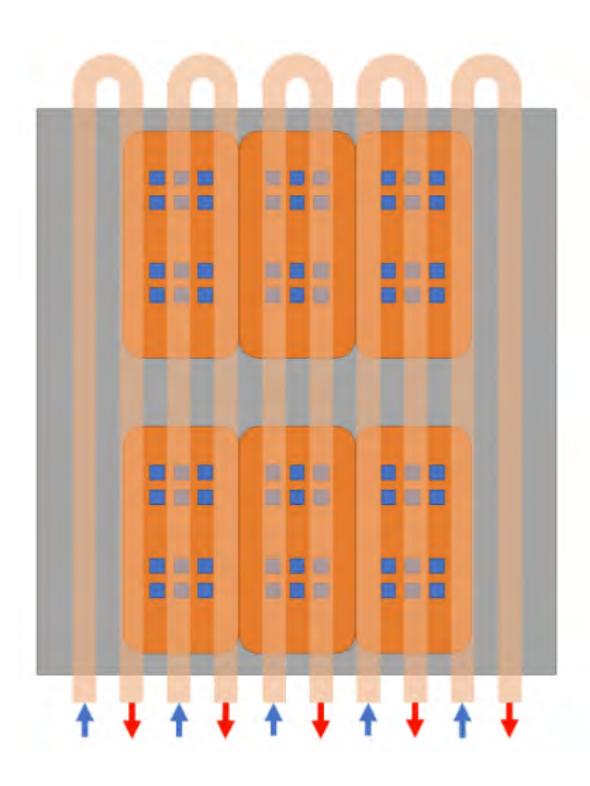


Figure 7-2: Cold plate arranged as a counter-flow heat exchanger Padilla et al. [31]

channels to the opposing side. Flow is directed back in the opposite direction via a 180° loop (u-tube). Water continues along the 3/8" channels and reintegrates in a 1" diameter outlet plenum. Water exits the plenum via the outlet piping attached on the same side of the cold plate as the inlet piping. Flow from the 3/8" cooling u-tubes were rotated 45° along the z-axis, so that the return piping sat in a lateral plane adjacent to the supply piping. The arrangement allowed for more cooling tubes to be designed adjacent to the iPEBB interface, therefore increasing the cooling capacity of the cold plate. The 3/8" return piping with the relatively warm return water lays away from the cooling interface so as to provide maximum cooling to the iPEBB. The design reduces the amount of piping needed for this configuration, which reduces the amount of head loss from pipe and valve fluid friction. The arrangement of both the inlet and outlet piping on one side of the iPEBB facilitates inspection and minimizes the iPEBB stack's spacial footprint, as seen in Fig. 7-4. At the time of design, the securing mechanism that moved the cold plate against and away from the iPEBB was unknown. This iteration maximized the interface surface availability for a potential securing mechanism design.

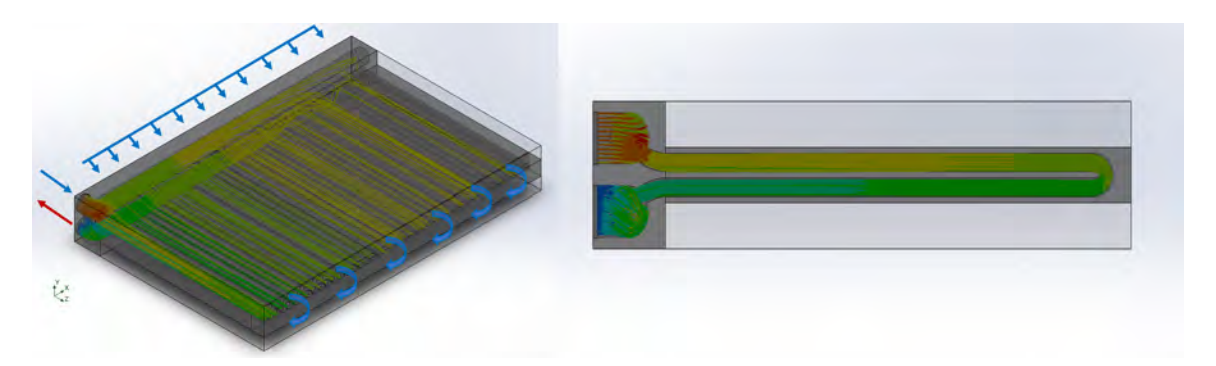


Figure 7-3: First iteration - single inlet, single outlet offset u-tube cold plate design

Non-uniform cooling distribution across the cold plate risked uneven thermal expansion and contraction of the cold plate and iPEBB materials. The potential distortion would likely cause a non-uniform compression of the thermal pad. The thermal pad is the component designed to lay between the iPEBB and cold plate and provide even heat transference between components. It performed its function when under proper compression between surfaces. Therefore, if uneven stresses compress the ther-

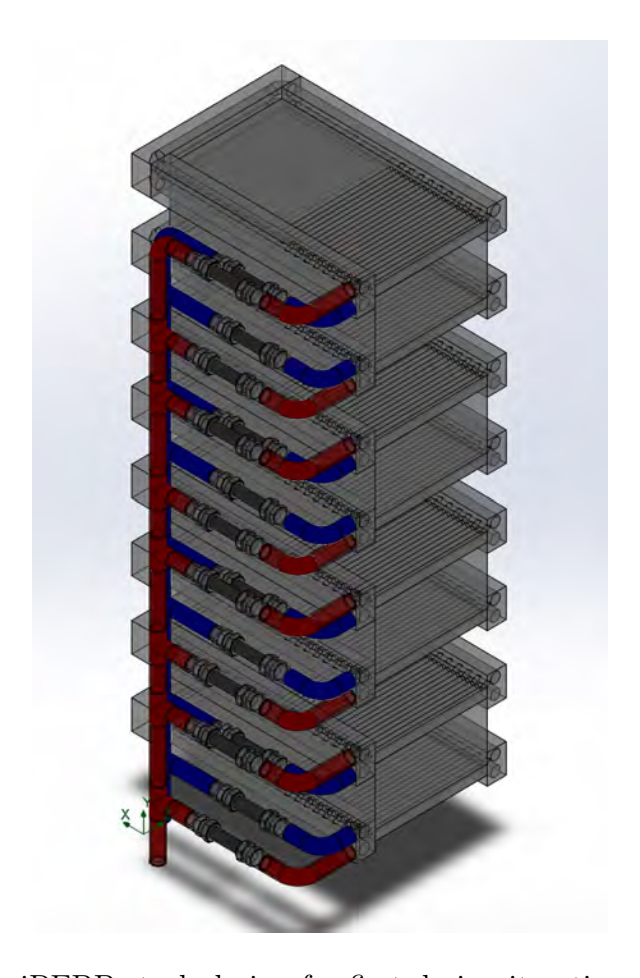


Figure 7-4: iPEBB stack design for first design iteration cold plates

mal pad it could fail to provide an adequate medium to remove heat from the iPEBB.

The subsequent design sought to mitigate the issue by providing even cooling from both sides of the cold plate.

#### 7.2 Second Design

The second design iteration, Fig. 7-5, was a double inlet, double outlet, opposing parallel flow design. Flow from each inlet piping, attached to the sides of the cold plate, and directed water into a 1" diameter plenum. In the inlet plenum, Water was directed through 3/8" alternating channels. Water continued along the 3/8" channels to the opposing sides' 1" outlet plenums. Water from the 3/8" channels reintegrated at the outlet plenums and exited the cold plate from their respective outlet pipe connected at the front of the cold plate. The design provided a more uniform cooling distribution at the expense of increasing pump head and the iPEBB stack's spatial footprint, as seen in Fig. 7-6. At the time of design, it was determined that the electrical connecting interface for the iPEBB would be situated on its back-facing surface. Placement of the inlet and outlet piping was such that if a cooling leak developed, it would involve less risk and increase the chances of early detection if the piping were located near the iPEBB's frontal areas. Additionally, placement of inlet and outlet piping near the front would facilitate maintenance and repair.

#### 7.3 Third Design

The third design iteration, Fig. 7-7, was a single inlet, single outlet, opposing parallel flow design. It was of a similar design to the previous iteration, except that it utilized a plenum bridging segment to reduce the amount of required piping. Flow from the inlet piping, attached to the side of the cold plate, directs water into a 1" diameter plenum. In the inlet plenum, some of the flow is directed into 3/8" alternating channels, while the remainder continues to flow along the plenum to the back of the cold plate. The water reaching the back of the cold plate is directed along the back-side to a secondary

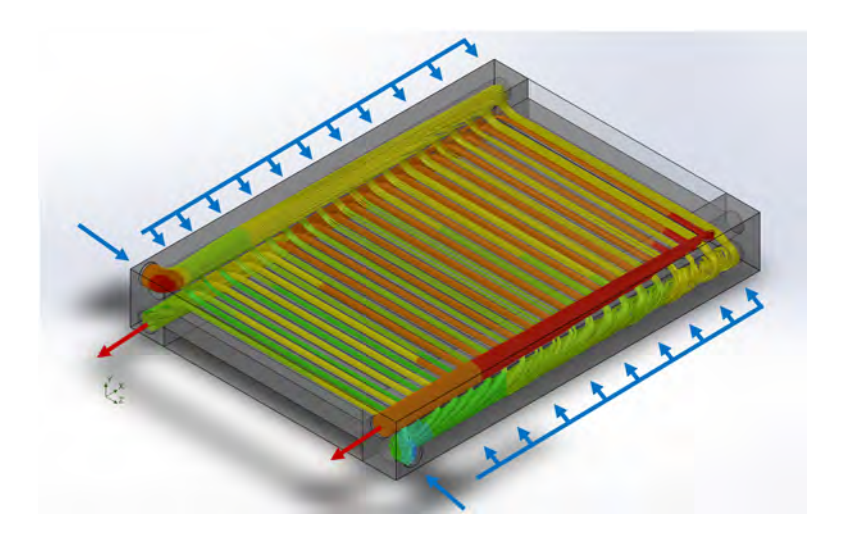


Figure 7-5: Second iteration - double inlet, double outlet, opposing flow cold plate design  ${\bf r}$ 

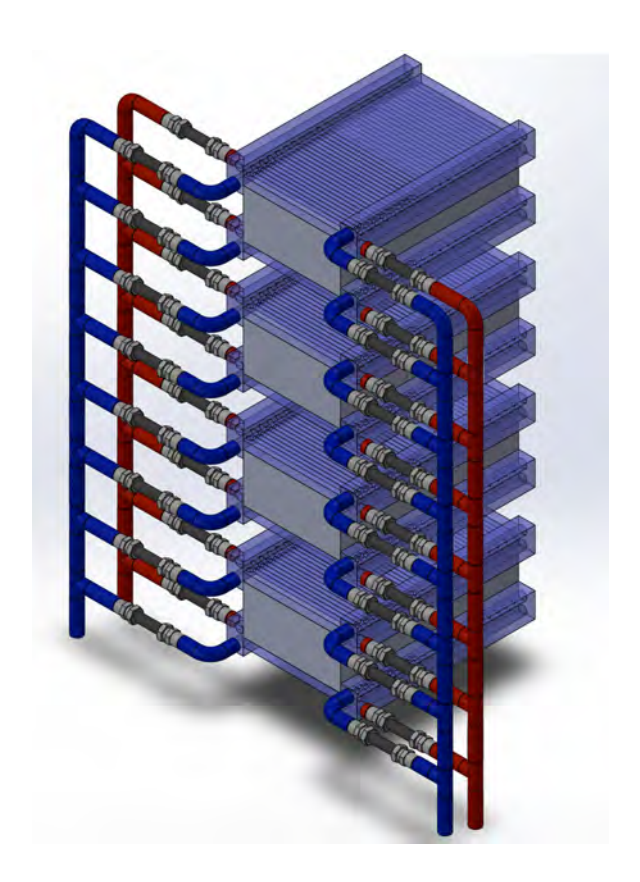


Figure 7-6: iPEBB stack design for second design iteration cold plates

inlet plenum on the right side of the cold plate. Water in this second inlet plenum is directed into its respective 3/8" alternating channels. Water continues along the 3/8" channels to their opposing sides' 1" diameter outlet plenums. Flow from the 3/8" channels originating from the first inlet plenum is directed to the back of the cold plate via the outlet plenum. The water reaching the back of the cold plate is directed along the back-side to an outlet plenum that reintegrates water from both inlet plenums. Water then exits the cold plate via the outlet piping on the same side and laterally adjacent to the inlet piping. The advantage of this design is that it allows for even cooling of the iPEBB, while reducing the piping head loss and minimizing the iPEBB's spatial footprint. Additionally, the design meets the military specification requiring each cold plate to have a single supply and return water connection [6]. The cold plate utilizes the iPEBB stack design from Fig. 7-6.

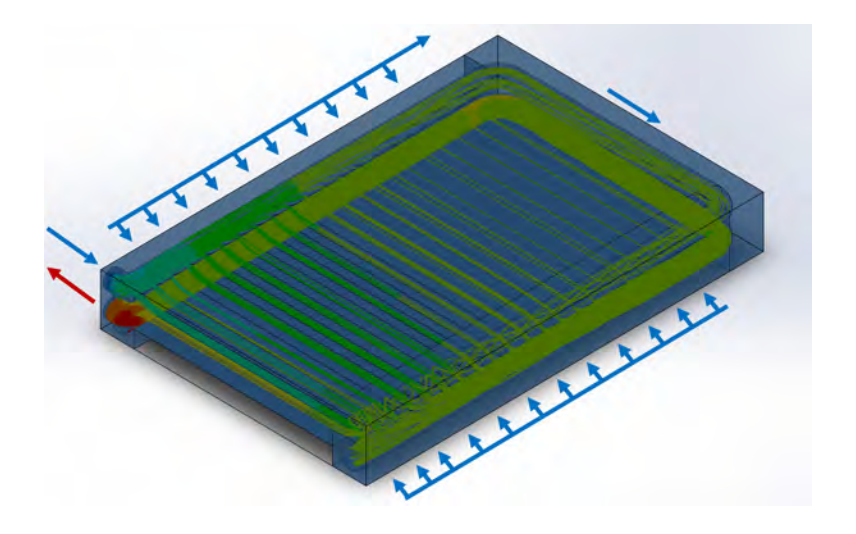


Figure 7-7: Third iteration - single inlet, single outlet, opposing flow cold plate design

#### 7.4 Final Design

The final design iteration, Fig. 7-8, utilizes a similar design to the previous iteration, except with a different placement of the inlet and outlet piping. Internal flow remains the same, while the inlet and outlet piping are located near the back end of the iPEBB and in concentric alignment with the axis of a hinge mechanism. Previous

design iterations assumed that if the cold plate moved for removal or installation of the iPEBB, a system of rigid hoses would permit a 1" lateral movement of the cold plates. The cold plate securing mechanism was finalized to a hinge-style design that would pivot along the back edges of the iPEBB. Placement of the inlet and outlet piping at the center of rotation removed the need for the lateral movement of the cold plate and the flexible hose system.

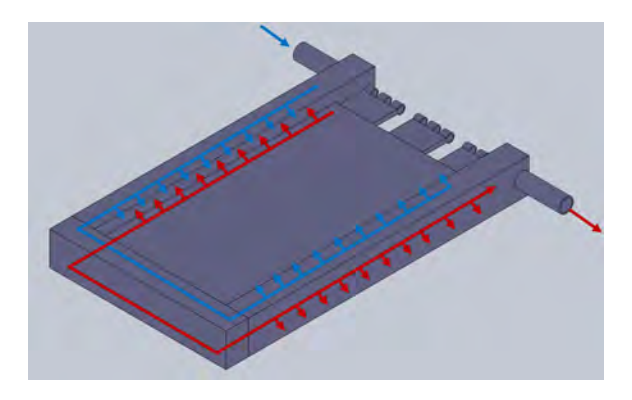


Figure 7-8: Cold plate arranged as a counter-flow heat exchanger

A fluid simulation was performed on the final cold plate design. The simulation assumed a demineralized water inlet pressure of  $100 \ lbf/in^2$  and a mass flow rate of  $0.5245 \ kg/s$ , or  $336 \ gpm$  divided equally among the 40 cold pates at 46 °C. Fig. 7-9 and 7-10 show the flow trajectories and pressure and velocity ranges across the model.

The flow velocities are projected to be well within the safe limits for the heat exchanger's internal components, but of sufficient magnitude to minimize the probability of biological surface fouling.

A pressure drop of approximately 0.2159  $lbf/in^2$  is calculated and meets the required design criteria of not exceeding a 10  $lbf/in^2$  pressure drop [6].

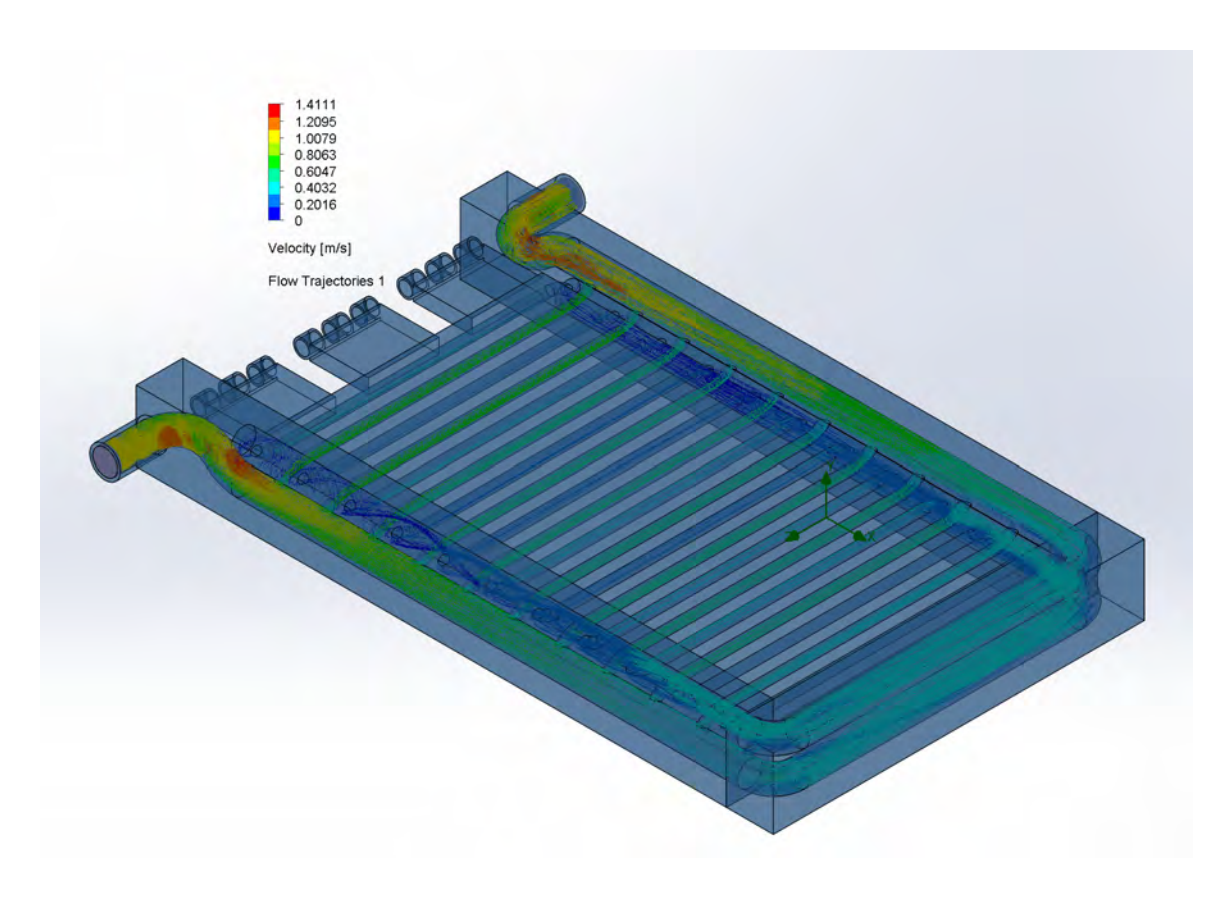


Figure 7-9: Cold plate demineralized water flow velocities

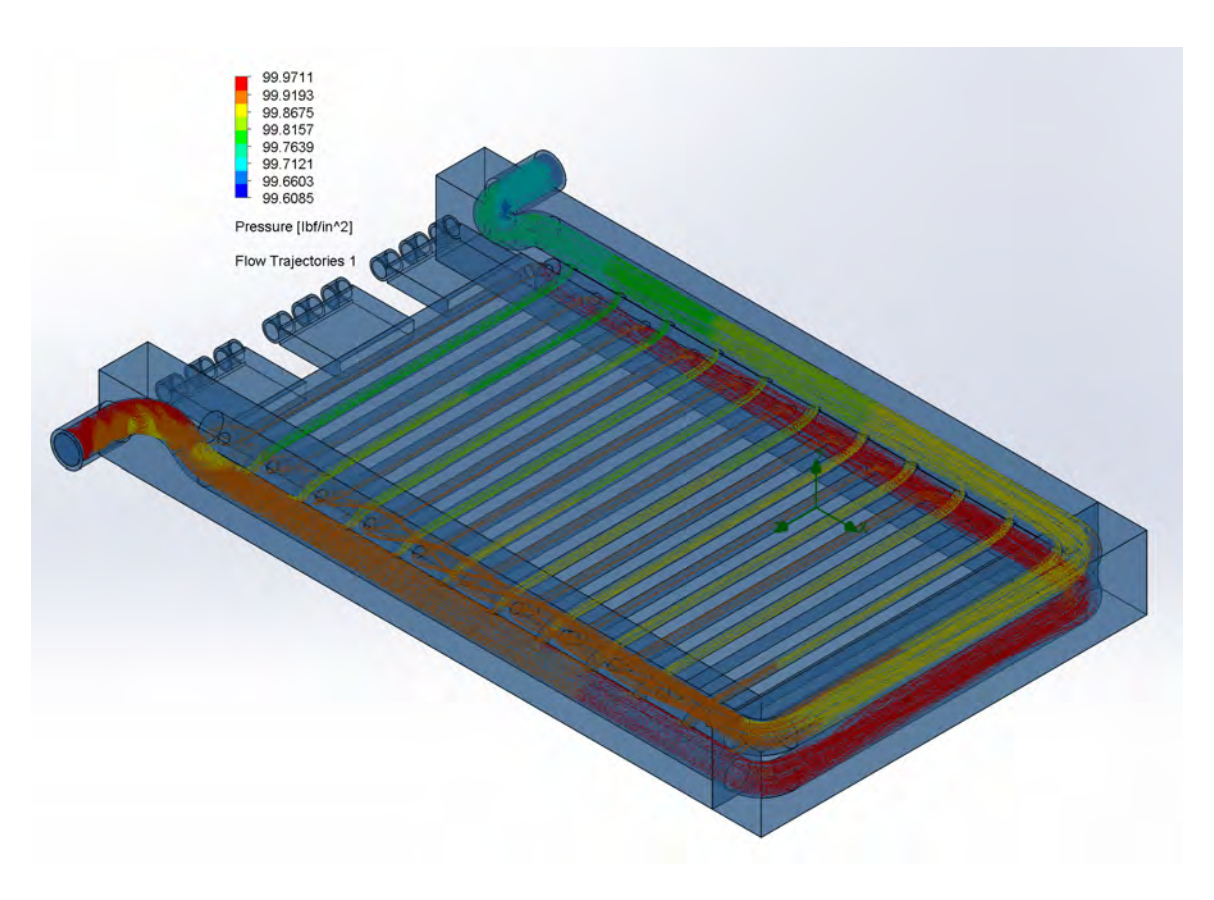


Figure 7-10: Cold plate demineralized water flow pressures

# Chapter 8

# Overall NiPEC Cooling System Architecture

#### 8.1 iPEBB, iPEBB Assembly, and iPEBB Stack

The iPEBB is installed manually into the electrical distribution system by an operator. It interfaces with the ship's system via connection ports on the rear face of the iPEBB. The connection ports from the iPEBB mate with their corresponding terminals, which are mounted on a rigidly affixed back-plate. The terminals are attached to cabling that networks the iPEBBs within the NiPEC compartment to the ship's loads, power sources, control systems, and other electrical system subsystems. The iPEBB is guided and aligned into position by a rail system attached to its side faces. It slides along the track until the connection is made at the rear, as seen in Figures 8-1 and 8-2. The number of electrical connectors has varied through different iPEBB design iterations. The most recent design features four rear-facing electrical connectors required for AC operations. However, the iPEBB figures displayed in this thesis represent a two-connector model limited to DC operations. It is assumed that the iPEBB's rear surface and electrical connections are maintained in position by an external force and securing mechanism.

Following the assumptions of Cooke et al. [3] with regards to geometry and arrangement, groups of iPEBBs are stacked in vertical alignment. The configuration

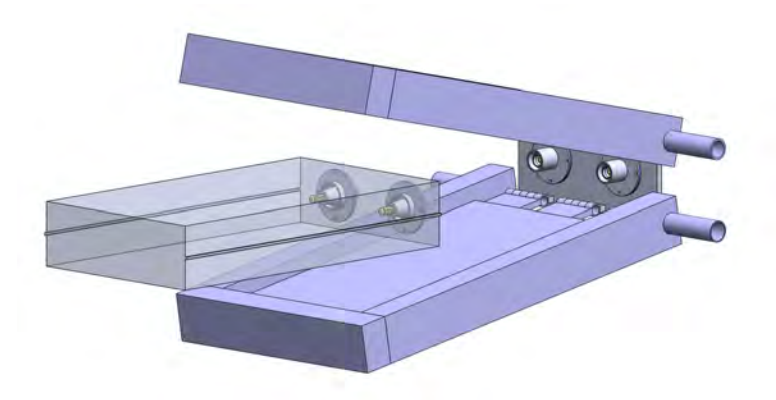


Figure 8-1: iPEBB being inserted into the operational position with cold plates in the stowed position.

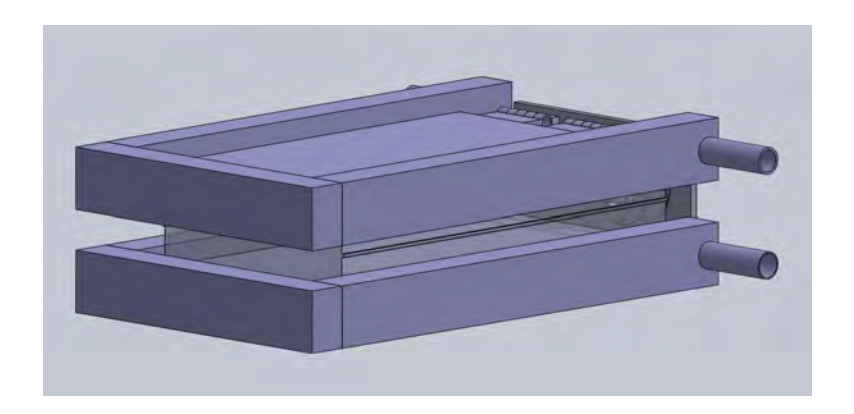


Figure 8-2: iPEBB inserted into the operational position with electrical connections made and cold plates positioned to provide cooling

makes effective use of spacial allowance and facilitates support system interfaces. The grouping of iPEBBs, termed iPEBB stack, is 69" tall. The width and depth of an iPEBB stack are, at a minimum, 15.811" and 21.685" respectively.

This study proposes that no electrical components be contained within the bottom 9 inches of the iPEBB stack due to the requirements of MIL-SPEC-3045. All transformers, controllers, and motors with electrical terminals or energized parts shall not be lower than the bottom sill of the compartment's main access door. The compartment is expected to be outfitted with a quick-acting watertight door (QAWTD) for damage control purposes. The minimum distance from the door's bottom sill to the ship's deck is 9 inches, which serves as a design basis for the iPEBB stack MIL-PRF-32482A. The exception to this requirement is for equipment located in machinery room levels, which should be considered for future system design iterations. The 9-inch specification is meant to prevent damage or loss to electrical equipment from compartment flooding. If flooding were to occur within the compartment, the QAWTD could be opened to direct the flooding out of the compartment before reaching vital electrical components.

The remaining 60" of reserved iPEBB stack height is equally distributed to four iPEBB assemblies. An iPEBB assembly is considered a grouping of one iPEBB, two thermal pads, and two cold plates, as seen in Fig. 8-2. Each iPEBB assembly requires a minimum of 12" of vertical space to accommodate the height of the assembly and the operating travel range of the cold plates. Though five iPEBB and cold plate assemblies could marginally fit within the budgeted space, the uncertainty of the securing mechanism's design and the final iPEBB design height conservatively suggest that four assemblies is a more feasible design approach.

When the iPEBB is situated in the iPEBB stack and makes the proper electrical connection at the back plate, the cold plates rotate down onto the thermal pad and iPEBB. Rotation occurs via a hinge system, which attaches each cold plate to the back plate at the rear of the iPEBB assembly. The axis of rotation is horizontal and perpendicular to the cold plate, as seen in Fig. 8-3 and 8-4. Each cold plate compresses its respective thermal pad against the iPEBB so that each component's

main heat transfer surface lays flush against the other. The thermal pad serves to promote even heat transference between the iPEBB and coldplate, which is challenged by surface imperfections, potential contaminants, and component alignment. The cold plates are pressed against the thermal pad and iPEBB by a securing mechanism, currently in design by Tomlinson [37], to maintain sufficient mating pressure and functionality. When the iPEBB is not installed, the cold plates are rotated away and maintained in a position to allow sufficient clearance for iPEBB installation. The securing mechanism is designed to provide a minimum of 1" of vertical clearance between the front edge of the cold plate and the top and bottom surfaces of the iPEBB, as seen in Fig. 8-5. 2 to 3 millimeters of clearance are provided at the rear of the assembly between the cold plates and the iPEBB as seen in Fig. 8-6. The clearances permit the unhindered travel of the iPEBB, with attached thermal pad, when it is inserted or removed from the installed position.

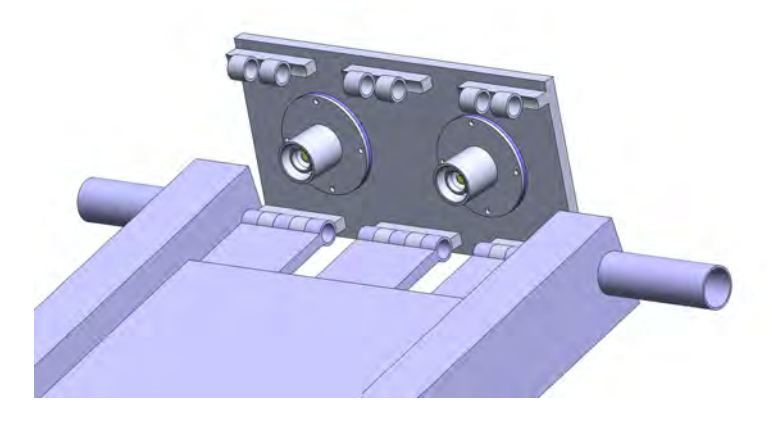


Figure 8-3: Unobstructed view of back-plate hinge mechanism and connection terminals

Cold plate inlet and outlet tailpipes are attached to the sides and near the rear of each cold plate. The tailpipes are in concentric alignment with the cold plate hinge mechanism. The configuration permits a straight or angled swivel fitting to connect the cold plate with the rest of the NiPEC cooling system. Swivel fittings, as seen in Fig. 8-7, allow the attached pipes or hoses to rotate while providing leak-free joint functionality. The cold plate tailpipe design arrangement minimizes the dynamic motion required of the piping system by using the swivel fitting's rotating movement.

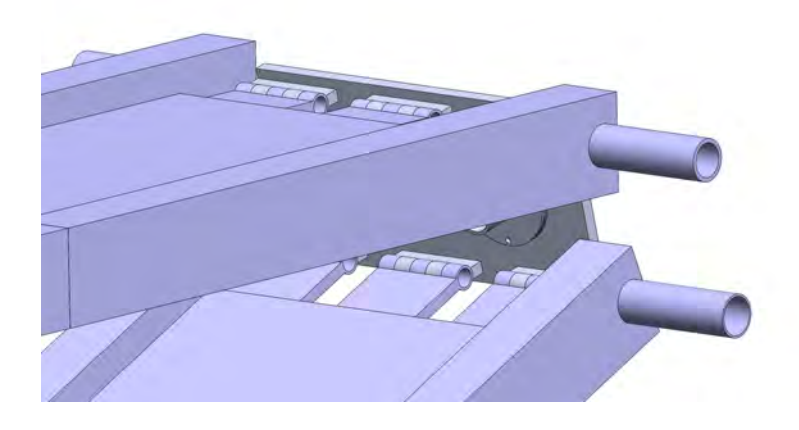


Figure 8-4: View of hinge mechanism connecting the cold plates to the back-plate

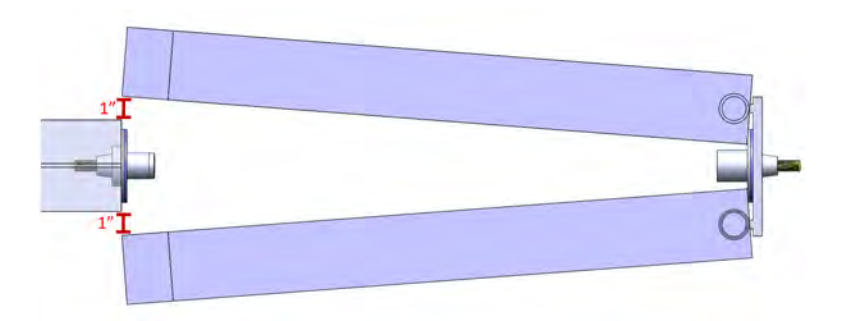


Figure 8-5: iPEBB and cold plate front edge vertical clearances during iPEBB insertion or removal

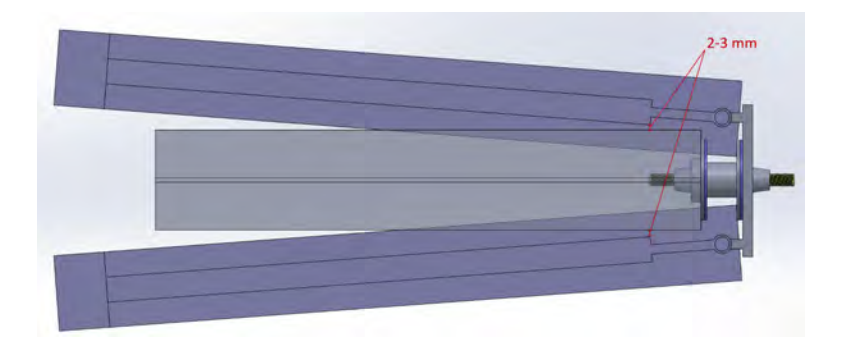


Figure 8-6: iPEBB and cold plate back edge vertical clearances during iPEBB insertion or removal  $\,$ 

A different cold plate surface mating approach would require the vertical travel of the cold plate towards and away from the iPEBB. If vertical travel of the cold plates was implemented, a flexible hose would have to be used to permit such motion. The minimum hose lengths, sans fittings, that are required for a flexible hose to permit vertical motion via an S-bend, as seen in Fig. 8-8, are calculated in Table 8.1. The values are calculated based on the minimum bend radii, hose diameters, and geometric arc length equations. Implementing the vertical motion design would require the installation of thousands of hoses though-out the ship solely for NiPEC cooling. Given the limitations and drawbacks of flexible hoses discussed in previous chapters, a hinge design with a swivel connection is the optimal solution as it negates the need for flexible hoses. Swivel joints are permitted for use in NiPEC cooling applications and are able to meet the system design limits such as pressure, temperature, and material MIL-DTL-18866K. The tailpipes are integrated into the cold plate by welding or machined processes to minimize the probability of joints leaking cooling fluid onto electrical components. Of note, MIL-HDBK-251 [23] recommends the use of a nonconductive coupling for connecting the cold plate to the cooling system. A nonconductive coupling mitigates the risk of electrical potential being transmitted from the iPEBB to the cooling system. The electrical potential could cause personnel injury, damage equipment, accelerate corrosion, and even cause the electrolysis of the cooling fluid. Further study and analysis and investigation is required for component implementation.

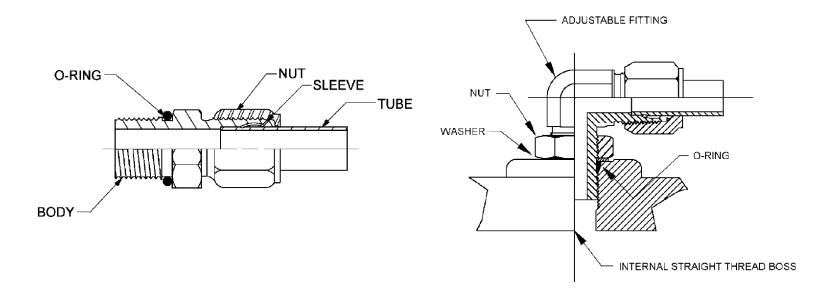


Figure 8-7: Straight and angled swivel fittings [18]

Table 8.1: Rubber flexible hose minimum lengths without fittings

Hose Size (in)	1/4	5/16	3/8	1/2	5/8	3/4	1	1-1/4	1-1/2	2
Minimum Hose Legnth (in)	3.51	3.72	4.04	4.34	4.73	5.13	5.46	6.03	6.51	7.30

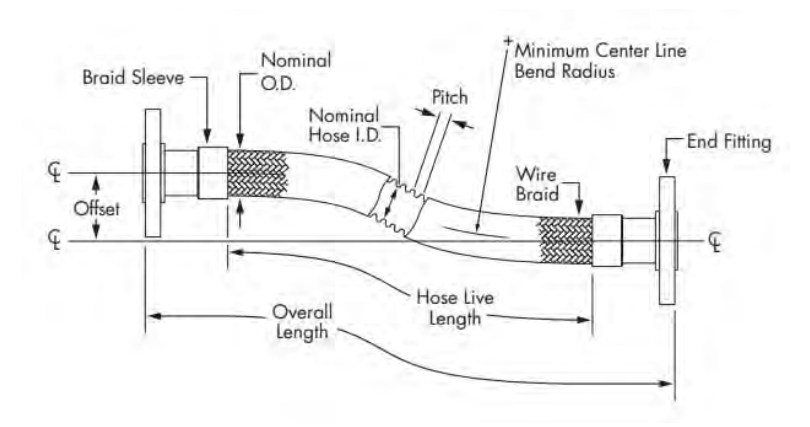


Figure 8-8: Example of an S-bend required for cold plate lateral movement [30]

#### 8.1.1 Condensation Mitigation

Since the demineralized cooling system is cooled by the ship's chilled water system, it is assumed that cold plate temperatures are capable of reaching 5-7 °C under various load conditions. Thus, condensation in marine environments can develop and pose issues of corrosion and electrical damage. iPEBB stack design must consider the risk of condensation as dew point temperatures are reached. The dew point temperature is calculated using dry bulb atmosphere temperatures, relative humidity, and psychometric charts, as seen in Fig. 8-9. The relative humidity within the compartment is assumed to be the same as the environment surrounding the ship, which is 80% relative humidity near the water's surface for most ocean environments. The compartment's dry-bulb temperature is assumed to be maintained at 70 °F. Therefore, at 80% relative humidity and a dry-bulb temperature of 70 °F, the dew point temperature is approximately 64 °F. Therefore, condensation is can be expected to form on exposed cold plate surfaces under the assumed thermal and cooling conditions.

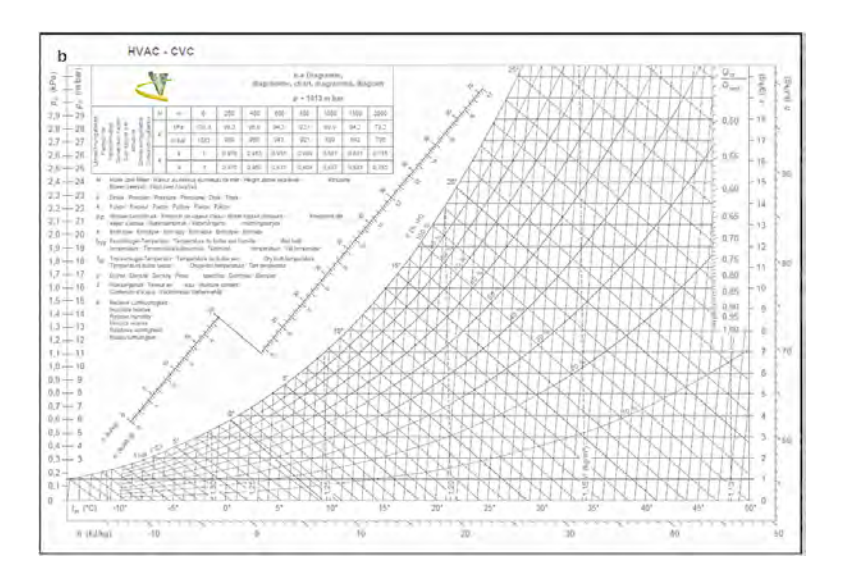


Figure 8-9: Psychometric chart at sea-level atmospheric pressures [2]

#### Fluid Flow Control

The following methods to prevent condensation were investigated based on their direct performance and minimal contribution to system complexity. Increasing the temperature of the chilled water system is limited in temperature range and operationally discouraged by DOD-STD-1399 [6]. Increasing the chilled water temperature risks cascading secondary effects to other chilled water-cooled systems and is therefore not a viable strategy.

Controlling chilled water or demineralized water flow through the NiPEC cooling system heat exchanger can increase the demineralized cooling water temperature above the dew point temperature and mitigate condensation risks. Using manual valve throttling or automatic flow regulating valves to control the chilled water flow through the heat exchanger could effectively maintain demineralized water temperatures above the dew point.

From a chilled water system perspective, regulating the chilled water flow to the several NiPEC cooling heat exchangers throughout the ship poses little risk under steady-state conditions or from minor changes in electrical heat loads. However, dynamic heat load conditions could risk causing ship-wide chilled water flow imbalances with other dependent systems. It is assumed that future chilled water system flow

capability shall be investigated and designed to support dynamic NiPEC heat loads.

Controlling demineralized cooling water flow through the heat exchanger or to the heat load components is a similarly feasible method to prevent condensation. However, demineralized water cooling flow to each component branch or supply header is achievable in a more discrete capability than the chilled water method. The drawback of regulating demineralized water flow is that using a two-way control valve could cause excessive pump head during periods of low heat load. Low heat loads would require throttling shut the control valve, restricting flow, and causing the pump to work harder and less efficiently. Using a three-way control valve to bypass the heat exchangers alleviates some of the added pump head. Regardless, regulating demineralized cooling water flow does not align with the design philosophy of providing efficient cooling flow with pipe diameter as the primary means of flow control. Therefore, chilled water flow control is the preferred method of mitigating condensation formation.

Regulating the chilled water flow manually to several compartments is cumbersome and infeasible based on varying system loads and operator capability. Thus, automatic means of flow control are more appropriate for the design scope and ship-wide implementation. However, automatic means still require local or remote monitoring to ensure proper system operation. The implementation of an automatic temperature regulating valve assumes it is installed on the chilled water inlet pipe of the NiPEC cooling heat exchanger. The valve uses a temperature sensing instrument to detect the demineralized water temperature in the supply header to the iPEBB stacks and adjust its position as needed. The use of a two-way temperature regulating valve is preferred, as using a three-way valve to bypass the heat exchangers inefficiently directs cooling water that could be used by other heat loads of the chilled water system. As temperature in the demineralized water header lowers, the temperature regulating valve will throttle shut to restore temperature to the preset temperature range. Similarly, the temperature regulating valve will throttle open to cool the demineralized water temperature. The motive force to position the valve could use electric, pneumatic, or hydraulic control mechanisms. The control mechanism should be designed in such a manner that its failure causes the valve to fully open until automatic or manual control is restored. In a casualty scenario, this feature would allow adequate cooling flow to be provided to the heat exchanger, which is not guaranteed if the valve were to fail in the shut or as-is position.

In determining the appropriate operating temperature range for the demineralized cooling water, assumptions from Section 2.1 and Padilla et al. [31] were utilized. The maximum heat load per semi-conductor switch is 167 W, and the total thermal resistance from the semi-conductor to the demineralized cooling water is approximately 0.6064 K/W. Thus, a temperature rise of 101.3 °C across the thermal interface is calculated using Eqn. 2.15. To maintain the semi-conductors within a safe operating temperature, a maximum threshold of 150 °C is assumed. The 150 °C takes into account a 30 °C safety margin at which semi-conductor damage is expected to occur. To provide the minimum cooling capability to the iPEBB, the demineralized water temperature must not exceed 48 °C (118.4 °F). Considering the calculated dew point temperature from before and the maximum demineralized water temperature, a supply header operating temperature band of 75-85 °F is recommended for the demineralized cooling system. The operating range provides an 11 °F buffer from condensation formation and a 33.5 °F margin for minimum cooling during peak heat load conditions.

The iPEBB stack design proposes the use of a controlled atmosphere cabinet as a secondary means to mitigate the risk of condensation with electronic components. The use of a cabinet to house the iPEBB stack provides significant advantages against the following challenges:

- Incidental contact with enclosed equipment
- Contamination by dust or foreign particulates
- Damage from liquid spray or splash
- Hydraulic fluid seepage
- Corrosive substances

#### • Arc flash or blast containment

The cabinet shall be 60 inches tall and sit 9 inches above the compartment's deck. Its width and depth shall be at a minimum 18 and 30 inches respectively to accommodate the size and operation of the iPEBB assembly. Each iPEBB and cold assembly shall be evenly spaced to occupy 15-inch high operating volumes. At the time of this research, there is no design requirement to physically partition the iPEBB assemblies. Thus, to facilitate atmospheric circulation within the cabinet, no partitions are implement in the design. Future design iterations may choose to incorporate partitions for structural anchoring or robustness but should consider the effects of internal air flow during design and modification. Perforated or partial partitions permit the passage of air flow but at the expense of incomplete iPEBB and cold plate encapsulation. Perforated partitions could promote arcing across the bores or cavities if exposed to electrical current and would therefore necessitate a non-conductive construction material or liner. The iPEBB rail alignment system is supported by triangular beams that span the depth of the cabinet and permit the passage of air flow. The inlet and outlet tailpipes would penetrate the cabinet at its side faces to allow connection to the demineralized cooling loop. A stuffing tube made of flexible gasketed material, such as rubber, would allow the cabinet to maintain atmosphere while permitting penetration. A flexible material would also allow for small misalignments as a result of hinge assembly yields from the applied stresses of the securing mechanism. Access to the cabinet shall be via a front panel door that extends the entire height of the cabinet. The door is secured in place by helical thumb screws along the door's perimeter that mate into the cabinet's front face perimeter edge. The design allows for complete door removal to facilitate access to all portions of the cabinet without obstruction. Multiple cabinets are able to be accessed simultaneously to facilitate maintenance without the obstruction of the door's swing from an adjacent cabinet. Naval electrical safety requirements for energized gear and initial voltage verification operations are eased in this configuration. The cabinet considers the constraints and requirements of possible iPEBB assembly securing mechanism designs. Further, detailed cabinet design features and requirements shall conform with MIL-DTL-2026E and MIL-DTL-108. An idealized model for an iPEBB stack cabinet is shown in Fig. 8-10.

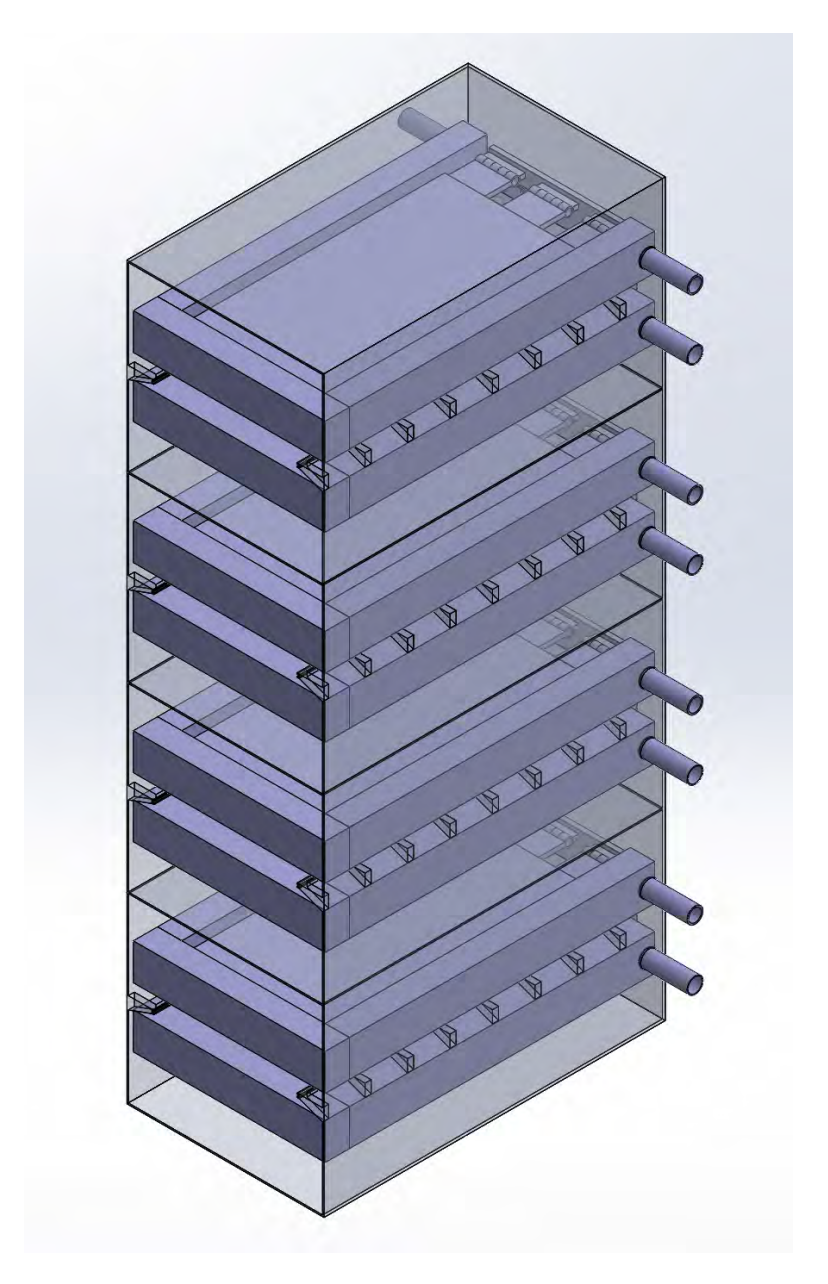


Figure 8-10: Idealized iPEBB cabinet

The cabinet's atmosphere, predominantly humidity, is controlled by a positive pressure unit (PPU). Commercial systems, similar to the EXAIR NEMA 4X [8], use compressed air and a vortex tube to supply cool, dry filtered air to enclosed cabinets. It is capable of lowering and maintaining the enclosure's atmosphere to  $\leq 45\%$  relative humidity and can provide up to 5,600 Btu/hr of cooling. Each iPEBB

stack is expected to emit approximately 137,000 Btu/hr at full load, which allows the PPU the potential to supplement the removal of approximately 4\% of the heat load. The PPU has no moving parts, which facilitates maintenance and operations. 100 psi compressed air, supplied by the ship's system or auxiliary compressor, passes through a micron filter and enters the vortex tube. The compressed air is cooled as it travels through the tube and enters the cabinet via a gasketed punch-through penetration. Non-conductive tubing is used to distribute cool, dry air to the components of concern. Air is expelled via exhaust ports on the vortex tube and released to atmosphere. The decibel rating of the devices range from 59 to 85 dBA, which is unlikely to cause hearing damage for prolonged exposure. The in-line micron filter removes dirt, moisture, and particulates before entering the vortex tube. The system can be constructed of corrosion-resistant materials suitable for marine environments. No hazardous refrigerants are used for operation as in other types of systems, minimizing the risk of personnel exposure and overall maintenance requirements. Compared to heat exchangers and heat pipes, no fans are required for circulation nor condensate collection system for operation. The vortex tube can be mounted on the cabinet's top or side faces. Application for the proposed cabinet design mounts the vortex tube on the cabinet's side face near the top. The placement provides a greater physical overhead margin for electrical cabling or additional iPEBB assemblies. An example of a PPU is shown in Fig. 8-11. Of note, the PPU is not meant to supplement the NiPEC cooling system but can provide cooling capable of negating the heating effects of warm air surrounding the cabinet.

The PPU air consumption is model dependent and ranges from 4 cfm to 80 cfm when in operation. It is capable of continuous or intermittent operations and uses a solenoid valve with an electronic control system to maintain the internal cabinet atmosphere. The intermittent model provides 1 cfm of air flow when the solenoid valve is shut, which prevents contaminants from entering the cabinet by maintaining it at pressures slightly higher than atmosphere. Assuming the proposed ship has 4 NiPEC corridors with about 12 compartments in each corridor and 5 cabinets in each compartment, the continuous air load when all solenoid valves were shut would be

240 cfm. A typical low-pressure air compressor onboard a ship is rated from 100 to 150 cfm, model dependent. Ships typically have several low-pressure air compressors, with some systems having dedicated compressors for special tasks capable of 2000 cfm. The PPU assumes the 100 psi air is drawn from humid atmospheric air conditions. Utilizing the ship's air dehydrators in combination with the compressors can yield even lower relative humidity controls.



Figure 8-11: Positive Pressure Unit Example [8]

#### 8.2 NiPEC System and Compartment Layout

The arrangement of NiPEC cooling system components and electrical distribution equipment within the reserved space is addressed to determine the feasibility of system implementation and determine the requirements for future system designs. Base assumptions are derived from [3] with regards to NiPEC compartment equipment layout and geometries. Modification of equipment characteristics and arrangement discussed in this section is based on [25] and [24] requirements.

As the primary focus of this study is the NiPEC cooling system, it is modeled to facilitate the operation and performance of its individual components and the collective framework. Maintenance and repair requirements are considered in the construction and allocation of system elements. Component builds, interfaces, and sub-components are designed, selected, or oriented to minimize the possibility of fluid leakage, and its severity when in proximity to electronic components. The arrangement of other components within the NiPEC compartment is driven by the optimization of the cooling system, as the designs of those systems have not been proposed or remain in design.

The NiPEC compartment and the systems it encompasses are categorized as 'vital' due to their critical function in providing continual operational ship capabilities. The compartment is required to provide protection from fumes, fire, and flooding to the personnel and equipment within. Furthermore, the compartment shall not sit adjacent to ship storerooms that contain hazardous materials. Given the expected corridor arrangement in the idealized ship model, the compartments will most likely be located below the ship's V-lines and are therefore required to have water-tight boundaries. If a compartment is located above the ship's V-lines, its boundaries shall be air-tight unless required to have a higher degree of protection. Aside from the compartment's normal access door, it is required to have an emergency egress/ingress route to a deck other than its own. For compartmental spatial coordination, emergency access is assumed to be via a raised quick-acting spring-balanced hatch of circular circumference that measures 30" in diameter with a dogging mechanism that protrudes 12" downward. The hatch shall be located in the overhead for compartments below the bulkhead deck and is assumed to reside in the corner of the compartment. The hatch will be accessed by a bulkhead-mounted ladder that spans the height of the compartment.

Component spacing permits access to equipment in accordance with Fig. 8-12, which considers human engineering criteria and anthropometric data from ASTM F1166 [24]. The spacing considers the movement and positioning of personnel and tools for maintenance and operations. The access path within the compartment shall

be free of obstruction and measure at least 36" in width along the path's length. The width provides sufficient space for two-way traffic, emergency egress, or passage of personnel during operations or maintenance within the iPEBB cabinet by another individual. Unobstructed headroom along the access path shall permit at least 77" of vertical clearance. The current compartment design achieves the requirement with a planned clearance of 84" plus an additional 18" of overhead space considered for light fixtures, wire runs, and ventilation ducts. Equipment shall be sized to allow for removal or installation via a path through the compartment's main access. The compartment shall be designed with an infrequent access panel or planned bulkhead removal footprint for equipment that cannot pass through the main access and shall be designed depending on the equipment's frequency of repair. The current NiPEC compartment design permits all components to transit via the main access.

Maintenance Posture	Light Clothing	Bulky Clothing	
	mm (inches)	mm (inches)	
Minimum height allowance for standing	1960 (77)	1981 (78)	
Minimum height allowance for crawling	788 (31)	864 (34)	
Maximum depth of objects which must be reached into	584 (23)	534 (21)	
Minimum width allowance for passing body	584 (23)	686 (27)	
Minimum thickness allowance for passing body	330 (13)	410 (16)	
Minimum height allowance for bending or kneeling	1220 (48)	1270 (50)	

Figure 8-12: Minimum machinery space working clearances [25]

Electrical distribution and control equipment shall not have their respective enclosure tops sit higher than 84" above the deck. A minimum of 42" of front operating space shall be required for the equipment's enclosure. 24" of clearance is required between the enclosure's back wall and the adjacent rear bulkhead to permit servicing of individual components or support equipment. On one side of the enclosure cabinet, or at the end of a row of cabinets, 24" of clearance is required. The other side of the enclosure cabinet, or row of cabinets, shall have a minimum clearance of 6" to the ship's structure. The compartment's arrangement was modified to meet the cri-

teria. A watertight barrier shall provide protection to the lower portion of enclosures containing electrical conditioning components. If the barrier is not integral to the enclosure, then it shall be provided with quick-opening drains. The iPEBB cabinet will provide the necessary watertight boundary to protect its internal components. Non-conductive and non-skid rubber matting shall be installed over the deck in front of and behind the electrical enclosures. The matting is expected to be no more than 0.5" in thickness and provide no significant change in vertical clearance.

The NiPEC cooling system design layout assumes that the components are not integrated into a single cooling unit architecture (i.e. cooling skids) for the purpose of maintenance and life-cycle growth. Liquid carrying pipes within the compartment shall best be within 36" of the most outward bulkhead which acts as a boundary between the heated portion of the ship and the unheated portion of the ship. A majority of the piping meets the 36" criteria with the exception of piping routed to and from the cooling system pumps, which have their own spatial requirements. Non-redundant pipes and cabling between vital components shall run in the most direct and orthogonal path as practical. Piping and cabling shall not be located behind deck-mounted front-serviced electronic equipment, such as iPEBB cabinets, if they are inaccessible. 30" of operating space shall be provided along the sides of the cooling pumps, with 36" of clearance provided at one end of the pump. For systems with more than one pump, 48" of operating space shell be provided between pumps unless a cooling skid arrangement is utilized. Interference removal for accessing pipes, cabling, and other components shall be kept to a minimum. When interference removal is required, it shall not be in such a manner that affects the ship's propulsion capability when underway. Electric cabling shall not be located above or adjacent to heat-generating components as practically possible. The wire runway connecting the iPEBB cabinets to the ship's electrical system is not located directly above the iPEBB cabinets. The wire runway is adjacent to the bulkhead that runs along the back side of the iPEBB cabinets.

Electrical components are oriented in such a manner that if an arc flash were to occur, it would minimize the chance of propelling front covers into watch stander

positions or areas containing flammable or combustible materials. The iPEBB cabinets are oriented such that front covers would be propelled across the compartment's main access path and against the bulkhead. As the NiPEC compartment will not be a continuously manned space the risk is abated. In relation to other machinery, electrical switchgear components, such as transformers, capacitors, and harmonic filters shall be located in their own compartment when practical; currently met by the NiPEC reserved space design basis. Electrical components are maintained at a distance from major NiPEC cooling system components to minimize the risk and severity from system leaks or ruptures. All major cooling components are located at one end of the compartment and within a 3"' tall basin with an installed deck drain. As no bilges are implemented or required of the compartment's design, the likelihood of compartment flooding is reduced. Compartment equipment shall be mounted to prevent accidental injury to personnel from mechanical systems. As mitigation, a majority of NiPEC cooling system components are located away from the compartment's main access path and rotating equipment within the compartment will have installed safety guards. Safety guards should be considered for installation around shafting, couplings, gears, a similar equipment with design considerations for maintenance access. Additional guidance for rotating machinery requires that the cooling pump's axis of rotation be aligned and horizontal to the ship's centerline when feasible. The current NiPEC cooling system arrangement does not meet this criteria, given the spatial requirements of the pumps and the spatial limitations of the idealized compartment. Future design iterations may choose to meet the requirement as ship compartment design is finalized.

Lastly, ship-wide electrical distributive system arrangement requires separating longitudinal runs by at least two vertical decks if possible, but at a minimum one deck of separation. The current design case for the four longitudinal corridors meets the requirement with one deck of vertical separation.

### Chapter 9

### Final System Design Summary

Taking all the research presented above into account, the following summarizes decisions made for the recommended NiPEC cooling system. A detailed and comprehensive explanation of the designs can be found in their respective chapters.

### 9.1 Heat Exchanger

Initial designs and simulations determined the requisite heat exchanger characteristics to robustly meet the needs of the NiPEC cooling system and collective design criteria. A two-pass heat exchanger utilizing cooling tube diameters sizes 1/2 in or 5/8 in should be pursued for further development and final system design. The heat exchanger's internal shell diameter should be sized to accommodate a cooling tube external surface area for a heat load of  $240 \ kW$  at a logarithmic mean temperature difference of  $27 \ ^{\circ}C$ . The estimated internal shell diameter and number of first pass cooling tubes should be approximately 10 to 14 in and 70 to 80, respectively. These values are ranged to meet the flow velocity and pressure drop criteria required of the heat exchanger. The heat exchanger's exposed tube length should be proportionally tailored to meet the required tube surface area and is estimated to be  $50to70 \ in$ . Single-segmented baffle sizing requires further investigation to determine the optimal cross-sectional area to promote heat transfer while minimizing the component's pressure drop. Optimizing the baffle geometry and arrangement will allow for a smaller

and more efficient heat exchanger. Serth [36] provides an in-depth methodology to determine the appropriate baffle characteristics and calculable pressure drops across the heat exchanger. The correction factors applied to the ideal heat transfer coefficient for demineralized water were conservative estimates. More refined values can be calculated during design optimization utilizing follow-on Bell-Delaware methods. The chilled water volumetric flow assumption requires a more capable and dedicated system than exists on current naval ships. A risk assessment should be conducted on the value of using a seawater-cooled heat exchanger for one of the two coolers, as ambient sea temperatures could provide sufficient cooling during non-peak conditions. If seawater cooling is not a viable solution, then a more robust chilled water infrastructure must be developed on future NiPEC ships. The thermal resistance from an internal iPEBB semi-conductor to the cold plate cooling liquid  $R_{Tot}$  developed by [31] served as a basis for initial system development. As iPEBB and cold plate designs are refined, and material thicknesses and heat transfer properties change,  $R_{Tot}$ must be considered for updated cooling system capacities. The heat exchanger design does not address the requirements for equipment shock testing and ship's motion resiliency. Investigation is required for on-ship implementation in accordance with MIL-DTL-901 [22] and DOD-STD-1399 [5].

### 9.2 Pump

The determination and analysis of the pump characteristics fall in line with expected estimates and comparable industry applications. A 23hp centrifugal pump with a 3.5in nominal outlet and 4in nominal inlet could provide sufficient cooling flow to the NiPEC compartment's iPEBBs at the most limiting heat load condition. Although the assumptions for equipment and piping head losses were conservative estimates, a continued analysis should be conducted as design iterations are refined. The equipment head loss assumptions used the maximum permissible values per military design requirements, and the piping estimates used 20% more than the expected lengths of piping. Of note, piping internal surface roughness was not implemented

into the analysis based on the variation amongst the selected materials and manufacturing techniques. Investigation into military piping specifications can provide initial estimates after determining the construction material [27]. The pump characteristics were based on the fluid thermal properties at the high end of the demineralized water temperature band. The basis for this assumption was to assess the effects of the available net positive suction head for the pump when vapor pressure was at its most limiting condition. Calculations and analysis were reperformed at feasible lowend temperatures for the demineralized water to assess the effects of water density on pumping power. The results showed that an increase of 1 hp (23 hp total) was required for low-temperature conditions at full flow. Lastly, a pump efficiency comparable to industry standards at full flow was utilized for calculations. As centrifugal pump efficiencies are normally better at the higher end of the pump's rated flow capacity, the range of lower operational efficiencies requires further investigation. However, until vendor-specific models are analyzed, cursory estimates are used. Pump motor, volute, and shafting characteristics can vary greatly between pump models, and the effects on mechanical, volumetric, and hydraulic efficiencies would be challenging to scope without vendor data.

#### 9.3 Expansion Tank

The expansion tank volume and minimum charge pressure were determined for the NiPEC cooling system. A reevaluation of component parameters should be performed as component sizes, geometries, and arrangement become more defined. No significant change in volume or pressure is expected based on maintaining one cooling system per NiPEC compartment. Small changes to the aforementioned cooling system parameters would maintain the total expansion tank volume in the range of 15to30gal.

#### 9.4 Pipes, Hoses, and Fittings

The marine atmosphere and ship's engineering environment strongly promote the selection of a corrosion-resistant material for the construction of NiPEC cooling system piping, fittings, and similar components. The performance of copper-nickel alloys in cooling system applications and their resiliency to various corrosion mechanisms make them the primary candidate in material selection among the permissible stainless steel and bronze alloys. Although stainless steel outperforms copper-nickel in the maximum safe piping flow velocities,  $3-4\ m/s$  vs  $13-15\ m/s$ , the current heat load and required volumetric flow rate of the compartment do not necessitate higher velocities. However, if one cooling system were to support multiple NiPEC compartments, then material selection should be reevaluated due to the limitations of shipboard piping diameters. Flexible hoses are not recommended for implementation in the current design. The cold plate to cooling system interface does not require the use of a flexible connection, and the drawbacks of flexible hose requirements are significant. Detailed piping, hose, and fitting criteria were summarized and referenced to facilitate immediate prototype material procurement and construction.

### 9.5 Water Chemistry Components

The cooling system requires the implementation of a two-phase resin bed to maintain the demineralized water particulate and ion free. A micron filter and y-strainer are employed for fine ( $\leq 0.5\mu m$ ) and coarse ( $> 0.5\mu m$ ) debris removal. Water chemistry specifications are delineated for the demineralized water and provide insight on how various criteria can be used to detect equipment casualties and troubleshoot issues. Cathodic protection is not required, provided material selection is as discussed. The premise of using high purity demineralized water is to mitigate the risk of electrical conduction through the cooling fluid. By reducing the ion content of the demineralized water, the chance of transmitting current from an iPEBB with an external shell potential can be minimized. Several design considerations are contingent on the

requirement to have high-purity water was the cooling medium for the cold plate. If the iPEBB design and safety margins can ensure the electrical potential is maintained within the iPEBB internals, then a risk assessment should reevaluate the possibility of using other cold plate cooling mediums currently limited by this constraint.

#### 9.6 Cold Plate

Initial cold plate designs were explored and a final recommendation was made based on the interfacing requirements with the iPEBB securing mechanism and the desire to minimize the likelihood of water contacting electronic components. The final design rotates about a hinge mechanism to apply pressure to the thermal pad and iPEBB for optimizing heat transfer between components. The cold plate aligns the inlet and outlet piping along the axis of rotation to avoid the use of flexible couplings capable of leaking water onto or near the iPEBB. The inlet and outlet piping are welded or machined into the cold plate and have a seamless design that greatly reduces the chance of leakage. Further analysis is required to determine the structural tolerance of the cold plate to static and dynamic loads.

### 9.7 Overall NiPEC Cooling System Architecture

The arrangement and specific operating geometries navigated the process by which the cold plates, iPEBB, and cooling system integrated with the iPEBB anchoring system. At the fluid temperatures achievable by the cooling system, condensation is a challenge at low load conditions if not managed properly. Condensation prevention is achievable through chilled water heat exchanger flow control and proper temperature control. The implementation of an iPEBB cabinet could protect each iPEBB stack from debris and condensation, and provide structural availability for sub-systems and components. A positive pressure atmosphere within the cabinet is capable of providing additional protection from penetrating fluids and fumes. Further investigation into iPEBB cabinet capabilities and requirements should be pursued for prototype

implementation. The NiPEC cooling system arrangement assumes that the pumps and heat exchangers are not assembled into a single cooling unit (*i.e.* cooling skid). An analysis of the requirements for all-inclusive cooling skids can address the space limitations encountered in the current NiPEC compartment model.

### Chapter 10

### Future Work and Conclusions

This thesis presents a first-pass design of a NiPEC liquid cooling system. Each element of the cooling system has been investigated, relevant standards and requirements have been documented, and recommendations have been made for the candidate problem. The proposed system is tailored to the shipboard environment for use by the sailors and technicians that operate and maintain the equipment. Deviation from the cited requirements risks the implementation of the system in the U.S. Navy's surface fleet.

#### 10.1 Future Work

There were three significant topics discovered in the process of this research which require further study. The topics discussed are not all-inclusive, but pose a significant challenge to the component and system architecture.

Variations in ship-wide NiPEC cooling system architectures should be evaluated. The number of cooling components required to support four corridors, with 12 compartments per corridor, denotes unwieldy operational and maintenance aspects under the current assumptions. This study developed a fully feasible system for a single NiPEC compartment. However, ship-wide implementation requires investigation into zonal cooling, super-loop, or other distributive cooling methods. The method could take advantage of the economies of scale while meeting the technical criteria addressed in this study. Additionally, this study did not address cooling system sur-

vivability, monitoring, safety, and control systems but are required for shipboard use and operator manageability.

iPEBB electrical isolation should be addressed and contained within the boundaries of the iPEBB. Given the large voltage capabilities of the iPEBB, electrical potentials permitted to travel outside the iPEBB shell could cause significant damage to equipment or personnel. Arcing across components, the electrolysis of the cooling liquid, accelerated corrosion, and other challenges multiply outside the bounds of the iPEBB. Electrical isolation can be equally, if not more difficult, to manage outside the iPEBB. Furthermore, MIL-HDBK-251 [23] states that electrical isolation and grounding should not be achieved via piping systems.

A thermal design criterion required of the iPEBB, and not currently addressed, is that it must be able to operate at full power within its temperature parameters for at least 8 hours at an ambient temperature of 35 °C with no new supply of cooling water [6]. iPEBB cabinet cooling could provide a back-up means of addressing this requirement and should be considered in accordance with specifications of MIL-DTL-2036 [19].

#### 10.2 Conclusion

Theoretical calculations and computer simulations presented in this thesis validate the concept that indirect liquid cooling of the iPEBB is possible and can be used for heat loads not capable of being managed by convective air cooling. The groundwork has been set for initial and comprehensive NiPEC cooling system design possibilities. Various flow conditions can be explored and simulated by building upon the provided CAD models and worksheets. The accumulated literature in this study can guide and further on-going and future NiPEC cooling research. Prototyping and advanced modeling can develop more sophisticated means of cooling and can now be pursued. Prototyping of the system and equipment to confirm the research presented herein is the next logical next step.

### Bibliography

- [1] Alfa Laval. Plate heat exchanger, 2015. URL https://www.alfalaval.com/contentassets/1a62e93b427c47ec9622df8366237a4d/imageoek7.png.
- [2] D. Beysens. The Physics of Dew, Breath Figures and Dropwise Condensation. Springer New York, New York, NY, 2022.
- [3] C. Cooke, C. Chryssostomidis, and J. Chalfant. Modular integrated power corridor. In *Electric Ship Technologies Symposium (ESTS)*, 2017 IEEE, pages 91–95. IEEE, 2017.
- [4] J. del Águila Ferrandis, J. Chalfant, C. M. Cooke, and C. Chryssostomidis. Design of a power corridor distribution network. In 2019 IEEE Electric Ship Technologies Symposium (ESTS), pages 284–292. IEEE, 2019.
- [5] DOD-STD-1399. Ship motion and attitude (metric). Department of Defense Interface Standard, July 1986. Chapter 301, Revision A.
- [6] DOD-STD-1399. Cooling water for support of electronic equipment. Department of Defense Interface Standard, June 2021. Chapter 532, Revision A.
- [7] DOE-HDBK-1018. Mechanical science volume 1. Department of Energy Fundamentals Handbook, 1 1993.
- [8] EXAIR. Nema 4x st. st. cabinet cooler® systems, cont oper, 2022. URL https://www.exair.com/n4xcc-cont.html.
- [9] R. Francis. Copper alloys in seawater: Avoidance of corrosion. Technical report, Copper Development Association Inc., 2016. URL https://www.copper.org/applications/marine/cuni/pdf/pub-225-copper-alloys-in-seawater-avoidance-of-corrosion.pdf.
- [10] R. Francis. Copper alloys versus stainless steels for seawater cooling systems the pros and cons. Technical report, The Nickel Institute, 2020.
- [11] C. D. A. Inc. Copper-nickel piping for off-shore platforms. Technical report, Copper Development Association Inc., 1987. URL https://www.copper.org/applications/marine/cuni/pdf/copper\_nickel\_piping\_708\_5.pdf.

- [12] C. D. A. Inc. Stainless steel in contact with other metallic materials. Technical report, The European Stainless Steel Development Association, 2009.
- [13] T. N. Institute. Copper-nickel alloys, properties and applications. Technical report, The Nickel Institute, 1982.
- [14] G. Kear, B. Barker, K. Stokes, and F. C. Walsh. Electrochemical corrosion behaviour of 90—10 Cu—Ni alloy in chloride-based electrolytes. *Journal of Applied Electrochemistry*, 2004.
- [15] J. H. Lienhard IV and J. H. Lienhard V. A Heat Transfer Textbook. Phlogiston Press, Cambridge, MA, 2020. URL https://ahtt.mit.edu/wp-content/uploads/2020/08/AHTTv510.pdf.
- [16] E. McCafferty. Introduction to Corrosion Science. Springer New York, New York, NY, 2010. URL https://doi.org/10.1007/978-1-4419-0455-3\_6.
- [17] MIL-DTL-15730. Coolers, fluid, naval shipboard hydrocarbon base oil and freshwater services. Department of Defense Detail Specification, June 2021. Revision N.
- [18] MIL-DTL-18866K. General specification for fittings, hydraulic tube, flared 37 degree and flareless. Department of Defense Detail Specification, July 2020. Revision K.
- [19] MIL-DTL-2036. Enclosures for electric and electronic equipment, naval ship-board. Department of Defense Detail Specification, June 2019. Revision E.
- [20] MIL-DTL-24136. General specification for hose, synthetic rubber, synthetic fiber reinforced, for flexible hose assemblies. Department of Defense Detail Specification, December 2021. Revision C.
- [21] MIL-DTL-24787. Fittings, end, type d (hose to hose, 90-degree elbow), reusable, for flexible hose assemblies. Department of Defense Detail Specification, September 2020. Chapter 5, Revision A.
- [22] MIL-DTL-901. Shock tests, h.i. (high-impact) shipboard machinery, equipment, and systems. Department of Defense Detail Specification, June 2017. Revision E.
- [23] MIL-HDBK-251. Reliability/design thermal applications. Department of Defense Handbook, January 2021.
- [24] MIL-STD-1472. Human engineering. Department of Defense Design Criteria Standard, September 2020. Revision H.
- [25] MIL-STD-3045. U.S. Navy surface ship machinery arrangements. Department of Defense Design Criteria Standard, March 2014.

- [26] MIL-STD-769. Insulation requirements for u.s. naval vessels. Department of Defense Standard Practice, June 2015. Revision K.
- [27] MIL-STD-777. Schedule of piping, valves, fittings, and associated piping components for naval surface ships. Department of Defense Standard Practice, February 2018. Revision F.
- [28] MIL-STD-889. Galvanic compatibility of electrically conductive materials. Department of Defense Standard Practice, 7 2021. Revision D.
- [29] Neutrium. Pressure loss from fittings excess heaf (k) method, 2012. URL https://neutrium.net/fluid-flow/pressure-loss-from-fittings-excess-head-k-method.
- [30] Omega Flex. Constant-flexing, 2022. URL https://www.omegaflex.com/wp-content/uploads/constant-flexing.jpg.
- [31] J. Padilla, J. Chalfant, C. Chryssostomidis, and C. Cooke. Preliminary investigation into liquid-cooled PEBBs. In 2021 IEEE Electric Ship Technologies Symposium (ESTS), August 2021.
- [32] H. Padleckas. Staright-tube heat exchanger, 2006. URL https://en.wikipedia.org/wiki/Shell\_and\_tube\_heat\_exchanger#/media/File: Straight-tube\_heat\_exchanger\_2-pass.PNG.
- [33] L. Petersen, C. Schegan, T. S. Ericsen, D. Boroyevich, R. Burgos, N. G. Hingorani, M. Steurer, J. Chalfant, H. Ginn, C. DiMarino, G. C. Montanari, F. Z. Peng, C. Chryssostomidis, C. Cooke, and I. Cvetkovic. Power electronic power distribution systems (PEPDS). ESRDC Website, www.esrdc.com, 2022.
- [34] C. Powell and H. Michels. Copper-nickel for seawater corrosion resistance and antifouling: A state of the art review. *Corrosion*, 2000. URL https://www.copper.org/applications/marine/Cu-Ni/properties/corrosion/corrosion\_resistance\_and\_antifouling.html#bio.
- [35] N. Rajagopal, R. Raju, T. Moaz, and C. DiMarino. Design of a high-frequency transformer and 1.7 kv switching-cells for an integrated power electronics building block (iPEBB). In *Electric Ship Technologies Symposium (ESTS)*, 2021 IEEE, IEEE, 2021.
- [36] R. W. Serth. Process Heat Transfer: Principles and Applications. Academic Press, Burlington, MA, 2007. URL https://mit-library.skillport.com/skillportfe/main.action?assetid=RW\\$41366:\_ss\_book: 28259#summary/BOOKS/RW\\$41366:\_ss\_book:28259.
- [37] C. Tomlinson. Design of securing mechanism for power converter in navy integrated power and energy corridor. Master's thesis, Massachusetts Institute of Technology, 2022.

- [38] S. Yan, G.-L. Song, Z. Li, H. Wang, D. Zheng, F. Cao, M. Horynova, M. S. Dargusch, and L. Zhou. A state-of-the-art review on passivation and biofouling of ti and its alloys in marine environments. *Journal of Materials Science and Technology*, 2018.
- [39] S. Yana, G.-L. Songa, Z. Lib, H. Wangb, D. Zhenga, F. Caoa, M. Horynovaa, M. S. Darguschc, and L. Zhoud. A state-of-the-art review on passivation and biofouling of Ti and its alloys in marine environments. *Materials Science and Technology*, 2017.
- [40] S. Yang, J. Chalfant, J. Ordonez, J. Khan, C. Li, I. Cvetkovic, J. Vargas, M. Chagas, Y. Xu, R. Burgos, et al. Shipboard PEBB cooling strategies. In 2019 IEEE Electric Ship Technologies Symposium (ESTS), pages 24–31. IEEE, 2019.

# Appendix A

## Pipe Fittings Flow Friction Values

Table A.1 shows the resistance coefficient values for various fittings. It is used in conjunction with Eqn. 3.2 to calculate the head loss produced by the respective fittings [29].

Table A.1: Resistance Coefficient Fitting Values [29].

Fitting	Type	K
45° Elbow	Standard $(R/D = 1)$	0.35
	Long Radius $(R/D = 1.5)$	0.2
90° Elbow Curved	Standard $(R/D = 1)$	0.75
	Long Radius $(R/D = 1.5)$	0.45
90° Elbow Square or Mitred		1.3
180° Bend	Close Return	1.5
Tee, Run Through	Branch Blanked	0.4
Tee, as Elbow	Entering in run	1
Tee, as Elbow	Entering in branch	1
Tee, Branching Flow		1
Coupling		0.04
Union		0.04
Gate valve	Fully Open	0.17
	3/4 Open	0.9
	1/2 Open	4.5
	1/4 Open	24
Diaphragm valve	Fully Open	2.3
	3/4 Open	2.6
	1/2 Open	4.3
	1/4 Open	21
Globe valve, Bevel Seat	Fully Open	6
	1/2 Open	9.5
Globe Valve, Composition seat	Fully Open	6
	1/2 Open	8.5
Angle valve	Fully Open	2
Butterfly valve	$\theta = 5^{\circ}$	0.24
	$\theta = 10^{\circ}$	0.52
	$\theta = 20^{\circ}$	1.54
	$\theta = 40^{\circ}$	10.8
	$\theta = 60^{\circ}$	118
Check valve	Swing	2
	Disk	10
	Ball	70
Foot valve		15
Water meter	Disk	7
	Piston	15
	Rotary (star-shaped disk)	10
	Turbine-wheel	6

# Appendix B

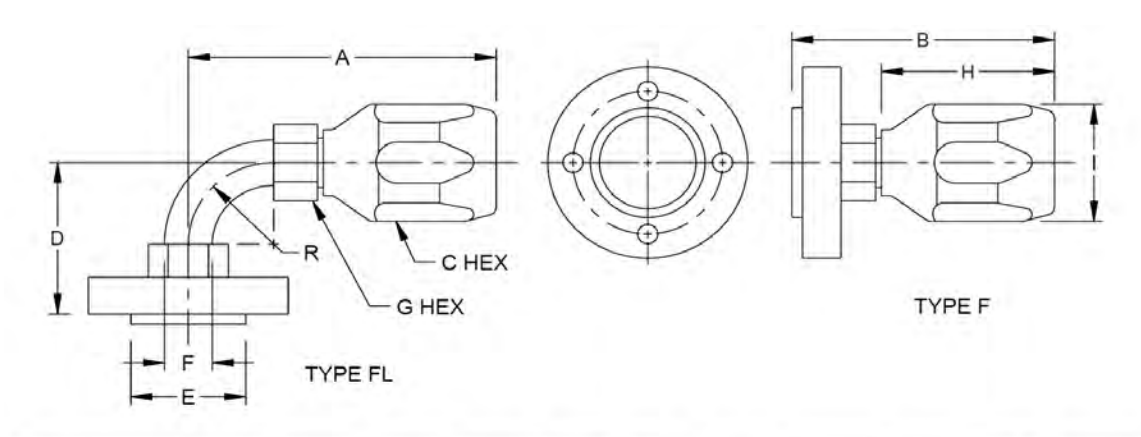
## Flexible Hose End Fittings

End fitting specification sheet number	End fitting type per specification sheet	End fitting description
24787/1 <sup>1/</sup>	F, FL, FFL	Flange to hose (straight, 90-degree elbow, or 45-degree elbow)
24787/2	A	37-degree flare swivel
24787/3 <sup>2/</sup>	C, CL	O-ring seal union (straight or 90-degree elbow)
24787/4 <sup>3/</sup>	E, EL, SC, TF, TM	Split clamp (straight, 90-degree elbow, or assembly), Tailpiece (female or male)
24787/5 <sup>2/</sup>	D	90-degree elbow

#### NOTES:

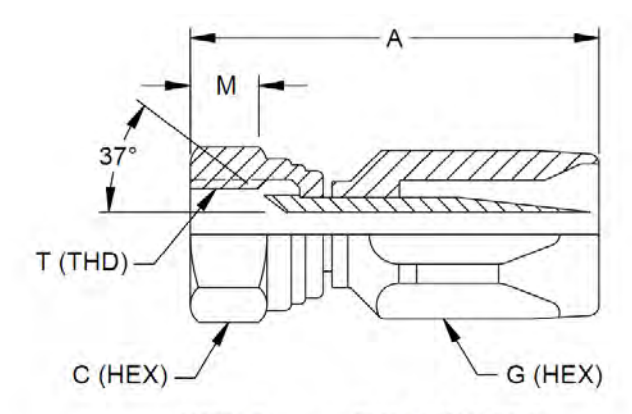
- $\frac{1}{2}$  This is for -16, -20, -24, and -32 hose dash sizes only.
- This does not include -4 or -5 hose dash sizes.
- $\frac{3}{2}$  This is for -32 hose dash size only.

Figure B-1: End fittings for use with flexible hoses [21]



Hose size	NOC	A	В	C	D	E	F		Н	I		
(dash number)	NPS	nom	nom	nom	nom	nom	nom	G	See n	ote 6	R	
-16	1/2	2.80	2.80	1.44	2.38	1.50	0.71	1.38	1.66	1.53	1.12	
-16	3/4	2.80	2.80	1.44	2.38	1.50	0.71	1.38	1.66	1.53	1.12	
-16	1	2.80	2.80	1,44	2.38	1.50	0.71	1.38	1.66	1.53	1.12	
-20	3/4	2.98	2.89	1.75	2.56	1.84	0.92	1.62	1.75	1.62	1.22	
-24	1	3.24	2.92	1.94	2.75	2.12	1.18	2.12	1.84	1.78	1.38	
-32	11/4	3.89	3.51	2.44	3.06	2.74	1.53	2.25	2.25	2.05	1.62	
-32	11/2	3.89	3.51	2.44	3.06	2.74	1.77	2.25	2.25	2.05	1.62	
-32	2	3.89	3.51	2.44	3.06	2.74	1.75	2.69	2.25	2.05	1.62	

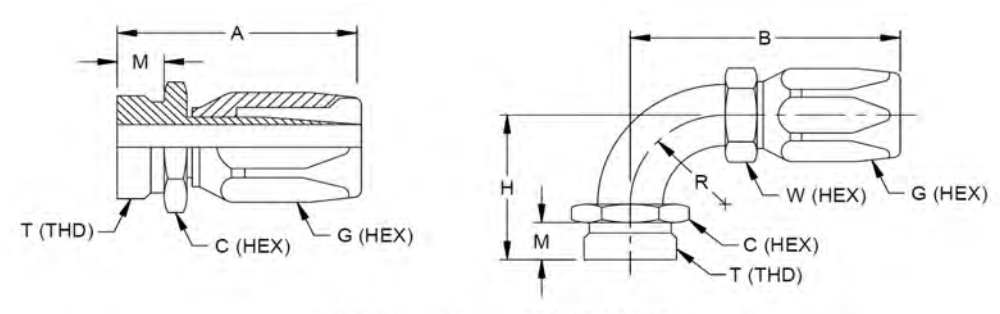
Figure B-2: Flange to hose - straight (F) and 90-degree elbow (FL) [21]



TYPE A - - - - SOLID SOCKET

Hose size (dash number)	Tube size (nom)	T Thread CL-2B	A max	C nom	G max	M ref
-4	1/4	7/6 - 20	1.75	0.56	0.62	0.35
-5	5/16	1/2 - 20	1.90	0.62	0.69	0.38
-6	3/8	½6 <b>-</b> 18	2.05	0.69	0.81	0.38
-8	1/2	3/4 - 16	2.52	0.88	0.94	0.43
-10	5/8	7/8 - 14	2.80	1.00	1.12	0.51
-12	3/4	1 - 1/16 - 12	3.15	1.25	1.25	0.57
-16	1	1 - 1/6 - 12	2.28	1.50	1.44	0.60
-20	11/4	1 - % - 12	3.00	2.00	1.75	0.64
-24	11/2	1 - 1/8 - 12	3.28	2.25	1.94	0.74
-32	21/2	1 - 7/8 - 12	3.88	2.88	2.44	0.76
-40	21/2	3 – 12	4.16	4.38	3.25	0.80

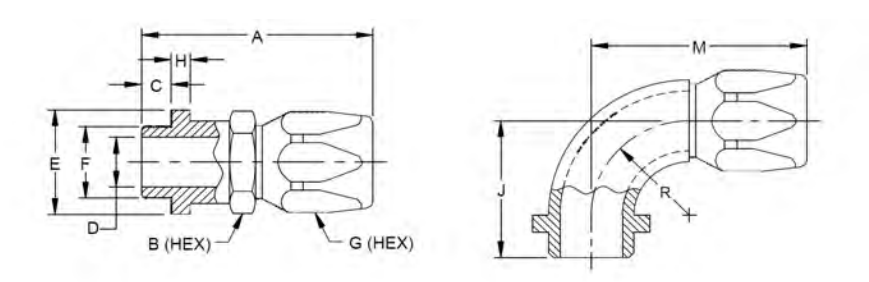
Figure B-3: 37-degree flare swivel (A) [21]  $\,$ 



TYPE C AND CL - - - - SOLID SOCKET

Hose size (dash number)	Tube size (nom)	T Thread CL-2B	A max	C nom	G max	M ref	B max	H max	R ref	W
-6	38	1-14 UNF	2.06	1.06	0.81	0.50	2.45	1.30	0.50	0.56
-8	1/4	1 - ¾6 - 12 UN	2.54	1.25	0.94	0.62	3.05	1.68	0.75	0.75
-10	3/8	1 - % - 12 UNF	2.75	1.44	1.12	0.62	3.57	1.99	1.00	0.81
-12	1/2	1 - % - 12 UNF	3.12	1.81	1.25	0.61	4.15	2.31	1.25	1.00
-16	3/4	2 - 12 UN	2.80	2.12	1.44	0.62	3.93	2.68	1.50	1.38
-20	1	2 - 16 - 12 UNS	3.14	2.38	1.75	0.75	4.27	3.17	1.75	1.62
-24	11/4	2 -3/4 - 12 UN	3.23	2.88	1.94	0.75	4.65	3.42	2.00	1.81
-32	11/2	3 - 1/16 - 12 UN	3.89	3.12	2.44	0.88	5.68	4.05	2.50	2.38

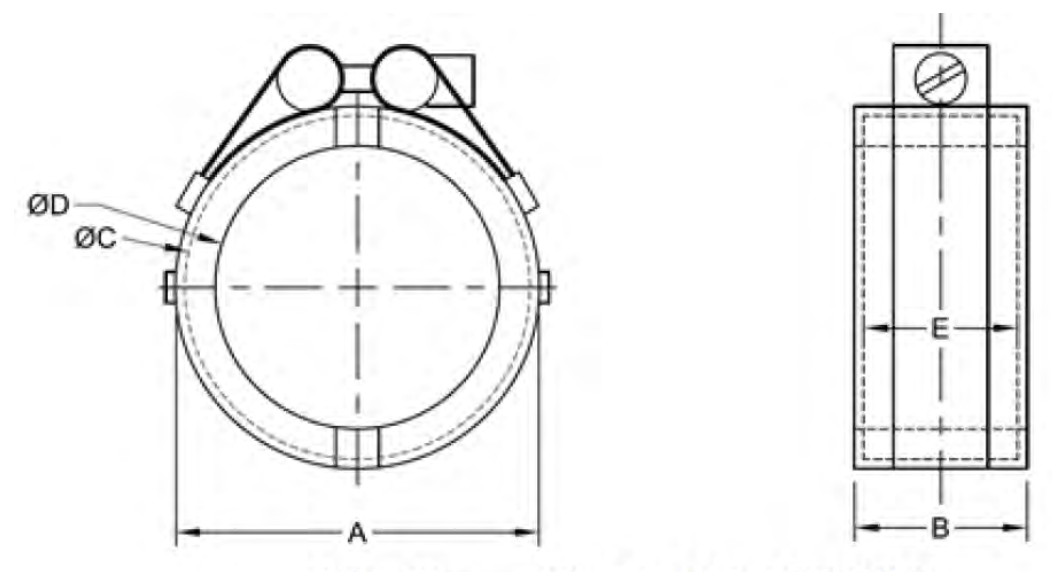
Figure B-4: O-ring seal union - straight (C) or 90-degree elbow (CL) [21]



TYPE E AND EL ----- SOLID SOCKET

Hose size (dash number)	NPS	A ref	B ref	C ±0.0025	D ref	E	F ±0,0025	G ref	H ±0.0025	J ref	M ref	R ref
-32	11/4	3.828	2.12	0.3345	1.53	2.433 ±0.005	1.7475	2.516	0.3195	2.81	3.891	1.62
-32	1½	3.796	2.12	0.3345	1.69	2.748 ±0.003	1.9975	2,516	0.3195	2.81	3.891	1.62
-40	2	4.094	2.62	0.3345	2.21	3.248 ±0.003	2.4975	3.266	0.3195	3.04	4.344	1.88
-40	21/2	4.188	3.25	0.3345	2,73	3.748 ±0.003	2.9975	3.891	0.3195	3.51	4.563	2.09

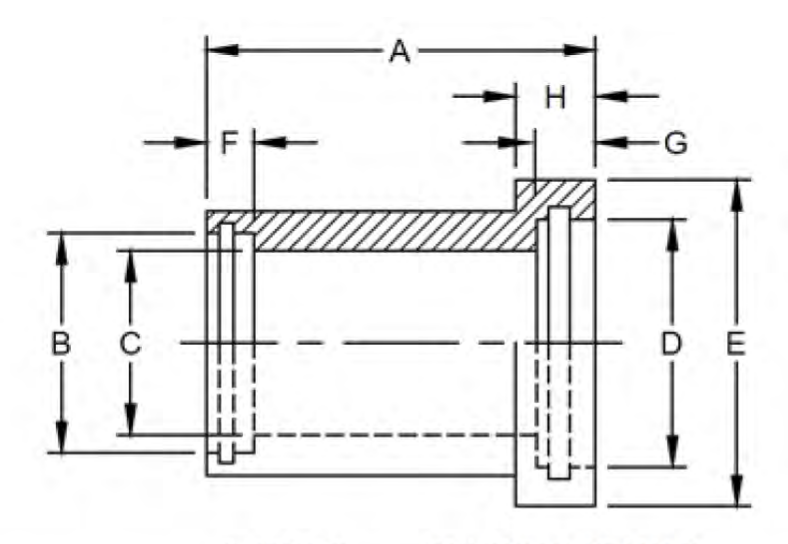
Figure B-5: Split clamp end fitting - straight (E) and 90-degree elbow (EL) [21]



TYPE SC ----- SPLIT CLAMP ASSEMBLY

NPS	A ref	B ref	C	D	E
11/4	3.000	1.310	2.439 +0.002 -0.003	2.125 ±0.010	0.875 ±0.006
11/2	3.312	1.310	2.760 ±0.004	2.437 ±0.010	0.875 ±0.006
2	4.00	1.380	3.260 ±0.004	2.937 ±0.010	0.880 ±0.006
21/2	4.420	1.440	3.761 ±0.004	3.437 ±0.010	0.937 ±0.006
	1		1	1	1

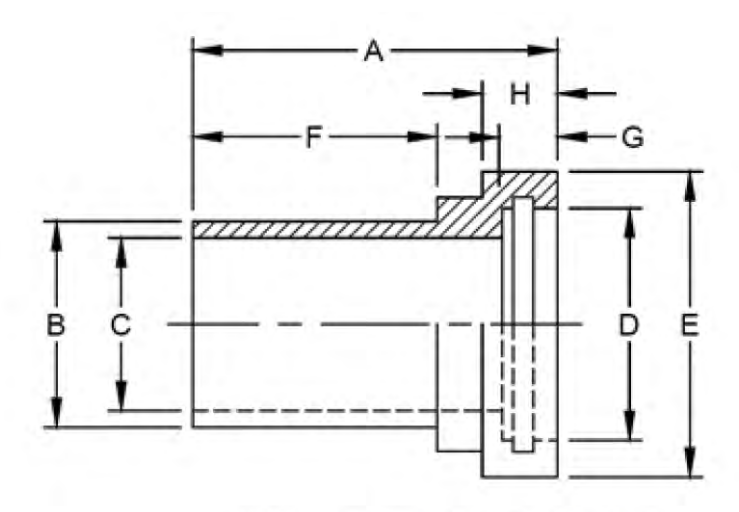
Figure B-6: Split clamp adapter assembly (SC) [21]  $\,$ 



TYPE TF ----- TAILPIECE, FEMALE

NPS	A ref	B +0.007 -0.000	C	D 8/	E 8/	F min	G <sup>8</sup> / +0.010 -0.000	Н
11/4	1.515	1.660	1.458 ±0.010	1.7575 ±0.0025	2.433 ±0.005	0.500	0.342	0.5435 ±0.0025
11/2	1.604	1.900	1.669 ±0.010	2.010 ±0.004	2.748 ±0.003	0.625	0.342	0.5435 ±0.0025
2	1.688	2.375	2.121 ±0.010	2.510 ±0.004	3.248 ±0.003	0.656	0.342	0.5435 ±0.0025
2½	1.890	2.875	2.591 ±0.010	3.010 ±0.004	3.748 ±0.003	0.781	0.342	0.6055 ±0.0025

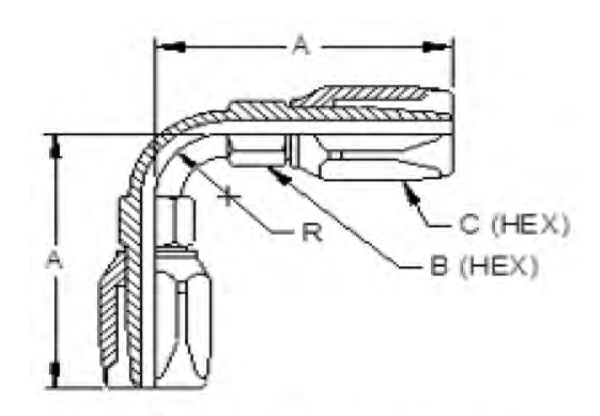
Figure B-7: Tailpiece female adapter (TF) [21]



TYPE TM ----- TAILPIECE, MALE

NPS	A ref	B +0.000 -0.007	C	<b>D</b> ½	E 7/	F +/-0.016	G <sup>7</sup> / +0.010 -0.000	H ½
11/4	1.963	1.660	1.413 ±0.005	1.7575 ±0.0025	2.433 ±0.005	1.125	0.342	0.5435 ±0.0025
1½	2.088	1.900	1.621 ±0.005	2.010 ±0.004	2.748 ±0.003	1.250	0.342	0.5435 ±0.0025
2	2.183	2.375	2.036 ±0.005	2.510 ±0.004	3.248 ±0.003	1.312	0.342	0.5435 ±0.0025
21/2	2.058	2.875	2.586 ±0.005	3.010 ±0.004	3.748 ±0.003	1.125	0.342	0.6055 ±0.0025

Figure B-8: Tailpiece male adapter (TM) [21]



TYPE D ---- SOUD SOCKET

Hose size (dash number)	A max	B nom	C max	R min
-6	2.45	0.56	0.81	0.50
-8	3.05	0.75	0.94	0.75
-10	3.57	0.81	1.12	1.00
-12	4.15	1.00	1.25	1.25
-16	3.93	1.38	1.44	1.50
-20	2.98	1/	1.75	1.22
-24	3.24		1.94	1.38
-32	3.89		2.44	1.62
-40	4.39		3.25	1.88

Figure B-9: 90-degree elbow [21]

### Appendix C

### Piping Construction Materials

The following tables list the pre-approved piping component materials aboard Navy surface ships. The information is from Table XVI in MIL-STD-777 [27] for Category C-1 and C-2 fluids, which is directed by note L-1-2 from Table XLVIII for L-1 fluids. The use of ethylene glycol/water solutions is required when piping systems impose anti-freeze protection, such as when piping is exposed to weather or outside the skin of the ship. C-1 and C-2 category fluids are freshwater, including feed, chilled water, condensate, electronic freshwater cooling, potable, freshwater firefighting, and gas turbine washdown, 200 psig/250 °F. L-1 category fluids are cooling, (electronic equipment, diesel equipment, diesel engine, and so forth) – ethylene glycol, freshwater solution, distilled water solution, 150 psig/200 °F. Not all metal alloys listed below are permitted for use when using demineralized water. A list of permissible metal alloys can be found in Table 5.1 and should be cross-referenced with the tables below.

Item	Types	Material	Applicable documents	Remarks
Pipe	Seamless	Copper	MIL-T-24107	0.065 inch min. wall thickness (see note C-1-1)
		GRP	MIL-P-24608	See 4.43
	Seamless or welded	Copper-nickel (90-10)	MIL-T-16420	
Valves	Gate, ¼ to 2 NPS	Bronze or copper-nickel	803-1385714	Union ends only
	Gate, 21/2 to 12 NPS		803-2177917	Flanged ends only
	Globe/angle stop/stop-check, ¾ to 2 NPS		803-4384536	Union ends only See note C-1-2
	Globe Y-pattern, 21/2 to 10 NPS		803-1385623	Flanged ends only
	Globe/angle check and stop-check. 2½ NPS and larger		803-1385541	100 psig max. Flanged ends only
	Swing-check, ¼ to 2 NPS		803-1385721	Umon ends only
	Swing-check, 2½ to 12 NPS		803-1385637	Flanged ends only
	Swing-check, ¼ NPS and above	Bronze, Nickel-aluminum-bronze or copper-nickel	MIL-V-17547	
	Relief	Bronze or copper-nickel	MIL-V-24332	
	Butterfly	Nickel-aluminum-bronze or copper- nickel	MIL-V-24624	Special flanges required
	Control	Bronze (nickel-copper trim or 300- series CRES trim) or copper-nickel	MIL-V-18030	100 psig max. Flanged ends only
	Pressure-reducing	Bronze or copper-nickel	ASTM F1370 including supplements	See 4.42

Figure C-1: Category C-1 and C-2, Freshwater, including feed, chilled water, condensate, electronic freshwater cooling, potable, freshwater firefighting, and gas turbine washdown,  $200 \text{ psig}/250 \text{ }^{\circ}\text{F}$  [27]

Item	Types	Material	Applicable documents	Remarks	
Valves - continued	Ball, ¼ to 2½ NPS	Bronze	803-5001003	Bronze body with bronze, copper-nickel end piece	
		Copper-nickel		Copper-nickel body with copper-nickel end piece	
	Ball, 3 to 6 NPS	Bronze or copper-nickel	803-5001004	6-NPS valve is butt-welded only	
Fittings	Silver brazing		MIL-DTL-1183		
	Butt-welding	Copper-nickel (90-10)	810-1385880	150 °F max.	
	Welded base by silver brazing end outlet boss	Copper-nickel (90-10 or 70-30)	803-1385950 or commercial	Welded to copper-nickel pipe run	
	Socket-welding	Copper-nickel	803-6397430		
	Belled end and couplings	Copper-nickel, MIL-T-16420	MSS SP-119	See 4.48	
	Socket (bonded)	GRP	MIL-P-24608		
	MAFs	Various	ASTM F1387	See 4.46	
Take-down joints	Silver brazing unions	Bronze	MIL-DTL-1183		
	Socket-welding flanges	Copper-nickel	803-6983512		
	Silver-brazed flanges	Bronze	MIL-PRF-20042, Class plain, 150 and 250 pounds	See notes C-1-3, C-1-4	
			803-1385892	Special flanges or butterfly valves, 180 °F max.	
	Socket-bonded flanges	GRP	MIL-P-24608	See 4.43, notes C-1-5, C-1-6	
Gaskets	Sheet	Non-asbestos	MIL-DTL-24696, Type II	Preferred gasket for butterfly valves	
		Nylon inserted rubber	804-5284201. Types 1. 2, or 4	See 4.26 as approved See note C-1-12	
		EPDM	MIL-DTL-22050		
	O-ring	Fluorocarbon	SAE-AMS7276		

Figure C-2: Category C-1 and C-2, Freshwater, including feed, chilled water, condensate, electronic freshwater cooling, potable, freshwater firefighting, and gas turbine washdown, 200 psig/250 °F - Continued [27]

	Item	Types	Material	Applicable documents	Remarks
Flange b	oolting	Bolts, screws, studs	Nickel-copper	ASTM F468, Alloy 400	See 4.16
		Nuts		ASTM F467, Alloy 400	
		Nuts, self-locking		NASM 25027/NASM 17828	
				MIL-DTL-32258	
NOTES					
C-1-1	The thickness	of copper tubing in condensate piping	shall be calculated using allowable	stresses for the fully annealed condition.	
C-1-2				nickel-chrome plated, with ½ NPS silver bra	
				, with raised metal seat and removable com	
C-1-3				lle; (4) valves shall be sized to suit the insta inmeter of the bolt holes in the line flanges	
C-1-3	250 psig flang		hanges in sizes 2 to 4 NPS, the di	ameter of the bolt hotes in the line hanges	shall be increased to match the
C-1-4			where temperatures do not exceed	150 °F. For temperature of 151 °F to 250 °	F, they shall be limited to 100
	psig and below				
C-1-5				oints are 200 psig at 150 °F and 100 psig at	
C-1-6			ted of copper-nickel pipe, with all	components (including but not limited to pi	pe, valves, fittings,
0.17		and flanges) either flanged or welded.		TO KIND OF A KIND OF A PROPERTY OF A PARTY O	
C-1-7	"W".			valves and branches to air conditioning coo	
C-1-8	For electronic products are n		wn systems, valve gland packing a	nd all other elastomers shall be compatible	with the fluid. Natural rubber
C-1-9		k valves subject to air pressure shall be	soft-seated.		
C-I-10	The sample co		aple water cooler shall be CRES co	omposition 304L in accordance with MIL-P	-24691/3, Grade 304L or
C-1-11	Where copper check valves in		s that supply water to equipment co	ontaining carbonated water dispensers, the	system shall have double
C-1-12	chlorides not t	o exceed 200 ppm.		ted for use in steam condensate systems sha	ill be tested for leachable
C-1-13		all not be used for freshwater fire figh			
C-1-14	Firemain pipin	ig and any source piping or fittings sha	II be welded for sizes 2 NPS and a	bove. Sizes 11/2 NPS and below may be we	lded or brazed.

Figure C-3: Category C-1 and C-2, Freshwater, including feed, chilled water, condensate, electronic freshwater cooling, potable, freshwater firefighting, and gas turbine washdown, 200 psig/250 °F - Continued [27]

### Appendix D

## Piping Insulation Materials

The following tables list the pre-approved insulation and lagging materials, specific to the NiPEC cooling system, for use aboard Navy surface ships. Concerning insulation selection and D-1, The 41 to 125 °F temperature range is the appropriate criteria for the design application. The air conditioning criteria are yet to be determined, but the space design is not expected to be open to the weatherdeck. The insulation is to be lagged with fibrous-glass cloth in accordance with MIL-C-20079. Removable and reusable insulation shall be installed on flexible hoses without lagging. Painting, splash guards, and metal sheathing shall be installed or applied in accordance with

		Nominal Thickness (inches)			
Pipe Size (inches)	Temperature Range (°F)	Non-Air Conditioned Spaces	Air Conditioned Spaces	Air Conditioned Spaces Open to Weatherdeck <sup>1/</sup>	
	-20 to -1	11/2	1	2	
All	0 to 40	1	3/4	11/2	
	41 to 125	3/4	1/2	1	

NOTE: Wherever possible, double layers or double thickness of insulation shall be used where piping is exposed to high humidity conditions. An example is a space that is in close proximity to the weather deck or outside doors and subject to outside air exposure.

Figure D-1: Thickness of anti-sweat and refrigerant insulation for piping [26]

		Nominal Thickness (inches)		
Temperature Range (°F)	Defense Specification	Non-Air Conditioned Spaces	Air Conditioned Spaces	
-20 to 40	MIL-PRF-32514	2	1	
41 to 125	MIL-PRF-32514	3/4	1/2	
	MIL-I-22023, Type I	1	1/2	

NOTE: In some cases, fibrous-glass thermal and sound absorbing insulation felt conforming to MIL-I-22023, Type I, Class 6 is used as an anti-sweat insulation for submarine tank tops.

Figure D-2: Thickness of anti-sweat and refrigerant insulation for machinery and equipment [26]

		Forn	n 1 – Tubular			
Wall thickness	(inches)	Length	(inches)	Inside diameter (i	nches)	
Dimension	Tolerance	Dimension	Tolerance	Dimension	Tolerance	
Up to 3/4, inclusive	-0 to +1/8		-1 to +4	Up to 1/2, inclusive	+1/16 to +5/32	
O 3/	-0 to +3/16	1/	-1 to +4	Over ½ to 2½, inclusive	+1/16 to +3/16	
Over 3/4				Over 2½	+½6to +½6	
		For	rm 2 – Sheet			
Thi	ckness (inches)	P.	1-27-2	Length and width (inches)		
Dimension		Tolerance	Dimension		Colerance	
Up to 1/4, inclusive		+3/32 to -1/32	Up to 6, inclu	sive	±1/4	
Over 1/4 to 1/2, inclusive		+3/32 to -1/32	Over 6 to 12, inclusive		±3/8	
Over 1/2 to 1, inclusive		±3/32	0.110		20/	
Over 1		±1/s	Over 12		±3%	
NOTE:  1 Lengths of tub	ular form or nu	mber of sheets sh	all be as specified	d (see 6.2).		

Figure D-3: Dimensional tolerance of form 1 – tubular insulation and form 2 – sheet insulation [26]

# Appendix E

## Ideal Tube Bank Correlation Graphs

An alternative method for deriving ideal tube bank correlations, such as the Colburn Factor, is by using the charts below for various tube pitch formations [36].

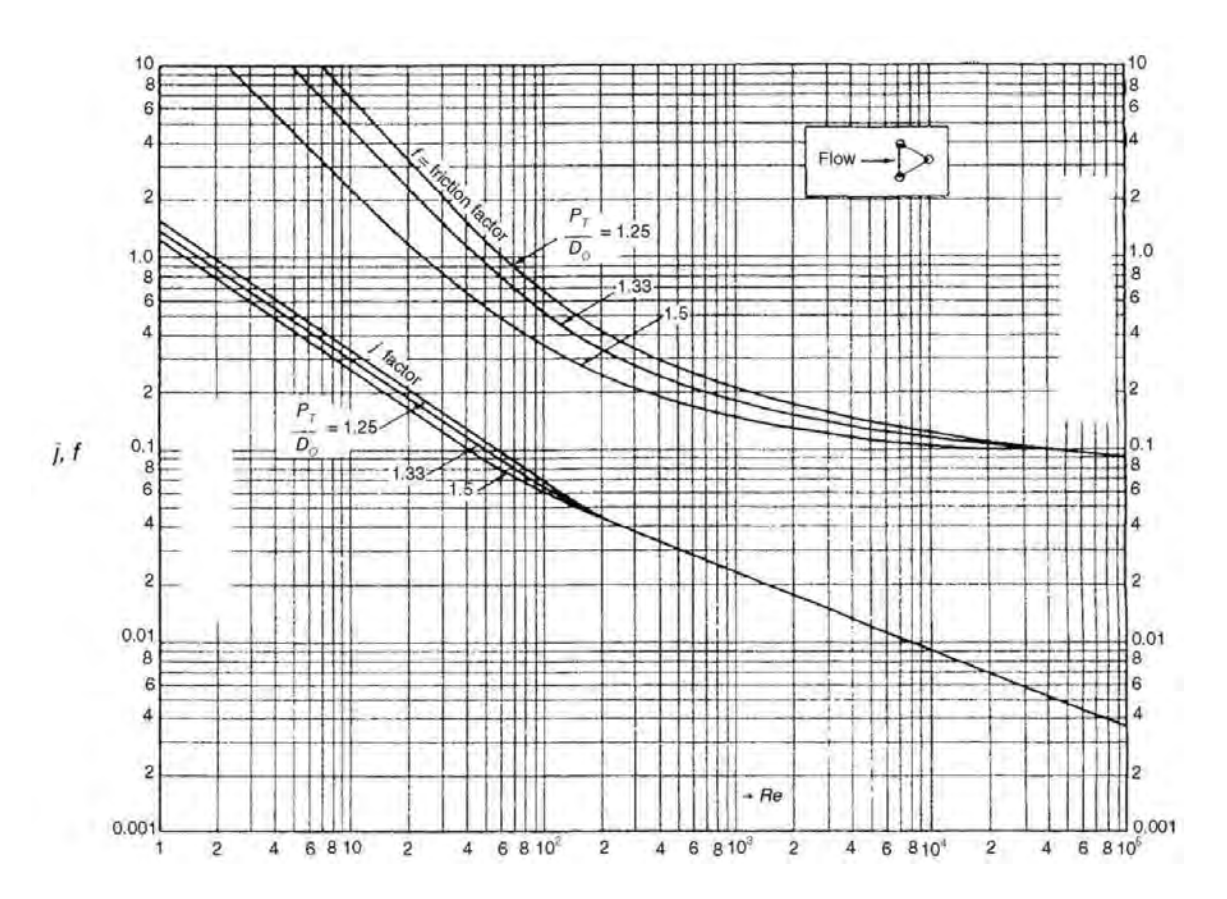


Figure E-1: Ideal tube bank correlation for triangular pitch [36]

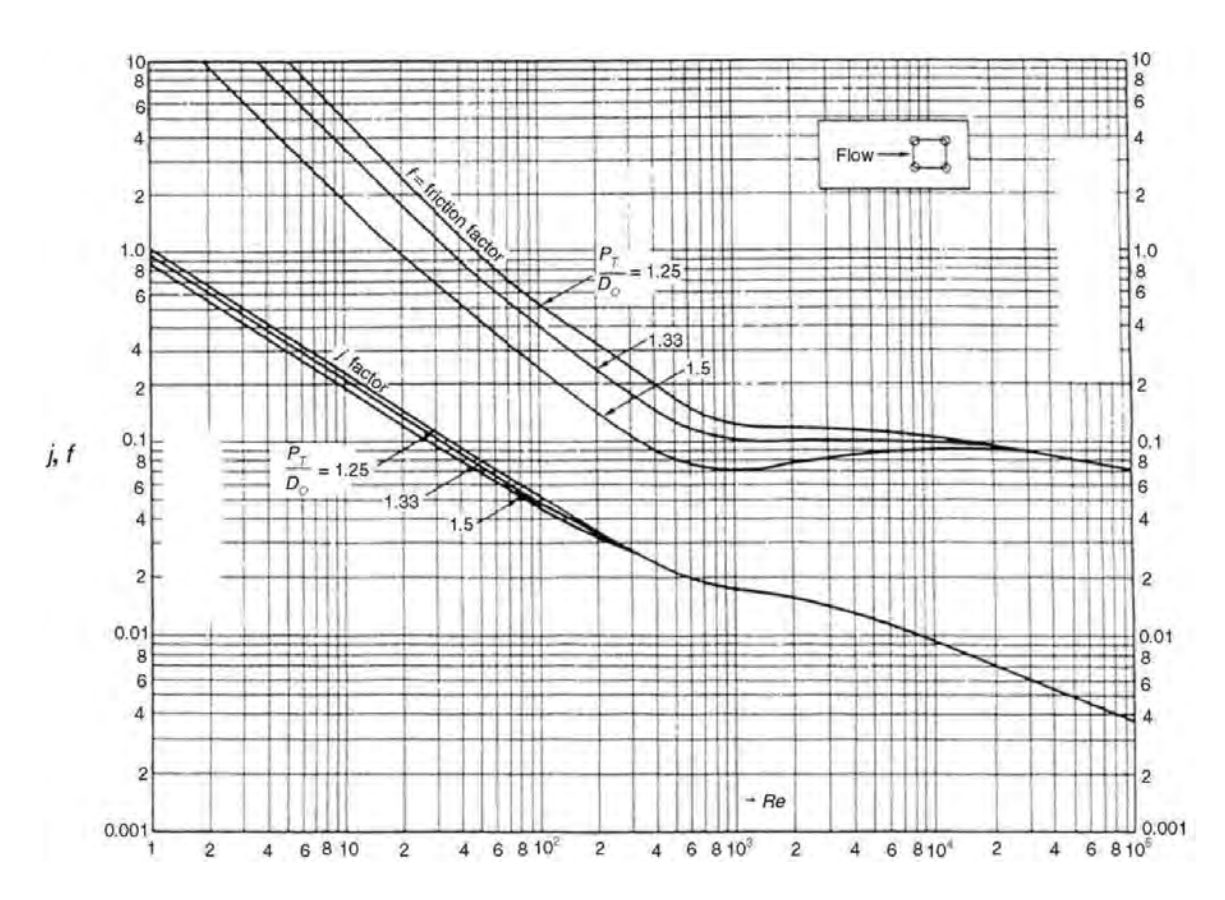


Figure E-2: Ideal tube bank correlation for square pitch [36]

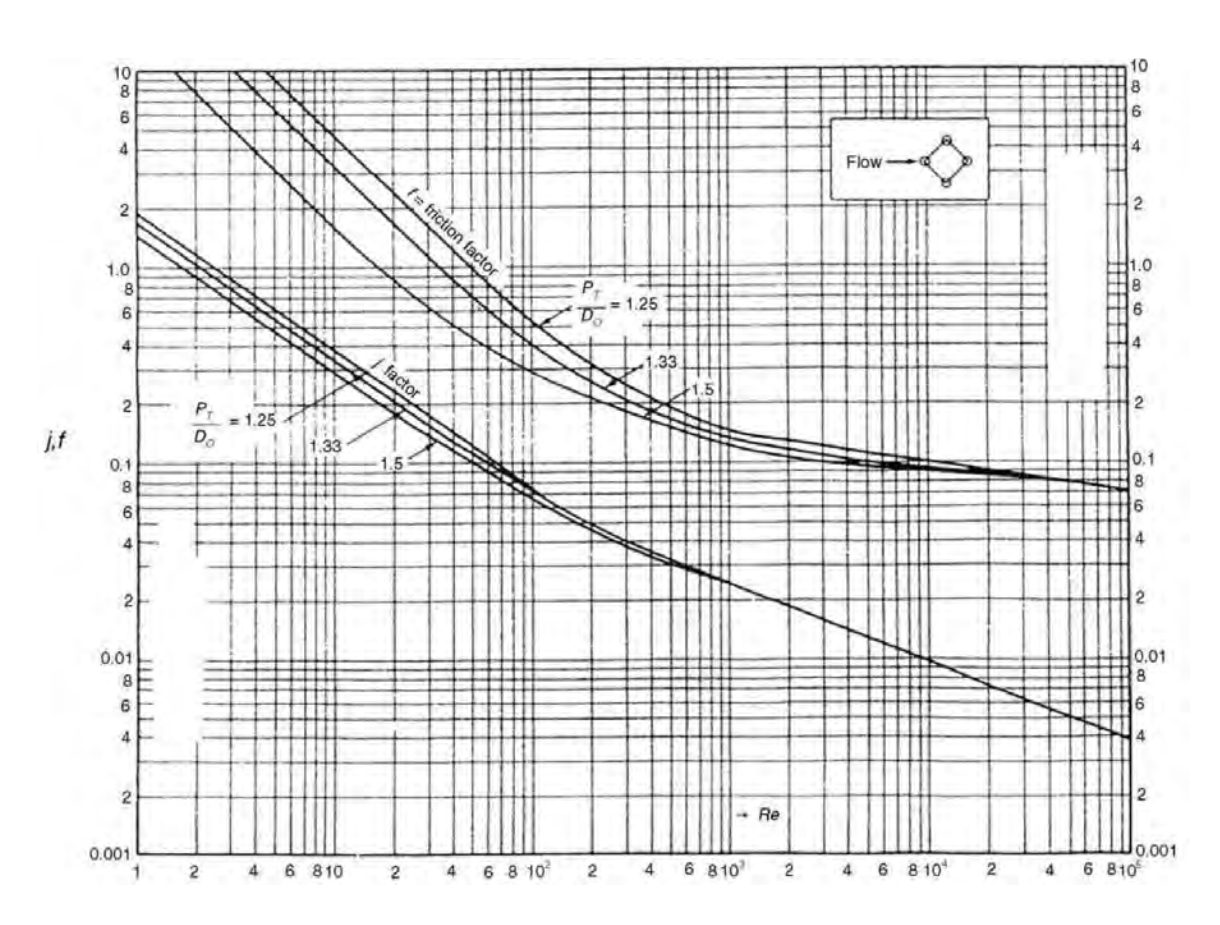


Figure E-3: Ideal tube bank correlation for diamond pitch [36]